Role of Age in Mitochondrial Susceptibility to 1,3-Dinitrobenzene-Induced Neurotoxicity

by

Laura L. Kubik

A dissertation submitted in partial fulfillment
of the requirements for the degree of
Doctor of Philosophy
(Toxicology)
in The University of Michigan
2014

Doctoral Committee:

Professor Martin A. Philbert, Co-Chair
Assistant Professor Laura Marie Rozek, Co-Chair
Professor Ari Gafni
Professor Rudy J. Richardson

DEDICATION

To my family and friends

ACKNOWLEDGEMENTS

Words simply cannot express the gratitude I have for the amount of support afforded to me by many, many individuals throughout this journey. I would like to first and foremost acknowledge the immeasurable levels of patience and guidance that my mentor, Dr. Martin Philbert, had bestowed upon me during my doctoral studies. Thank you, Dr. Philbert, for helping me work through many "growing pains" as a scientist and a professional throughout my dissertation. It was an honor and a privilege working in your lab. I would also like to thank Dr. Laura Rozek, Dr. Ari Gafni, and Dr. Rudy Richardson for serving on my committee and for providing scientific direction at multiple points throughout my dissertation. I sincerely appreciate the time and effort you devoted to the project.

I would also like to thank the members of the Philbert Lab, both past and present, that contributed to a fun and productive research experience: Dr. Stephen Steiner, Dr. Yipei Wang, Dr. Sonja Capracotta, Ian Speirs, Jackie Latham, Rory Landis, Drew Jureziz, Dr. Angela Dixon, and Jennifer Fernandez. Additionally, I would like to recognize the camaraderie and friendship of multiple members of the EHS department (past and present): Dr. Craig Harris, Dr. Rita Loch-Caruso, Dr. Dana Dolinoy, Dr. Kelly Bakulski, Dr. Lauren Tetz, Dr. Cassandra Korte, Iman Hassan, Erica Boldenow, Muna Nahar, Dr. Kelly Ferguson, Justin Colacino, Dr. Nichole Hein, Caren Weinhouse, Lisa Marchlewicz, Kari Sant, and Nancy Polderdyke. Beyond the department, I would like to thank Dr. Ingrid Bergin, Dr. Henriette Remmer, Kim Walacavage, and Wendy Rosebury-

Smith. I would also especially like to recognize Sylvia Koski, who may be described as nothing less than a master of scheduling.

I would also like to thank my family – mom and dad, I can't thank you enough for instilling the importance of hard work and perseverance; my cousin Caitlyn Galloway for always being there; and my brothers (Jake, Andy, Luke, and Adam) for teaching me how to recognize what's worth fighting for.

Lastly, I express my deepest gratitude to my husband and best friend Corey – for your support, patience, understanding, and love.

TABLE OF CONTENTS

DEDICATION ii

ACKNOWLEDGEMENTS iii

LIST OF FIGURES vii

LIST OF TABLES ix

LIST OF ABBREVIATIONS xi

ABSTRACT xiii

CHAPTER

I. Introduction 1

References 10

II. Stability of the Mitochondrial Membrane Potential Confers Susceptibility to 1,3-DNB Neurotoxicity 13

Introduction 13

Materials & Methods 14

Results 21

Discussion 26

References 42

III. Determine Whether or not the Degree of DNB-Induced Oxidation of Mitochondria-Related Proteins in Susceptible Brainstem Regions is Dependent on Age 44

Introduction 44

Materials & Methods 46

Results 50

Discussion 52

References 73

IV. Are There Differences in Compensatory Molecular Pathways between Younger and Older Brainstem Mitochondria following 1,3-DNB Exposure? 77

Introduction 77

Materials & Methods 79

Results 81

Discussion 84

References 99

V. Conclusion and Future Directions 102

References 119

LIST OF FIGURES

Figure 1.1 Age-Related Vulnerability to DNB-Induced Neurotoxicity 9

Figure 2.1. Mitochondrial Aspect Ratio and Time to First Mitochondrial Flickering Decrease as a Function of Passage Number in Immortalized Astrocytes Exposed to DNB 31

Figure 2.2. Proliferation Rates in High Passage and Low Passage Immortalized Astrocytes 32

Figure 2.3. Immunocytochemistry on Primary Neurons for Cell Identification 33

Figure 2.4. Free Intracellular Calcium Concentrations in Neurons Co-cultured with Low Passage or High Passage Immortalized Astrocytes Exposed to 600uM DNB 34

Figure 2.5. Free Intracellular Calcium Concentrations in Neurons Co-cultured with Low Passage or High Passage Immortalized Astrocytes Exposed to 400uM DNB 35

Figure 2.6. Free Intracellular Calcium Concentrations in Neurons Co-cultured with Low Passage or High Passage Immortalized Astrocytes Exposed to 200uM DNB 36

Figure 2.7. Free Intracellular Calcium Concentrations in Neurons Co-cultured with Low Passage or High Passage Immortalized Astrocytes Exposed to 100uM DNB 37

Figure 2.8. Free Intracellular Calcium Concentrations in Neurons Co-cultured with Low Passage or High Passage Immortalized Astrocytes Exposed to 50uM DNB 38

Figure 2.9. Mitochondrial Membrane Potential in Co-cultured Neurons Exposed to 600uM DNB 39

Figure 2.10. Viability of Co-cultured Immortalized Astrocytes by DNB Concentration and Passage Number 40

Figure 2.11. ATP Concentrations in Co-cultured High Passage and Low Passage Immortalized Astrocytes 41

Figure 3.1. Histology of Deep Cerebellar Nuclei in 1mo Male F344 Rats Exposed to DNB 62

Figure 3.2. Histology of Deep Cerebellar Nuclei in 3mo Male F344 Rats Exposed to DNB 63

Figure 3.3. Histology of Deep Cerebellar Nuclei in 18mo Male F344 Rats Exposed to DNB 64

Figure 3.4. Effects of DNB on Global Oxidation of Mitochondria-Related Proteins (MRPs) 65

Figure 3.5. Average Fold-Change and Percentage of Significantly Oxidized Brainstem and Cortex MRPs 68

Figure 3.6 Carbonylation Detection in 1mo F344 Rats 70

Figure 3.7 Carbonylation Detection in 3mo F344 Rats 71

Figure 3.8 Carbonylation Detection in 18mo F344 Rats 72

Figure 4.1. MRP Normalized Spectral Abundance Factor (NSAF) Fold-Changes in Brainstem 88

LIST OF TABLES

Table 3.1. Conditions and Mortality Rates of Male F344 Rats Sacrificed 24h After Last Exposure 60

Table 3.2. Conditions and Mortality Rates of Male F344 Rats Sacrificed 12h After Last Exposure 61

Table 3.3. Effects of DNB on Regional MRP Oxidation 66

Table 3.4 Effects of Age on Regional MRP Oxidation 67

Table 3.5. Pathways Significantly Oxidized by DNB in Brainstem 69

Table 4.1. Pathways Significantly Upregulated or Downregulated in Brainstem of Control Rats 89

Table 4.2. Identification of MRPs in Pathways Significantly Upregulated or Downregulated in Brainstem of Control Rats 90

Table 4.3. Pathways Significantly Upregulated or Downregulated in Brainstem of DNB-Exposed Rats 91

Table 4.4. Identification of MRPs in Pathways Significantly Upregulated or Downregulated in Brainstem of DNB-Exposed Rats 92

Table 4.5. Fold-Change Values of MRPs Significantly Changed in Brainstem of Control 1mo Rats 93

Table 4.6. Fold-Change Values of MRPs Significantly Changed in Brainstem of DNB-Exposed 1mo Rats 94

Table 4.7. Fold-Change Values of MRPs Significantly Changed in Brainstem of Control 3mo Rats 95

Table 4.8. Fold-Change Values of MRPs Significantly Changed in Brainstem of DNB-Exposed 3mo Rats 96

Table 4.9. Fold-Change Values of MRPs Significantly Changed in Brainstem of Control 18mo Rats 97

Table 4.10. Fold-Change Values of MRPs Significantly Changed in Brainstem of DNB-Exposed 18mo Rats 98

LIST OF ABBREVIATIONS

1mo	1 month old
3mo	3 month old
18mo	18 month old
ATP	Adenosine Triphosphate
BrdU	Bromodeoxyuridine
DAPI	4’,6-diamidino-2-phenylindole
DNA	Deoxyribonucleic Acid
DNB	1,3-Dinitrobenzene
DMEM	Dulbecco’s Modified Eagle’s Medium
DMSO	Dimethyl Sulfoxide
DPBS	Dulbecco’s Phosphate Buffered Saline
DSU	Disk Scanning Unit
ELISA	Enzyme-Linked Immunosorbent Assay
ETC	Electron Transport Chain
FWHM	Full Width at Half Maximum
GFAP	Glial Fibrillary Acidic Protein
GFP	Green Fluorescence Protein
GOTerm	Gene Ontology Term
HBSS	Hank’s Balanced Salt Solution
HEPES	4-(2-hydroxyethyl)-1-piperazineethanesulfonic acid
HPLC	High Performance Liquid Chromatography
HP	High Passage
KCl	Potassium Chloride
LP	Low Passage
MPT	Mitochondrial Permeability Transition
MPTP	1-methyl-4-phenyl-1,2,3,6-tetrahydropyridine
MRP	Mitochondria-Related Proteins
mtDNA	Mitochondrial DNA
MS	Mass Spectrometry
mtPTP	Mitochondrial Permeability Transition Pore
ND	Neutral Density
NeuN	Neuronal Nuclei
NPC	Neural Progenitor Cells
NSAF	Normalized Spectral Abundance Factor

PFA	Paraformaldehyde
RFP	Red Fluorescence Protein
RLU	Relative Luminescence Units
ROS	Reactive Oxygen Species
SAF	Spectral Abundance Factor
SDS-PAGE	Sodium Dodecyl Sulfate Polyacrylamide Gel Electrophoresis
TMRM	Tetramethylrhodamine Methyl Ester
ULAM	Unit for Laboratory Animal Medicine
VC	Vehicle Control

ABSTRACT

The prevalence of neurodegenerative disease is projected to increase in proportion to the doubling of older Americans over the coming decades. While age is the principle epidemiologic factor, it is likely that the development of these complex neuropathological entities is multifactorial and reflects the accumulation of chemical, physical and/or biological insults to the CNS. The Superfund chemical, 1,3-Dinitrobenzene (DNB), is an industrial intermediate in the production of dyes, plastics, and explosives. DNB selectively targets astrocytes in brainstem nuclei innervated by the 8th cranial nerve. The toxicity of DNB has been previously linked to dysfunction in astrocyte mitochondria. This study focuses on the susceptibility of key astrocytic mitochondrial proteins to selective and specific oxidation following exposure to DNB *in vitro* and *in vivo*. Using an immortalized cortical astrocyte culture, passage number provided a useful surrogate for age *in vitro*. In a co-culture system containing immortalized astrocytes and primary neurons, low passage immortalized astrocytes are able to protect neurons in DNB exposure (whereas high passage immortalized astrocytes are not); additionally, low passage immortalized astrocytes are better able to survive DNB exposure in co-culture than high passage immortalized astrocytes. Additionally, *in vivo* data shows that proteins in older mitochondria are more susceptible to oxidation by DNB than the ones from young organelles, and mitochondria-related

proteins are more highly expressed in young control animals than in older animals (both control and DNB-exposed). This data suggests that aging increases mitochondrial susceptibility to DNB-induced neurotoxicity. Using a high throughput proteomic approach with subsequent pathway analysis, it was determined that cation transmembrane transporter, nucleoside-triphosphatase, pyrophosphatase, and hydrolase activity pathways are selectively vulnerable to oxidation in *older* mitochondria. These results provide compelling evidence that environmental chemicals such as DNB may aid in the acceleration of injury to specific brain regions by inducing oxidation of sensitive mitochondrial proteins.

CHAPTER I

INTRODUCTION

Public Health Significance

As of 2010, 40 million Americans were over the age of 65 (representing 13% of the total population) (1). This number is expected to grow to 87 million by the year 2050 (1). Age is a major risk factor for a number of neurodegenerative diseases, including Parkinson's Disease (2), Alzheimer's Disease (3), and dementia (4) [of which 65% is caused by Alzheimer's Disease in those 65 years and older (5)]. The prevalence of neurodegenerative disease will likely rise as the number of older Americans doubles over the coming decades. This presents a significant public health problem for the following reasons: 1) survival for those diagnosed with neurodegenerative diseases is 11.7 years in patients diagnosed with dementia at 65 years of age (6); 2) care for those with neurodegenerative disease is expensive; and 3) there are currently no cures for neurodegenerative diseases.

The development of neuropathic states over time involves multiple contributing and causative factors. Thus, understanding the differences between healthy brain aging and the accumulation of neural damage over the life course of the individual (including exposures to environmental contaminants) will aid in the identification of critical *tipping points* in the process of neurodegeneration.

Cellular and Mitochondrial "Aging" and Neural Susceptibility

Although astrocytes can retain the ability to replicate throughout the lifespan, neurons are post-mitotic. New neurons and astrocytes can, however, arise from neural progenitor cells (NPCs) in the adult mammalian brain (7). These multipotent NPC populations are spatially restricted to the subgranular layer of the dentate gyrus in the hippocampus and the subventricular zone of the lateral ventricles (8). Because most regions of the brain do not contain NPCs from which new neurons may arise, the age of neurons between different regions of the adult brain may differ. Therefore, the biochemical demands on astrocytes in these regions may differ as a result. Additionally, aging causes a significant decrease in neuronal progenitor proliferation and in migration of new neurons in adult rat hippocampus (9). Aging of a cell, therefore, not only refers to an accumulation of functional changes in astrocytic daughter cells, but also to the accumulation of functional changes in postmitotic neurons and the multipotent NPCs from which new astrocytes and neurons may be derived.

The accumulation of posttranslational modifications to proteins, such as oxidation, can, over time, result in alterations in structure and function. During the aging process, astrocyte populations amass functional changes to proteins in multiple pathways that are detrimental to their ability to perform neuroprotective functions, including increased expression of mutant huntingtin in mice (10). Additionally, because neurons don't replicate, the neurons that persist postnatally through adulthood accrue damaging posttranslational modifications, such as oxidation (11), (12), (13) (14). Therefore, astrocytes must accommodate the "aged" neuronal environment in adult

mammals, when they themselves are at a higher risk for dysfunction as a result of the aging process.

As mammals get older, mitochondria have a propensity to accumulate damage (oxidized proteins (15), mutated mtDNA (16), (17), etc.), which is often colloquially referred to as mitochondrial aging. However, mitochondrial "aging" within the brain is a complex and dynamic process; these organelles have the ability to fuse together (fusion), and to split from one mitochondrion into two distinct mitochondria (fission). Mitochondria undergo these fusion and fission events in response to the immediate cellular microenvironment. Mitochondrial fission events segregate mitochondrial contents (mtDNA, electron transport chain (ETC) enzymes, antioxidants, reactive oxygen species (ROS), etc.) into two distinct mitochondria. Mitochondrial fusion events, conversely, mix these contents from two mitochondria into one mitochondrion. Although mitochondrial fusion and fission is dynamic, these events aren't stochastic. As a function of age in culture, fusion events decreased as fission rates increased in rotenone-exposed rat primary cortical neurons; the opposite was true in control primary neurons (18). Fusion events, followed by near immediate fission of the previously fused mitochondrion, also increased in frequency in rotenone-exposed rat primary cortical neurons (18). Therefore, not only can mitochondrial fusion and fission events be linked, age in culture also influences the frequency and type of mitochondrial dynamic events.

Mitochondrial remodeling processes occur throughout the life course. However, when mitochondria are significantly damaged, they are eliminated via autophagy or can be segregated from the remaining mitochondrial population by fusing with an adjacent healthy mitochondrion (19). Autophagous processes themselves decline in efficiency

with age (20), increasing the risk of the accumulation of damaged mitochondria in a time-dependent manner. It is crucial that damaged mitochondria are appropriately removed from cells; this is crucial not just for the health of the aging individual, but their offspring as well. Recently, it was discovered that maternally transmitted mtDNA mutations in mice can induce aging phenotypes and abnormal brain development in offspring mice (21).

Environmental Exposure to Neurotoxicants during Aging

Age is a primary risk factor for the development of neurodegenerative disease. However, due to the unknown etiology of most late-onset neurodegenerative diseases, exposures to neurotoxicants over the life course have been postulated to play a role. Causal determinations between environmental exposures (both discrete exposures and chronic exposures) and development of neurodegenerative diseases in humans have proven difficult to achieve. The most convincing evidence of associations between exposures and onset of neurodegenerative diseases have come from occupational exposures to heavy metals in humans; mechanistic data investigating these links in laboratory animals have provided some insight, and likely include disruption of iron and/or zinc homeostasis (reviewed by Cannon and Greenamyre) (22). Altogether, the exact mechanisms by which environmental exposures cause or contribute to the development of neurodegenerative disease have remained elusive.

Occupational exposure to manganese in welders is one of the most well studied exposures attempting to establish neurotoxicants in the etiology of neurodegenerative diseases. There is also a need for characterizing environmental exposure to

manganese as a contributor to neurotoxicity across the life course, in addition to what is known of occupational exposures (23). Manganese exposure causes an array of neuromuscular symptoms, many of which overlap with parkinsonism (24) (also referred to as idiopathic Parkinson's Disease in the literature). Epidemiologic studies have linked advanced age and occupational exposure to manganese with poorer performance in neurobehavioral tests than age-matched controls (25). The mechanism of manganese neurotoxicity has been explored in developing, adult, and aged rats: in neonatal rats, manganese exposure caused an increase in dopamine and norepinephrine, whereas in adult rats, it caused a decrease in dopamine (26); in brainstem of aged rats, chronic manganese exposure depleted noradrenaline, dopamine, and glutathione levels, while increasing amino acid oxidation (27). This data suggests that older rats are more susceptible to the neurotoxic effects of manganese exposure, including oxidative stress in the brainstem. This increased susceptibility due to age is also likely to be true for other neurotoxicants that cause oxidative stress, including 1,3-Dinitrobenzene (DNB).

1,3-Dinitrobenzene-Induced Regional and Cellular Susceptibility in Brain

1,3-Dinitrobenzene (DNB), a Superfund chemical, is an industrial intermediate used in the production of dyes, explosives, and plastics. In humans, DNB exposure causes ataxia, dizziness, and nausea. In rats, DNB exposure causes methemoglobinemia and ataxia, with bilaterally symmetrical spongiform lesions evident in areas of the brainstem innervated by the 8th cranial nerve (28). *In vivo,* initial cellular targets of DNB exposure include glia (astrocytes, oligodendrocytes) and the vasculature, followed by involvement of neurons (28). Because DNB-induced lesions

closely resemble those observed in acute energy deprivation syndromes, it was hypothesized that the mechanism of toxicity of DNB in the glia of the brainstem involved a disruption of mitochondrial function, likely involving a disturbance in redox balance within the mitochondria (28).

Cellular Susceptibility

Exposure to DNB causes differential mitochondrial sensitivity in cultured neurons compared to astrocytes. Neuroblastoma cells (SY5Y) exposed to DNB exhibited mitochondrial reduction potential nearly ten times lower than that of DNB-exposed C6 glioma cells, while inducing the mitochondrial permeability transition (MPT) in both C6 and SY5Y cells (29). Additionally, DNB exposure inhibits the pyruvate dehydrogenase complex in C6 glioma cells (30). Mitochondrial permeability transition pore (mtPTP)-induced cell death is governed by a specific group of proteins, including Bcl-X_L, Bcl-2, and Bax. C6 glioma cells express significantly more Bcl-X_L than SY5Y cells exposed to DNB, while conversely, SY5Y neuroblastoma cells expressed significantly higher levels of Bcl-2 and Bax compared to C6 cells (29). These data suggest that a compromise of the mitochondrial membrane potential plays a role in the differential susceptibility to DNB in neurons and astrocytes.

DNB exposure causes increased production of ROS and loss of mitochondrial membrane potential in immortalized astrocytes, while at the same time producing distinct carbonylation profiles of organellar proteomes (namely mitochondrial) (31). This indicates that while DNB induces higher ROS production within the cell overall, specific carbonylation of mitochondrial proteins in astrocytes may ultimately affect their neuroprotective capability and contribute to the mechanism of toxicity of DNB.

Regional Susceptibility

Region-specific investigations of mitochondrial function within brainstem and cortex in DNB exposure provide evidence of a change in Bcl-X_L expression in cortical astrocytes, but not brainstem astrocytes (32). Additionally, DNB exposure inhibits mitochondrial succinate dehydrogenase activity in both brainstem and cortical astrocytes; this inhibition was prevented by mtPTP inhibitors bongkrekic acid and cyclosporin A in brainstem astrocytes only (33). This evidence supports the premise that regional susceptibility is specific to opening of the mtPTP. Opening of the mtPTP can be caused by increases in ROS. Increases in DNB-induced ROS in brainstem mitochondria, as measured by specific carbonylated mitochondrial proteins, have been shown (Dr. Stephen Steiner, unpublished data).

Research Gaps to be Addressed by this Dissertation

It has been established that damage to macromolecules accumulates during aging, and that there is considerable cellular and regional variability in the brain regarding susceptibility to these accumulations. Mechanisms with which oxidative damage to proteins is removed and antioxidant stores are replenished attenuate in the brain over time. DNB exposure results in regionally-confined lesions, with specific cellular targets within those regions. DNB causes decreases in selected enzymatic functions in astrocyte mitochondria, increases in proteomic oxidation in immortalized astrocyte mitochondria, and shifts in mtPTP dynamics in brainstem and cortical mitochondria. Exposure to environmental neurotoxicants, such as DNB, can exacerbate the limits to which the aging brain can efficiently respond.

Therefore, it is hypothesized that (Figure 1.1):

Aging increases mitochondrial susceptibility to neurotoxicity induced by 1,3-DNB by causing mitochondrial membrane instability in astrocytes, oxidation of specific pathways in mitochondria-related proteins in brainstem, and altering expression profiles of mitochondria-related proteins.

Specific Aim 1) Stability of mitochondrial membrane potential confers susceptibility to 1,3-DNB toxicity

Specific Aim 2) Determine whether or not the degree of 1,3-DNB-induced oxidation of MRPs in susceptible brainstem regions is dependent on age

Specific Aim 3) Determine whether or not there are differences in compensatory molecular pathways between younger and older brainstem mitochondria in 1,3-DNB exposure

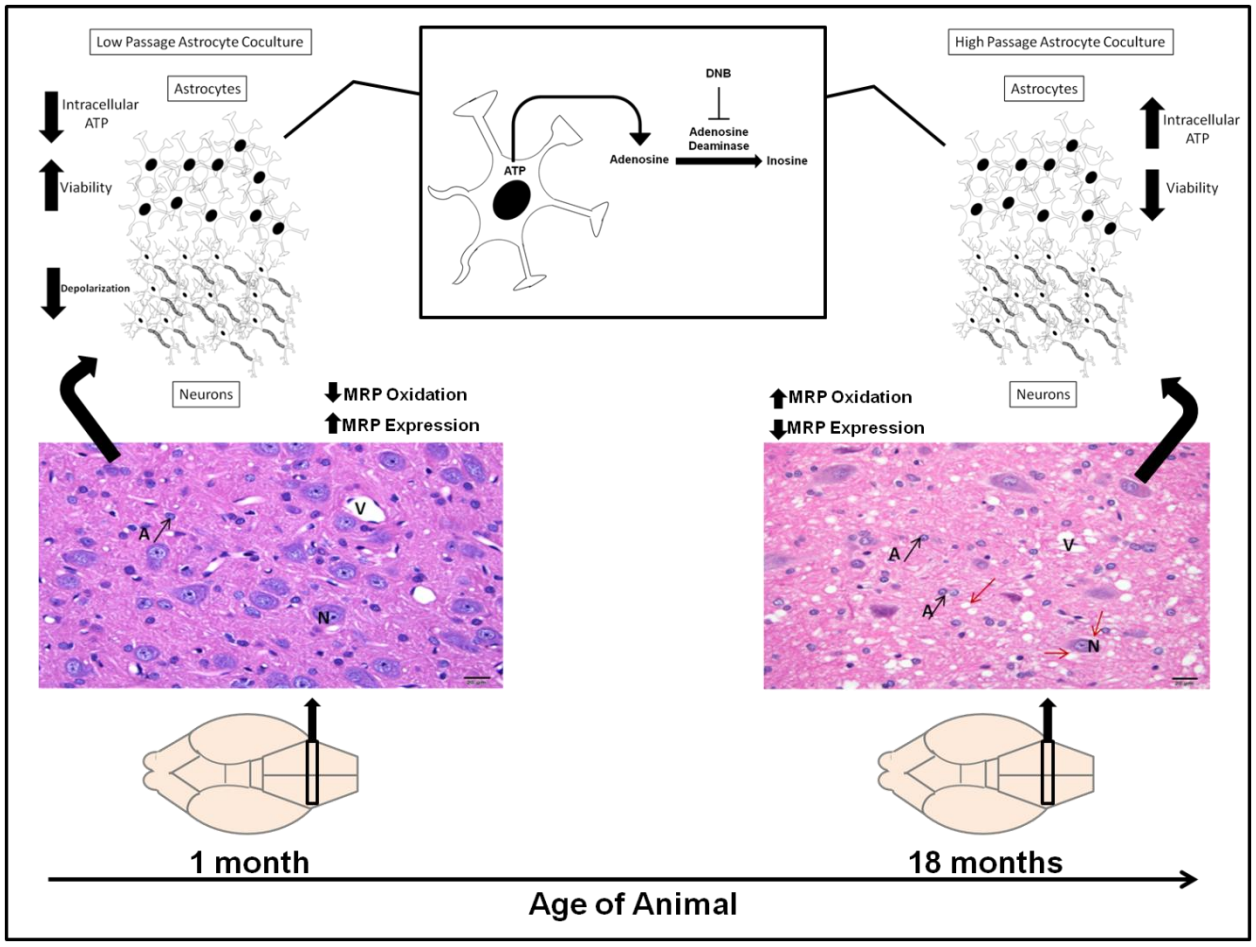

Figure 1.1 Age-Related Vulnerability to DNB-Induced Neurotoxicity
Exposure to DNB causes spongiform lesions in the brainstem in old animals, with increased vacuolation of the neuropil. Because mitochondria accumulate damage over time during the aging process, mitochondria related proteins (MRP) within the brainstem of older animals are more vulnerable to DNB-induced damage than younger animals. Brainstem astrocytes are a cellular target of DNB; *in vitro,* low passage co-cultured astrocytes were better able to survive DNB exposure compared to high passage co-cultured astrocytes, and were able to better perform neuroprotective functions, such as preventing neuronal depolarization. Low passage co-cultured astrocytes exhibit lower intracellular ATP compared to high passage co-cultured astrocytes, indicating that low passage astrocytes may release more ATP into the extracellular space (which can be dephosphorylated to adenosine) and therefore can better silence neurons compared to high passage co-cultured astrocytes in response to DNB exposure. Because DNB inhibits adenosine deaminase (Wang, et al. 2012), DNB itself directly contributes to the prevention of the conversion of adenosine to inosine and may therefore contribute to an increase in extracellular adenosine. *(N = Neuron, A = Astrocyte, V = Vasculature, Red Arrow = Vacuolation)*

REFERENCES

1. Statistics FIFoA-R. Older Americans 2012: Key Indicators of Well-Being. In: Statistics FIFoA-R, editor. Washington, D.C: U.S.: U.S. Government Printing Office; 2012.

2. Moghal S, Rajput AH, D'Arcy C, Rajput R. Prevalence of movement disorders in elderly community residents. Neuroepidemiology. 1994;13(4):175-8.

3. Lindsay J, Laurin D, Verreault R, Hebert R, Helliwell B, Hill GB, et al. Risk factors for Alzheimer's disease: a prospective analysis from the Canadian Study of Health and Aging. Am J Epidemiol. 2002;156(5):445-53.

4. Fratiglioni L, Launer LJ, Andersen K, Breteler MM, Copeland JR, Dartigues JF, et al. Incidence of dementia and major subtypes in Europe: A collaborative study of population-based cohorts. Neurologic Diseases in the Elderly Research Group. Neurology. 2000;54(11 Suppl 5):S10-5.

5. Lobo A, Launer LJ, Fratiglioni L, Andersen K, Di Carlo A, Breteler MM, et al. Prevalence of dementia and major subtypes in Europe: A collaborative study of population-based cohorts. Neurologic Diseases in the Elderly Research Group. Neurology. 2000;54(11 Suppl 5):S4-9.

6. Xie J, Brayne C, Matthews FE. Survival times in people with dementia: analysis from population based cohort study with 14 year follow-up. BMJ. 2008;336(7638):258-62. PMCID: 2223023.

7. Eriksson PS, Perfilieva E, Bjork-Eriksson T, Alborn AM, Nordborg C, Peterson DA, et al. Neurogenesis in the adult human hippocampus. Nat Med. 1998;4(11):1313-7.

8. Gage FH, Kempermann G, Palmer TD, Peterson DA, Ray J. Multipotent progenitor cells in the adult dentate gyrus. J Neurobiol. 1998;36(2):249-66.

9. Kuhn HG, Dickinson-Anson H, Gage FH. Neurogenesis in the dentate gyrus of the adult rat: age-related decrease of neuronal progenitor proliferation. J Neurosci. 1996;16(6):2027-33.

10. Bradford J, Shin JY, Roberts M, Wang CE, Li XJ, Li S. Expression of mutant huntingtin in mouse brain astrocytes causes age-dependent neurological symptoms. Proc Natl Acad Sci U S A. 2009;106(52):22480-5. PMCID: 2799722.

11. Smith CD, Carney JM, Starke-Reed PE, Oliver CN, Stadtman ER, Floyd RA, et al. Excess brain protein oxidation and enzyme dysfunction in normal aging and in

Alzheimer disease. Proc Natl Acad Sci U S A. 1991;88(23):10540-3. PMCID: 52964.

12. Nicolle MM, Gonzalez J, Sugaya K, Baskerville KA, Bryan D, Lund K, et al. Signatures of hippocampal oxidative stress in aged spatial learning-impaired rodents. Neuroscience. 2001;107(3):415-31.

13. Aksenova MV, Aksenov MY, Carney JM, Butterfield DA. Protein oxidation and enzyme activity decline in old brown Norway rats are reduced by dietary restriction. Mech Ageing Dev. 1998;100(2):157-68.

14. Cakatay U, Telci A, Kayali R, Tekeli F, Akcay T, Sivas A. Relation of oxidative protein damage and nitrotyrosine levels in the aging rat brain. Exp Gerontol. 2001;36(2):221-9.

15. Perluigi M, Di Domenico F, Giorgi A, Schinina ME, Coccia R, Cini C, et al. Redox proteomics in aging rat brain: involvement of mitochondrial reduced glutathione status and mitochondrial protein oxidation in the aging process. J Neurosci Res. 2010;88(16):3498-507.

16. Miquel J, Economos AC, Fleming J, Johnson JE, Jr. Mitochondrial role in cell aging. Exp Gerontol. 1980;15(6):575-91.

17. Barja G. Mitochondrial oxygen consumption and reactive oxygen species production are independently modulated: implications for aging studies. Rejuvenation Res. 2007;10(2):215-24.

18. Arnold B, Cassady SJ, VanLaar VS, Berman SB. Integrating multiple aspects of mitochondrial dynamics in neurons: age-related differences and dynamic changes in a chronic rotenone model. Neurobiol Dis. 2011;41(1):189-200. PMCID: 3021420.

19. Sheng ZH, Cai Q. Mitochondrial transport in neurons: impact on synaptic homeostasis and neurodegeneration. Nat Rev Neurosci. 2012;13(2):77-93.

20. Gottlieb RA, Carreira RS. Autophagy in health and disease. 5. Mitophagy as a way of life. Am J Physiol Cell Physiol. 2010;299(2):C203-10. PMCID: 2928637.

21. Ross JM, Stewart JB, Hagstrom E, Brene S, Mourier A, Coppotelli G, et al. Germline mitochondrial DNA mutations aggravate ageing and can impair brain development. Nature. 2013;501(7467):412-5. PMCID: 3820420.

22. Cannon JR, Greenamyre JT. The role of environmental exposures in neurodegeneration and neurodegenerative diseases. Toxicol Sci. 2011;124(2):225-50. PMCID: 3216414.

23. Hudnell HK. Effects from environmental Mn exposures: a review of the evidence from non-occupational exposure studies. Neurotoxicology. 1999;20(2-3):379-97.

24. Calne DB, Chu NS, Huang CC, Lu CS, Olanow W. Manganism and idiopathic parkinsonism: similarities and differences. Neurology. 1994;44(9):1583-6.

25. Wastensson G, Sallsten G, Bast-Pettersen R, Barregard L. Neuromotor function in ship welders after cessation of manganese exposure. Int Arch Occup Environ Health. 2012;85(6):703-13.

26. Seth PK, Chandra SV. Neurotransmitters and neurotransmitter receptors in developing and adult rats during manganese poisoning. Neurotoxicology. 1984;5(1):67-76.

27. Desole MS, Miele M, Esposito G, Migheli R, Fresu L, Enrico P, et al. Monoaminergic systems activity and cellular defense mechanisms in the brainstem of young and aged rats subchronically exposed to manganese. Neurosci Lett. 1994;177(1-2):71-4.

28. Philbert MA, Nolan CC, Cremer JE, Tucker D, Brown AW. 1,3-Dinitrobenzene-induced encephalopathy in rats. Neuropathol Appl Neurobiol. 1987;13(5):371-89.

29. Tjalkens RB, Ewing MM, Philbert MA. Differential cellular regulation of the mitochondrial permeability transition in an in vitro model of 1,3-dinitrobenzene-induced encephalopathy. Brain Res. 2000;874(2):165-77.

30. Miller JA, Runkle SA, Tjalkens RB, Philbert MA. 1,3-Dinitrobenzene-induced metabolic impairment through selective inactivation of the pyruvate dehydrogenase complex. Toxicol Sci. 2011;122(2):502-11. PMCID: 3155080.

31. Steiner SR, Philbert MA. Proteomic identification of carbonylated proteins in 1,3-dinitrobenzene neurotoxicity. Neurotoxicology. 2011;32(4):362-73. PMCID: 3158615.

32. Phelka AD, Sadoff MM, Martin BP, Philbert MA. BCL-XL expression levels influence differential regional astrocytic susceptibility to 1,3-dinitrobenzene. Neurotoxicology. 2006;27(2):192-200.

33. Phelka AD, Beck MJ, Philbert MA. 1,3-Dinitrobenzene inhibits mitochondrial complex II in rat and mouse brainstem and cortical astrocytes. Neurotoxicology. 2003;24(3):403-15.

CHAPTER II

Stability of the Mitochondrial Membrane Potential Confers Susceptibility to 1,3-DNB Neurotoxicity

INTRODUCTION

Notable age-related declines in mammalian mitochondrial function have been linked to the normal and accelerate degeneration of brain and other organs. In aging human brains, neuronal and glial mitochondrial metabolism decreases in both neurons and glia and are likely responsible for the steady overall loss of function due to the dependence of neurons on astrocytes for collateral metabolic and physical support, and for maintenance of the composition of the extracellular environment (1). Astrocytes participate actively in neuroprotective functions, such as scavenging excess extracellular glutamate (2), and regulating extracellular calcium and potassium concentrations (3). Astrocytes with functionally intact mitochondria supply energy equivalents in the form of adenosine triphosphate (ATP) that is required to maintain important neuroprotective functions (4). Thus, the accumulation of (bio)chemical and physical insults to brain mitochondria over time can result in a deterioration in these neuroprotective astrocyte functions in older mammals. Exposure to neurotoxicants that selectively target astrocyte mitochondria may, therefore, exacerbate existing or acquired metabolic imbalances as a result of aging.

1,3-Dinitrobenzene (DNB) is an industrial synthetic intermediate that produces focal, bilaterally symmetrical lesions in the brainstem similar to those seen in acute energy deprivation syndromes (5). It has been established that astrocytes within the brainstem are a principal cellular target in DNB exposure (4), and that astrocyte mitochondria are an organellar target in DNB exposure (6), (7), (8), (9), (10). Astrocytes release adenosine as a neuroprotective mechanism (11). Extracellular adenosine increases significantly in immortalized astrocyte monoculture with corresponding increases in DNB concentrations (12), suggesting that DNB exposure causes astrocytes to expend their energetic resources toward neuroprotective functions, perhaps at the expense of other cellular functions.

This study seeks to establish evidence of a relationship between age in culture (passage number of immortalized astrocytes) and the degree to which astrocytes can maintain neuroprotective functions. Both monoculture astrocytes and cocultures of immortalized astrocytes and primary neurons are employed to investigate this relationship.

MATERIALS AND METHODS

Cell Culture

Immortalized astrocytes (DI-TNC_1) were obtained from the American Type Culture Collection and maintained in a humidified incubator at 37°C and 5% CO_2. Growing media for DI-TNC_1 astrocytes consisted of Dulbecco's Modified Eagle's Medium (DMEM, 25mM D-Glucose, 1mM sodium pyruvate), 10% Fetal Bovine Serum,

and 1% Antibiotic/Antimycotic. Media and additives were vacuum filtered for sterilization prior to use.

Primary neurons were isolated from E18 Sprague-Dawley rat cortex, obtained from BrainBits, LLC and maintained in a humidified incubator at 37°C and 5% CO_2. Isolation of neurons was performed according to the protocol by BrainBits. Briefly, glass coverslips were coated with 50µg/mL Poly-D-Lysine and allowed to adhere at least one hour at 37°C. Coverslips were then subsequently rinsed with sterile water 3 times and then allowed to dry under the sterile hood. Cortices were dissociated with 2mg/mL papain in Hibernate E media without calcium (BrainBits, LLC) using a fire-polished glass Pasteur pipette. Papain solution was removed and Hibernate E media (BrainBits, LLC) was added to the dissociated tissue. Tissue was allowed to settle, supernatant was spun down to pellet the neurons, and then the pellet was resuspended in Neurobasal media supplemented with B-27, Glutamax, and 1% Antibiotic/Antimycotic (all from Invitrogen). Neurons were diluted and then plated at $1.2x10^5$ cells per coverslip. After 3 hours, half of the media was removed and fresh supplemented Neurobasal media was used to rinse the coverslips 3 times. Media was then changed every 4-5 days afterward.

Mitochondrial Flickering Detection and Analysis

DI-TNC_1 astrocytes were plated onto glass coverslips and grown to ~30-50% confluence (18-24 hours) in an incubator (5% CO_2, 37°C). Growing media was replaced with DNB dosing media (serum-free DMEM). One hour after exposure to DNB, 10% FBS was supplemented back into the media. Fifteen minutes prior to imaging, the dosing media was aspirated, cells were rinsed gently with Dulbecco's

phosphate buffered saline (DPBS), and 100nM tetramethylrhodamine methyl ester (TMRM) (in 4-(2-hydroxyethyl)-1-piperazineethanesulfonic acid/Hanks' Balanced Salt Solution: HEPES/HBSS buffer) was added. After a fifteen minute incubation period, the TMRM solution was replaced with HEPES/HBSS buffer and the cells were imaged.

Cells were imaged on an Olympus IX-800 disk scanning unit (DSU) microscope at intervals of 500ms for 60 seconds. Light intensity of the mercury lamp was maintained at a constant wattage output, measured by a light meter, so as to maintain imaging consistency and to control for phototoxicity. During imaging, the cells were maintained in an environmental chamber (Pathology Devices), set at 5% CO_2, 37°C, and 60% humidity. The microscope was controlled using SlideBook software (version 5.0), and image loops were reviewed immediately following image acquisition.

Bromodeoxyuridine (BrdU) Proliferation Assay in Immortalized Astrocytes

DI-TNC_1 astrocytes were plated onto 96-well plates at $5x10^3$ cells per well and grown to confluence (24 hours) in an incubator (5% CO_2, 37°C). Growing media was replaced with DNB dosing media (serum-free DMEM). One hour after exposure to DNB, 10% FBS was supplemented back into the media. The manufacturer's instructions for the BrdU ELISA (Roche) were followed. Briefly, BrdU labeling solution was added to the wells and allowed to incubate 2-20 hours after exposure to either 100uM or 600uM DNB (or a v/v equivalent of DMSO as a vehicle control). At each time point (2h, 4h, 8h, 12h, 16h, 20h) the labeling solution was removed from the wells and the cells were processed as directed for colorimetric detection of BrdU incorporation.

Immunocytochemistry – Primary Neuron Identification

Sprague-Dawley rat E18 cortical tissue (BrainBits, LLC) was dissected as directed by the protocol. Neurons were cultured on poly-D-lysine glass coverslips for 5-7 days and used for co-culture experiments with astrocytes. Neurons were fixed with 4% paraformaldehyde, rinsed with DPBS, and incubated with 4',6-diamidino-2-phenylindole (DAPI) alone as a negative control or with DAPI, anti-glial fibrillary acidic protein (GFAP) conjugated with Alexafluor-488 to identify astrocytes, and anti-neuronal nuclei (NeuN) conjugated with Alexafluor-555 to identify neurons (red). Neurons were imaged on an Olympus IX-800 DSU microscope and images were saved using Slidebook software (version 5.3).

Ca2+ Visualization using Fluo-4 AM in Primary Neurons

Rat E18 cortical tissue (BrainBits, LLC) was dissected as directed by the protocol. Neurons were cultured for 5-7 days in Neurobasal media (Invitrogen) supplemented with Glutamax, B-27 and antibiotic-antimycotic (Invitrogen) on poly-D-lysine coated glass cover slips and co-cultured with either high passage or low passage DI-TNC_1 astrocytes using Corning® Trans-well inserts. After 24h had elapsed, neurons and DI-TNC_1 astrocytes were exposed to 50uM, 100uM, 200uM, 400uM, or 600uM DNB (or v/v equivalent of DMSO (vehicle control; VC)). At time points at which first flickering was observed in DNB exposures in monoculture DI-TNC_1 astrocytes, the dosing media was removed, the insert containing DI-TNC_1 astrocytes was removed, and 1uM Fluo-4 (Invitrogen), dissolved in Pluronic (Invitrogen) was delivered to neurons in HEPES/HBSS buffer. After a 30 minute incubation in an incubator (5% CO_2, 37°C),

Fluo-4 was removed, cells were rinsed 2x with HEPES/HBSS buffer, and incubated with HEPES/HBSS buffer for 30 minutes in the incubator. Coverslips were mounted on an imaging chamber, 900µl of HEPES/HBSS buffer was added to the chamber, and baseline images were captured (60 images, 1s intervals). At 60s, 100µl of 1M potassium chloride (KCl) was added to the chamber (100mM working concentration) to induce depolarization of the neuron; images were continuously taken for 5 more minutes to monitor the Ca^{2+} wave during depolarization. Thapsigargin was used as a positive control for intracellular calcium following KCl-induced depolarization.

JC-1 Visualization of Mitochondrial Membrane Potential in Primary Neurons

Sprague-Dawley rat E18 cortical tissue (BrainBits, LLC) was dissected as directed by the protocol. Neurons were cultured for 5-7 days in Neurobasal media (Invitrogen) supplemented with Glutamax, B-27 and antibiotic-antimycotic (Invitrogen) on poly-D-lysine coated glass cover slips and co-cultured with either high passage or low passage DI-TNC_1 astrocytes using Corning® Trans-well inserts. After 24h had elapsed, neurons and DI-TNC_1 astrocytes were exposed to 600uM DNB, v/v equivalent of DMSO (vehicle control; VC), or 5uM FCCP (positive control for mitochondrial depolarization). At time points at which first flickering was observed in DNB exposures in monoculture DI-TNC_1 cells at 600uM DNB, the dosing media was removed, the insert containing DI-TNC_1 cells was removed, and buffer (HEPES/HBSS) containing 5uM JC-1 was added. Neurons were incubated with JC-1 at 37°C for 30 minutes. Following this 30 minute step, neurons were rinsed 3x with HEPES/HBSS buffer and visualized on an Olympus IX-800 DSU microscope (20x). During imaging, the cells were maintained in

an environmental chamber (Pathology Devices), set at 5% CO_2, 37°C, and 60% humidity. The following camera settings were used for capturing images: red fluorescence protein (RFP) (Neutral Density 4 (ND4)); green fluorescent protein (GFP) (ND4); Range around current: 1um, # planes: 10, step size: 0.1um. Scale bars were added (Annotations tab in Slidebook) and Z-stack was exported as TIF files, MultiDimensional View was exported as a TIF file.

Trypan Blue Exclusion – Determination of DI-TNC_1 Astrocyte Viability

DI-TNC_1 astrocytes were co-cultured on Corning® Trans-well inserts for 24h in wells containing primary neurons, adhered to coverslips, derived from rat E18 cortical tissue (BrainBits, LLC). The co-culture media (Neurobasal, Glutamax, B-27, antibiotic-antimycotic) was removed and fresh co-culture media with varying concentrations of DNB and VC was added for the following lengths of time: 600uM = 3.5h; 400uM = 9h; 200uM 12h; 100uM = 20h; 50uM = 22h (these time points and concentrations are directly aligned with the time points and concentrations found to induce first flickering and morphological changes in LP DI mitochondria). DI-TNC_1 astrocytes were rinsed with DPBS, trypsinized, and resuspended in DMEM. Cell resuspensions were added to Trypan Blue (1:1) and cells were counted using a Countess™ automated cell counter (Sigma).

ATP Concentration Assay in Co-cultured Immortalized Astrocytes

Sprague-Dawley rat E18 cortical tissue (BrainBits, LLC) was dissected as directed by the protocol. Neurons were cultured for 5-7 days in Neurobasal media (Invitrogen) supplemented with Glutamax, B-27 and 1% antibiotic/antimycotic

(Invitrogen) on poly-D-lysine coated glass cover slips and co-cultured with either high passage or low passage DI-TNC_1 astrocytes using Corning® Trans-well inserts. After 24h had elapsed, neurons and DI-TNC_1 astrocytes were exposed to 50uM, 100uM, 200uM, 400uM, or 600uM DNB (or v/v equivalent of DMSO (vehicle control; VC)). At time points at which first flickering was observed in DNB exposures in monoculture DI-TNC_1 astrocytes, the dosing media was removed and the ATPLite™ luminescence ATP concentration detection assay (PerkinElmer®) was performed as directed by the manufacturer.

Statistical Analysis

Fluorescence microscopy data measuring free intracellular calcium in neurons (Figures 2.4-2.8) were graphed as a percentage of fluorescence intensity induced by addition of KCl; a one-way ANOVA with Tukey's test for multiple comparisons was used to determine significant differences between the exposures, with $p<0.05$ considered statistically significant (Prism software, version 5.0, GraphPad). Viability of co-cultured astrocytes (Figure 2.10) was expressed as the mean live cell count ± SEM, normalized to the vehicle control, and values for low passage and high passage astrocytes were pooled for comparison by Student's t-test, with $p<0.05$ considered statistically significant. ATP levels in astrocytes were shown as relative luminescence units and normalized to the vehicle control. A one-way ANOVA with Tukey's test for multiple comparisons was used to compare the effect of each concentration of DNB on low and high passage astrocyte ATP levels; $p<0.05$ was considered a significant difference between the means for each group (Prism software, version 5.0, GraphPad).

RESULTS

Mitochondrial Aspect Ratio and Time to First Mitochondrial Flickering in DI-TNC$_1$ astrocytes exposed to DNB

DNB-induced changes in mitochondrial aspect ratio and concurrent induction of first mitochondrial flickering events are shown in Figure 2.1. A mitochondrial "first flickering event" is defined, for the purposes of this study, as the first detectable loss of membrane potential, followed immediately by the regain of the membrane potential. Mitochondrial flickering was measured using the mitochondrial-specific, potentiometric fluorescent dye TMRM, and aspect ratio was measured using MitoTracker® Deep Red. Higher passage DI-TNC$_1$ astrocytes exhibited earlier first flickering events (solid blue line) and decreased aspect ratio (dashed blue line) in comparison to lower passage DI-TNC$_1$ astrocytes (time to first flickering event = solid red line, aspect ratio = dashed red line). A regression model ($\beta_0 + \beta_1 \log(\text{DNB Concentration}) + \beta_2 \log(\text{Exposure time})$) was run separately for both mitochondrial first flickering and aspect ratio values, and showed that trends were statistically significant between passage groups ($p<0.05$). A range of concentrations of DNB were used for the experiment (600uM, 400uM, 200uM, 100uM, and 50uM). For both passage groups, the higher the concentration of DNB, the earlier the average first flickering event occurred. Decreases in aspect ratio were concurrent with detection of first mitochondrial flickering events.

Proliferation Rates in High Passage and Low Passage DI-TNC$_1$ astrocytes

DI-TNC$_1$ astrocyte proliferation rates were measured using an enzyme-linked immunosorbent assay (ELISA) for BrdU incorporation into cellular deoxyribonucleic acid (DNA) to determine whether or not DNB causes a passage-dependent decrease in cell

proliferation. While there were no statistically significant differences in proliferation rates between high passage DI-TNC_1 astrocytes and low passage DI-TNC_1 astrocytes or between vehicle control and DNB-exposed cells within each passage group, some proliferation trends do emerge (Figure 2.2): high passage DI-TNC_1 astrocytes' growth curve peaks and then plateaus, whereas low passage astrocytes keep proliferating past 20 hours, in both control and DNB-exposed groups.

Immunocytochemistry on Primary Neurons for Cell Identification

Immunocytochemistry experiments to identify the purity of primary neuron cultures used for co-culture experiments identified the cultures to be at least 81% neurons on average (Figure 2.3.).

Free Intracellular Calcium Concentrations in Neurons Co-cultured with Low Passage or High Passage Immortalized Astrocytes Exposed to 600uM, 400uM, 200uM, 100uM, 50uM DNB

Free intracellular calcium was detected using the fluorescent dye Fluo-4AM and induction of neuronal depolarization by KCl addition. This was done to determine whether or not lower passage astrocytes were better able to defer or prevent depolarization in neurons during DNB exposure than higher passage astrocytes. Thapsigargin (1uM) was used as a positive control for intracellular calcium, as it blocks the sarco/endoplasmic Ca2+ ATPase and raises intracellular calcium stores (13). Because adenosine is a neuroprotective metabolite (14), 5uM adenosine was used as an additional control by itself, and was also used as a co-treatment with DNB. Exposures to DNB were parallel with time-points and concentrations that induced the first flickering event (as shown in Figure 2.1).

At 600uM DNB, neurons co-cultured with low passage DI-TNC_1 astrocytes showed statistically significantly lower levels of intracellular calcium than thapsigargin ($p<0.05$) (Figure 2.4), as did neurons co-cultured with high passage DI-TNC_1 astrocytes ($p<0.001$). Additionally, adenosine alone caused a decrease in neuronal intracellular calcium that was statistically significantly lower in both low passage ($p<0.05$) and high passage ($p<0.001$) co-cultured neurons compared to thapsigargin (Figure 2.4). However, in neurons co-cultured with high passage DI-TNC_1 astrocytes, there was a statistically significant difference between thapsigargin and adenosine/600uM DNB co-treatment ($p<0.001$). There were no statistically significant differences between vehicle control and 600uM DNB neuronal intracellular calcium measurements.

In co-cultures exposed to 400uM DNB, there were no statistically significant differences between 400uM DNB, the vehicle control, adenosine, adenosine/400uM DNB co-treatment, or thapsigargin in neurons co-cultured with low passage DI-TNC_1 astrocytes (Figure 2.5). Intracellular calcium in both adenosine and adenosine/400uM DNB co-treatment were statistically significantly lower than thapsigargin ($p<0.01$) in neurons co-cultured with high passage DI-TNC_1 astrocytes. Again, there were no statistically significant differences between vehicle control and 400uM DNB neuronal intracellular calcium measurements.

Both high passage ($p<0.001$) and low passage ($p<0.05$) co-cultures exposed to 200uM DNB exhibited significantly lower intracellular calcium in neurons between 200uM DNB and thapsigargin, adenosine and thapsigargin, and adenosine/200uM DNB co-treatment and thapsigargin (Figure 2.6). Additionally, in neurons co-cultured with

high passage DI-TNC_1 astrocytes, the vehicle control was significantly lower than thapsigargin (Figure 2.6).

Neurons co-cultured with low passage DI-TNC_1 astrocytes exposed to 100uM DNB exhibited a significantly lower intracellular calcium concentration compared to thapsigargin ($p<0.05$), as did adenosine compared to thapsigargin ($p<0.05$) and the vehicle control compared to adenosine/100uM DNB co-treatment ($p<0.05$) (Figure 2.7). There were several significant differences in intracellular calcium concentration between exposures in neurons co-cultured with high passage DI-TNC_1 astrocytes: adenosine ($p<0.001$), vehicle control ($p<0.05$), and adenosine/100uM DNB co-treatment ($p<0.001$) were all lower than thapsigargin (Figure 2.7). Additionally, neurons co-cultured with high passage DI-TNC_1 astrocytes exposed to 100uM DNB showed a significantly higher intracellular calcium concentration than adenosine alone ($p<0.05$) or adenosine/100uM DNB co-treatment ($p<0.01$) (Figure 2.7).

The following exposures elicited significantly lower neuronal co-culture intracellular calcium concentrations compared to thapsigargin in low passage DI-TNC_1 astrocyte co-cultures: 50uM DNB ($p<0.001$), adenosine (0.01), and adenosine/50uM DNB co-treatment ($p<0.01$) were significantly lower than thapsigargin; whereas neuronal intracellular calcium in the vehicle control was significantly higher than adenosine ($p<0.05$), adenosine/DNB co-treatment ($p<0.05$), and 50uM DNB ($p<0.001$) (Figure 2.8, red asterisks). Neuronal intracellular calcium was significantly higher in thapsigargin treatment compared to 50uM DNB exposure ($p<0.05$), the vehicle control ($p<0.01$), adenosine ($p<0.001$), and adenosine/50uM DNB co-treatment ($p<0.001$) in high passage DI-TNC_1 astrocyte co-cultures (Figure 2.8).

Mitochondrial Membrane Potential in Co-Cultured Neurons Exposed to 600uM DNB

Mitochondrial membrane potential in co-cultured neurons was measured using the cationic carbocyanine dye JC-1. This experiment was performed to determine whether or not DNB exposure caused depolarization of neuronal mitochondria dependent on the passage number of the DI-TNC_1 astrocytes with which they were cultured. Neurons co-cultured with high passage DI-TNC_1 astrocytes exposed to 600uM DNB exhibit more depolarized mitochondria compared to their counterparts co-cultured with low passage DI-TNC_1 astrocytes (Figure 2.9).

Viability of High Passage and Low Passage Co-Cultured DI-TNC_1 Astrocytes Exposed to DNB

To determine whether or not low passage DI-TNC_1 astrocytes are better able to survive DNB exposure than high passage DI-TNC_1 astrocytes while co-cultured with neurons, a trypan blue exclusion assay was performed to determine the cell viability of co-cultured DI-TNC_1 astrocytes . The total number of live cells was higher for both control and DNB-exposed high passage co-cultured DI-TNC_1 astrocytes compared to low passage (Figure 2.10). When normalized to the control, however, low passage DI-TNC_1 astrocytes exhibited relatively higher viability, of which no comparison was statistically significant. When the normalized live cell counts were pooled for each passage group, viability of high passage DI-TNC_1 astrocytes were statistically significantly lower than low passage DI-TNC_1 astrocytes.

ATP Measurements in Co-Cultured DI-TNC_1 Astrocytes Exposed to DNB

Because high passage DI-TNC_1 astrocytes are functionally different from low passage DI-TNC_1 astrocytes in that they are less able to protect neurons (Figures 2.4-

2.8), exhibit an unstable mitochondrial membrane potential (Figure 2.1), and exhibit decreased viability in co-culture in DNB exposure (Figure 2.10), an ATP assay was performed to determine whether or not high passage DI-TNC_1 astrocytes have lower ATP concentrations than low passage. A luminescence assay from PerkinElmer®, ATPLite™, was used to determine relative ATP levels between high and low passage cells. The ATPLite™ assay utilizes luciferin to catalyze an enzymatic reaction converting ATP, D-Luciferin, and O_2 to oxyluciferin, adenosine monophosphate, inorganic diphosphate, CO_2, and light. This light is measured by a luminometer; the amount of measured light correlates to the amount of ATP in the cells. At all concentrations of DNB (600uM, 400uM, 200uM, 100uM, and 50uM), measured ATP levels were lower for low passage co-cultured DI-TNC_1 astrocytes than high passage (Figure 2.11). However, there were no statistically significant differences between any of the DNB concentrations and controls.

DISCUSSION

The data demonstrate that in monoculture, mitochondria in high passage DI-TNC_1 astrocytes are more susceptible to DNB-induced alterations in mitochondrial morphology and mitochondrial membrane potential than low passage DI-TNC_1 astrocytes. Passage #-dependent susceptibility was determined to be dependent on both the concentration of DNB and length of exposure: the higher the concentration of DNB exposure, the earlier a mitochondrial first flickering event would occur concurrently

with a decrease in aspect ratio. At each concentration of DNB, the higher the passage number, the earlier mitochondria had exhibited a first flickering event and concurrent morphological change.

Existing literature shows evidence supporting the relationship between a decrease in mitochondrial membrane potential and change in mitochondrial shape, and a related decrease in mitochondrial function (15). This evidence, combined with novel data put forth in this chapter showing that high passage DI-TNC_1 astrocytes co-cultured with neurons are less likely to survive DNB exposure than low passage DI-TNC_1 astrocytes suggests that perturbations to mitochondria in monoculture DI-TNC_1 astrocytes correspond with a decrease in co-cultured DI-TNC_1 astrocyte viability. It is possible that the onset of the first flickering event is an early indicator of DNB-induced metabolic stress in monoculture DI-TNC_1 astrocytes, which is likely exacerbated when DI-TNC_1 astrocytes are in a co-culture system. A novel aspect of this research is that the relationship between mitochondrial membrane potential, mitochondrial aspect ratio and astrocyte viability is mediated by the passage number of the astrocytes themselves, suggesting that passage number may be an *in vitro* proxy for *in vivo* cellular age.

High passage DI-TNC_1 astrocytes showed attenuated proliferation compared to low passage DI-TNC_1 astrocytes. Additionally, low passage DI-TNC_1 astrocytes did not exhibit deviations from proliferation rates when exposed to 600uM DNB. In high passage DI-TNC_1 astrocytes exposed to 600uM DNB, however, proliferation rates decreased. Because cellular proliferation is an “energy-expensive” process and requires functional mitochondria, this could indicate one or more of the following regarding mitochondria in high passage DI-TNC_1 astrocytes compared to their lower

passage counterparts: 1) that there are fewer mitochondria overall, 2) that they contain the same number of mitochondria (or more), but there are fewer *functional* mitochondria in high passage DI-TNC_1 astrocytes, or 3) that there are fewer mitochondria overall, and that they are less functional than in low passage DI-TNC_1 astrocytes. It is most likely the second is true, as it has been shown that mitochondrial DNA (mtDNA) copy number increases with age in rodent brain (16) (indicating more mitochondria overall), mitochondrial enzyme activity decreases in the aging brain (17), and mtDNA mutations (18) and oxidative mtDNA damage increase (19). However, measures of mtDNA (copy number, mutations, and oxidative damage) and enzyme activity in different regions of the brain are not necessarily reflective of what is occurring between and within cell types in those regions, and is likely differential between neurons and astrocytes.

Both high and low passage DI-TNC_1 astrocytes prevented depolarization (as measured by monitoring intracellular Ca^{2+} after KCl addition) in co-cultured neurons when exposed to 600uM or 400uM DNB. However, in co-culture, high passage DI-TNC_1 astrocytes exposed to high concentrations of DNB (600uM and 400uM) prevented depolarization of neurons when co-treated with adenosine and DNB together; this was not observed with low passage DI-TNC_1 astrocytes. It's possible that low passage DI-TNC_1 astrocytes had the ability to precondition the extracellular space with adenosine endogenously, which resulted in no significant differences in depolarization in low passage co-cultured DI-TNC_1 astrocytes when exposed to both adenosine and the highest concentrations of DNB used (600uM and 400uM).

Overall, neurons co-cultured with low passage co-cultured DI-TNC_1 astrocytes exhibited a more pronounced decrease in intracellular neuronal Ca^{2+} when exposed to

DNB, suggesting that low passage DI-TNC_1 astrocytes are better equipped to perform neuroprotective functions than high passage DI-TNC_1 astrocytes. This supposition is bolstered by data shown in this chapter in which DNB exposure causes increased mitochondrial depolarization in neurons co-cultured with high passage DI-TNC_1 astrocytes compared to neurons co-cultured with low passage DI-TNC_1 astrocytes.

ATP has been shown to be a major signaling molecule released from astrocytes into the extracellular environment, stimulated by glutamate (3), high potassium concentrations (20), and other stimuli. In this study, ATP concentrations were higher in high passage DI-TNC_1 co-cultured astrocytes than in low passage astrocytes, which wasn't expected. This could, however, be explained partially by the fact that the astrocytes required trypsinization and subsequent resuspension in media to release them from the co-culture device to be analyzed for ATP concentrations in a separate 96-well plate. Because the astrocytes were removed from the original co-culture media (in which there was the opportunity for crosstalk with neurons and the necessary neurotransmitters and extracellular metabolites), the replacement of the experimental media with fresh media would not have allowed for measurement of extracellular ATP that may have been secreted by the astrocytes in response to DNB exposure. Therefore, the data from this chapter may be reflective of only intracellular ATP stores.

This data suggests that low passage co-cultured DI-TNC_1 astrocytes may be continually shuttling ATP into the extracellular space in response to futile redox cycling of DNB, where it can be catabolized further into adenosine (21). Additionally, it has previously been shown that the addition of extracellular ATP to astrocyte/neuron co-cultures results in resistance to oxidative injury as robust in primary astrocytes from old

mice as in young mice (22). Because low passage DI-TNC_1 astrocytes were better able to survive DNB exposure when co-cultured with neurons, the data also suggests that low passage DI-TNC_1 astrocytes contain mitochondria that are able to expend ATP to the extracellular environment while maintaining higher overall viability in contrast with co-cultured high passage DI-TNC_1 astrocytes.

In summary, this study provides novel evidence of increased passage number as a surrogate for age in immortalized DI-TNC_1 astrocyte mono- and co-culture. Mitochondria in high passage DI-TNC_1 astrocytes demonstrated an increased susceptibility to DNB exposure compared to low passage, which ultimately correlated with a decrease in their function in co-culture with neurons. Future studies will need to elucidate possible polymorphic phenotypic differences between high and low passage DI-TNC_1 astrocytes that may define the functional differences observed in this study.

ACKNOWLEDGEMENTS

This research was supported by the NIH (2R01 ES08846) and the NIEHS (2T32 ES007062). We would like to thank Jackelyn Latham, Rory Landis, Ian Speirs, Dr. Nichole Hein, and Jennifer Fernandez for their assistance on this project.

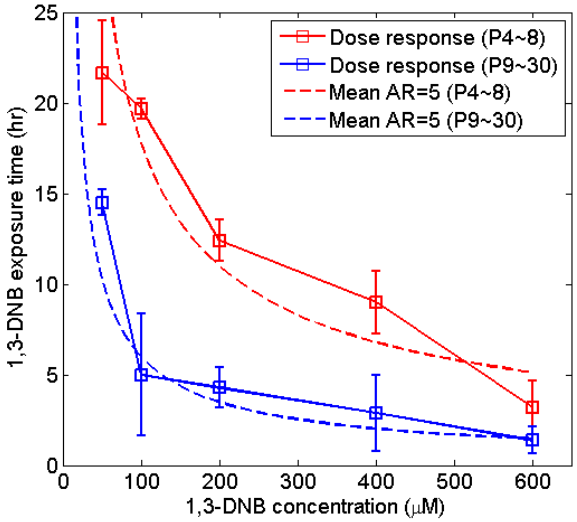

Figure 2.1. Mitochondrial Aspect Ratio and Time to First Mitochondrial Flickering Decrease as a Function of Passage Number in Immortalized Astrocytes Exposed to DNB Low Passage # (Passage 4 through Passage 8; "P4~P8") and High Passage # (Passage 9 through Passage 30; "P9~P30") immortalized astrocytes exposed to varying concentrations of DNB. Solid blue and red lines show trends for time in hours to first mitochondrial flickering event; all β values were statistically significant ($p<0.05$) for first mitochondrial flickering trends. Dashed blue and red lines show trends for mean aspect ratio (AR). Dashed blue and red lines show mean aspect ratio (AR) =5 predicted from following regression model: mean aspect ratio = $\beta_0 + \beta_1 \log(\text{DNB Concentration}) + \beta_2 \log(\text{Exposure time})$; All β values were statistically significant ($p<0.05$) for AR trends.

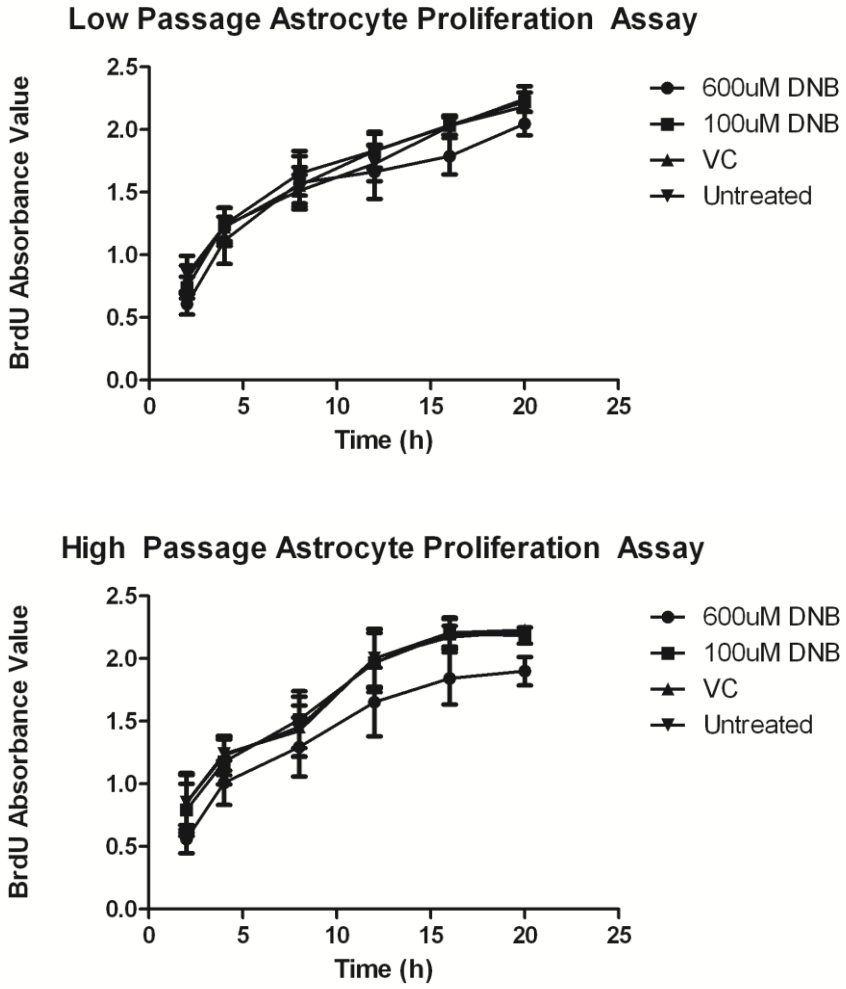

Figure 2.2. Proliferation Rates in High Passage and Low Passage Immortalized Astrocytes
Bromodeoxyuridine incorporation ELISA measured in LP (P4-P8) and HP (P19-P26) monoculture immortalized astrocytes exposed to either 100uM or 600uM or v/v equivalent of DMSO as a vehicle control (VC). Untreated cell proliferation was also assessed.

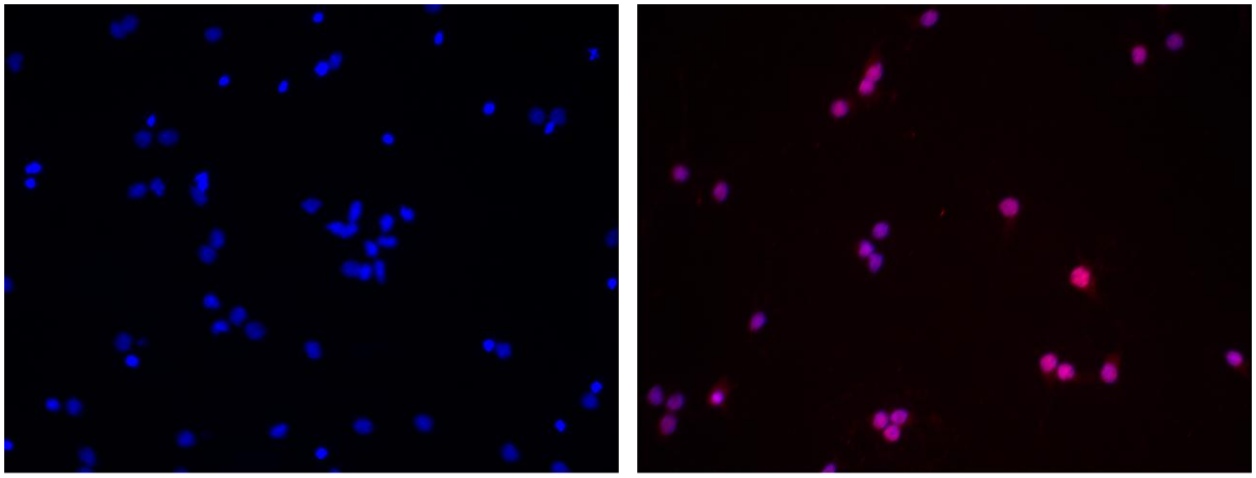

Figure 2.3. Immunocytochemistry on Primary Neurons for Cell Identification
Rat E18 cortical neurons were cultured on glass coverslips for 5-7 days and used for co-culture experiments with astrocytes. Neurons were fixed with 4% paraformaldehyde and incubated with DAPI alone as a negative control (left panel) or with DAPI, anti-glial fibrillary acidic protein (GFAP) conjugated with Alexafluor-488 to identify astrocytes (green), and anti-neuronal nuclei (NeuN) conjugated with Alexafluor-555 to identify neurons (red). Average % neurons across all cultures for co-culture experiments = 81% (n=10).

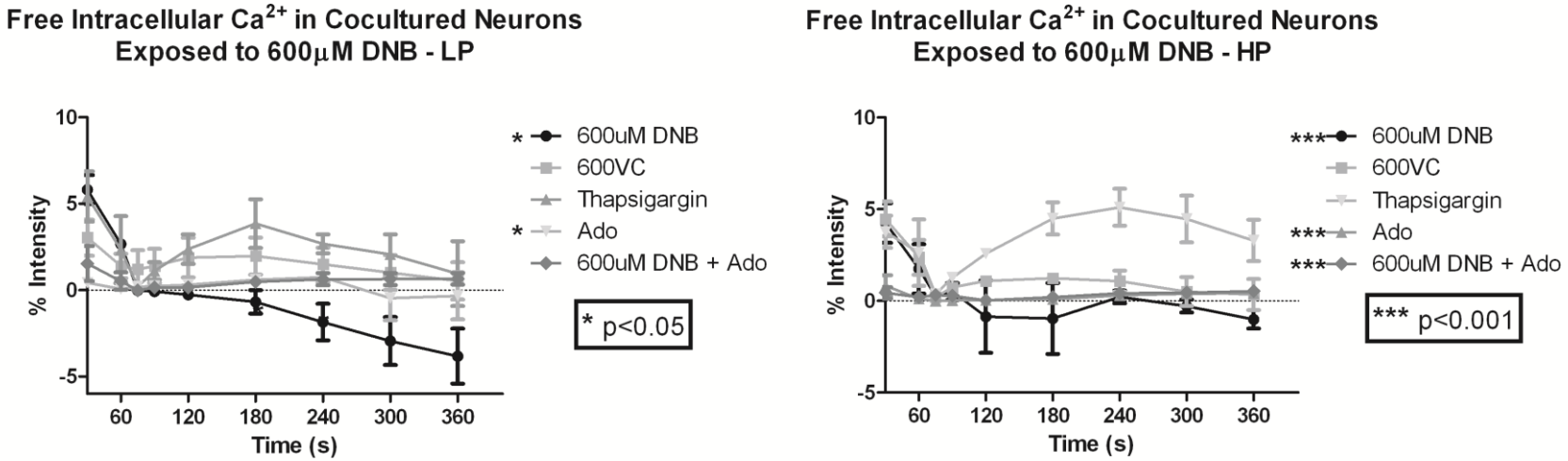

Figure 2.4. Free Intracellular Calcium Concentrations in Neurons Co-cultured with Low Passage or High Passage Immortalized Astrocytes Exposed to 600uM DNB

Low passage immortalized astrocytes (Left panel) and High Passage (Right Panel) were co-cultured with primary cortical neurons and exposed to 600uM DNB or the equivalent v/v amount of DMSO. Fluo-4 AM fluorescent dye was added to neurons to measure free intracellular Ca^{2+} concentrations. Sixty images were taken at 1s intervals prior to the addition of KCl; 300 images were taken at 1s intervals following KCl addition. The average fluorescence intensity of the field of view for each time point was calculated as a percent of the minimum average fluorescence induced by KCl addition. For comparisons across the entire time course of the experiment, a 1-way ANOVA with Tukey's Multiple Comparison Test was performed; *asterisks denoting a statistically significant difference between an exposure and thapsigargin are indicated in the legend next to the exposure that was significantly different from thapsigargin.*

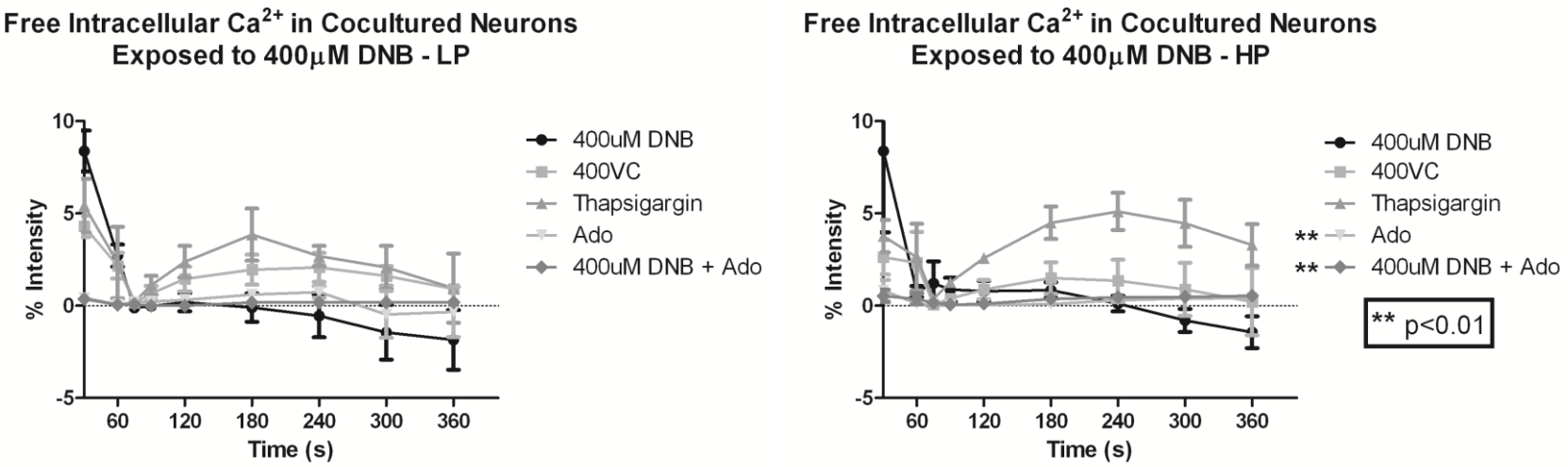

Figure 2.5. Free Intracellular Calcium Concentrations in Neurons Co-cultured with Low Passage or High Passage Immortalized Astrocytes Exposed to 400uM DNB

Low passage immortalized astrocytes (Left panel) and High Passage (Right Panel) were co-cultured with primary cortical neurons and exposed to 400uM DNB or the equivalent v/v amount of DMSO. Fluo-4 AM fluorescent dye was added to neurons to measure free intracellular Ca^{2+} concentrations. Sixty images were taken at 1s intervals prior to the addition of KCl; 300 images were taken at 1s intervals following KCl addition. The average fluorescence intensity of the field of view for each time point was calculated as a percent of the minimum average fluorescence induced by KCl addition. For comparisons across the entire time course of the experiment, a 1-way ANOVA with Tukey's Multiple Comparison Test was performed; *asterisks denoting a statistically significant difference between an exposure and thapsigargin are indicated in the legend next to the exposure that was significantly different from thapsigargin.*

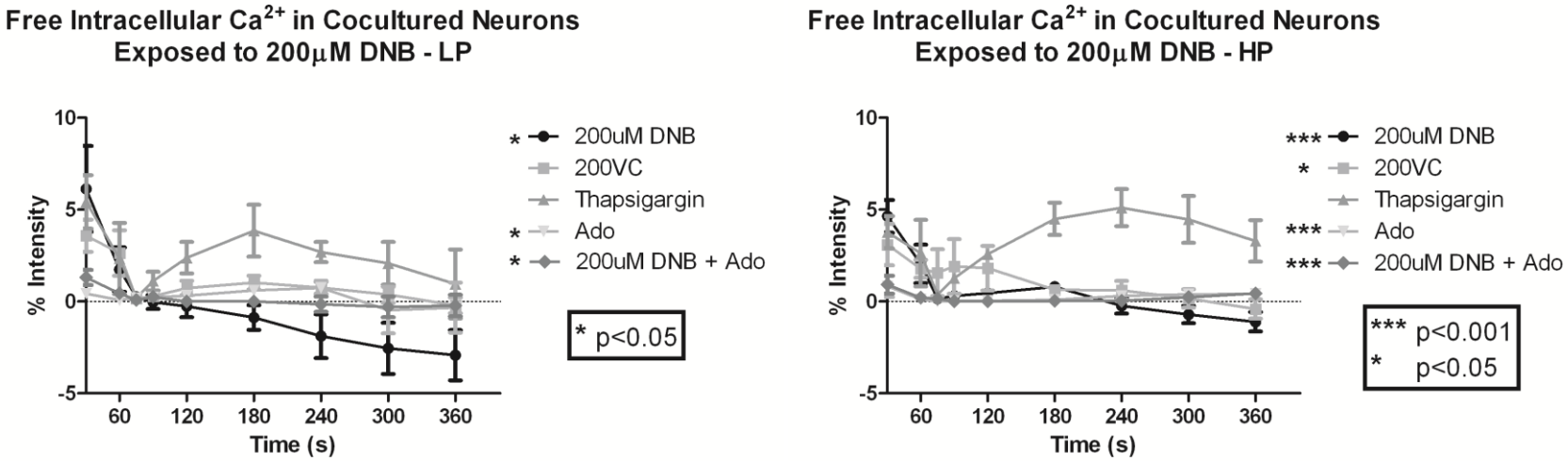

Figure 2.6. Free Intracellular Calcium Concentrations in Neurons Co-cultured with Low Passage or High Passage Immortalized Astrocytes Exposed to 200uM DNB

Low passage immortalized astrocytes (Left panel) and High Passage (Right Panel) were co-cultured with primary cortical neurons and exposed to 200uM DNB or the equivalent v/v amount of DMSO. Fluo-4 AM fluorescent dye was added to neurons to measure free intracellular Ca^{2+} concentrations. Sixty images were taken at 1s intervals prior to the addition of KCl; 300 images were taken at 1s intervals following KCl addition. The average fluorescence intensity of the field of view for each time point was calculated as a percent of the minimum average fluorescence induced by KCl addition. For comparisons across the entire time course of the experiment, a 1-way ANOVA with Tukey's Multiple Comparison Test was performed; *asterisks denoting a statistically significant difference between an exposure and thapsigargin are indicated in the legend next to the exposure that was significantly different from thapsigargin.*

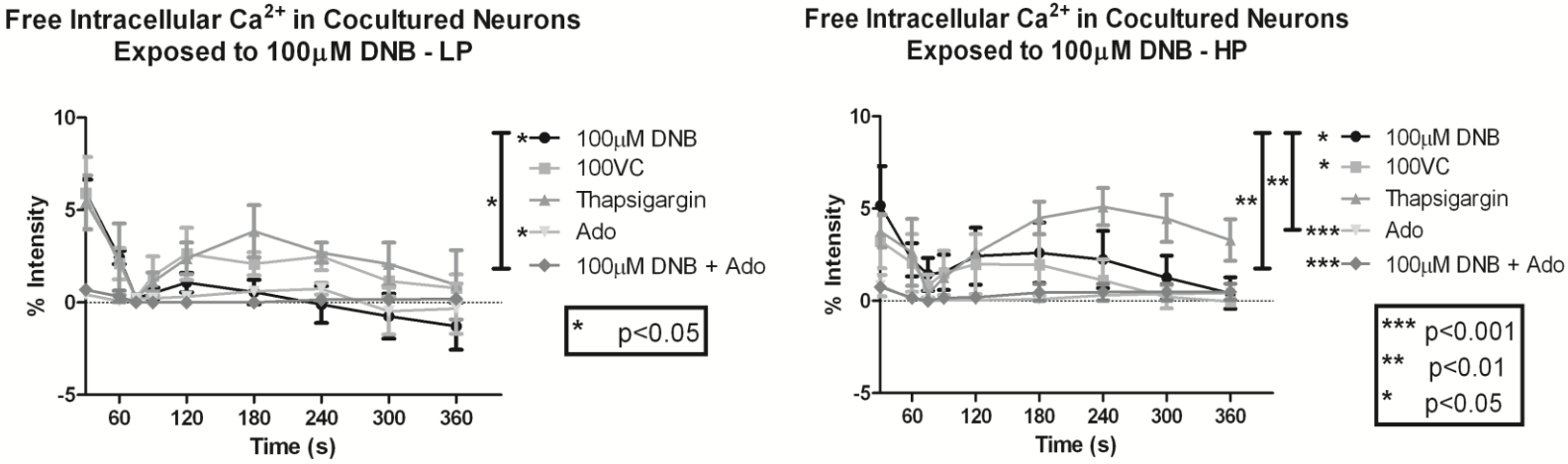

Figure 2.7. Free Intracellular Calcium Concentrations in Neurons Co-cultured with Low Passage or High Passage Immortalized Astrocytes Exposed to <u>100uM DNB</u>

Low passage immortalized astrocytes (Left panel) and High Passage (Right Panel) were co-cultured with primary cortical neurons and exposed to 100uM DNB or the equivalent v/v amount of DMSO. Fluo-4 AM fluorescent dye was added to neurons to measure free intracellular Ca^{2+} concentrations. Images were taken at 1s intervals prior to the addition of KCl; 300 images were taken at 1s intervals following KCl addition. The average fluorescence intensity of the field of view for each time point was calculated as a percent of the minimum average fluorescence induced by KCl addition. For comparisons across the entire time course of the experiment, a 1-way ANOVA with Tukey's Multiple Comparison Test was performed; *asterisks denoting a statistically significant difference between an exposure and thapsigargin are indicated in the legend next to the exposure that was significantly different from thapsigargin. Statistically significant differences between 100uM DNB and other exposures are denoted by a bar between 100uM DNB and that exposure (level of significance denoted in legend).*

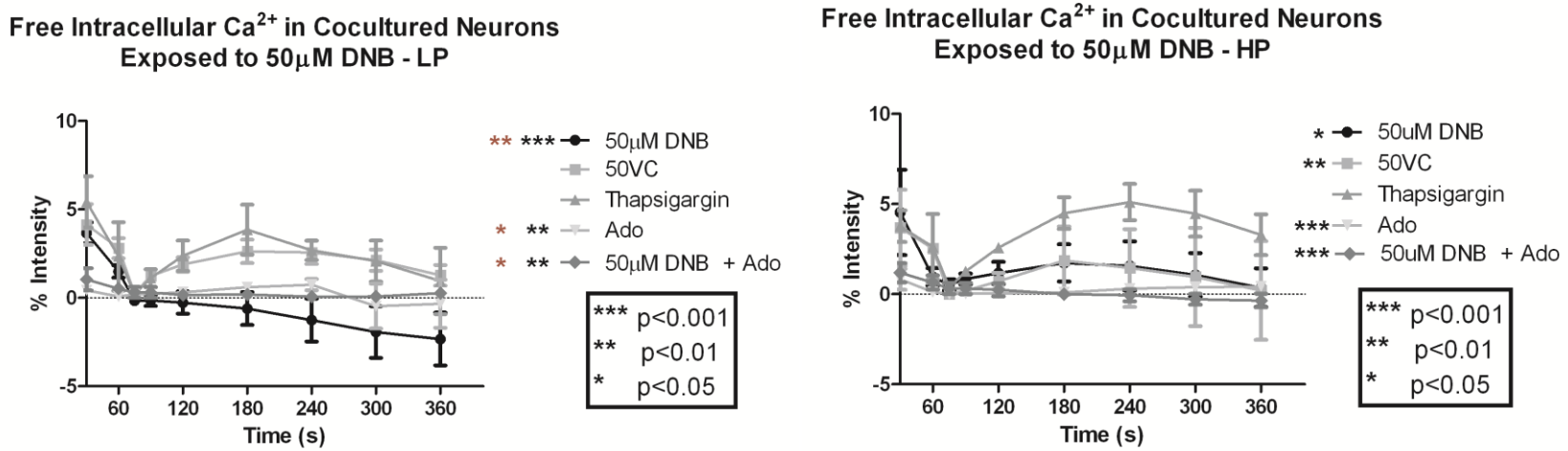

Figure 2.8. Free Intracellular Calcium Concentrations in Neurons Co-cultured with Low Passage or High Passage Immortalized Astrocytes Exposed to 50uM DNB

Low passage immortalized astrocytes (Left panel) and High Passage (Right Panel) were co-cultured with primary cortical neurons and exposed to 50uM DNB or the equivalent v/v amount of DMSO. Fluo-4 AM fluorescent dye was added to neurons to measure free intracellular Ca^{2+} concentrations. Sixty images were taken at 1s intervals prior to the addition of KCl; 300 images were taken at 1s intervals following KCl addition. The average fluorescence intensity of the field of view for each time point was calculated as a percent of the minimum average fluorescence induced by KCl addition. For comparisons across the entire time course of the experiment, a 1-way ANOVA with Tukey's Multiple Comparison Test was performed; *asterisks denoting a statistically significant difference between an exposure and thapsigargin are indicated in the legend next to the exposure that was significantly different from thapsigargin (black asterisks); red asterisks denote a significant difference between the vehicle control and the denoted exposure.*

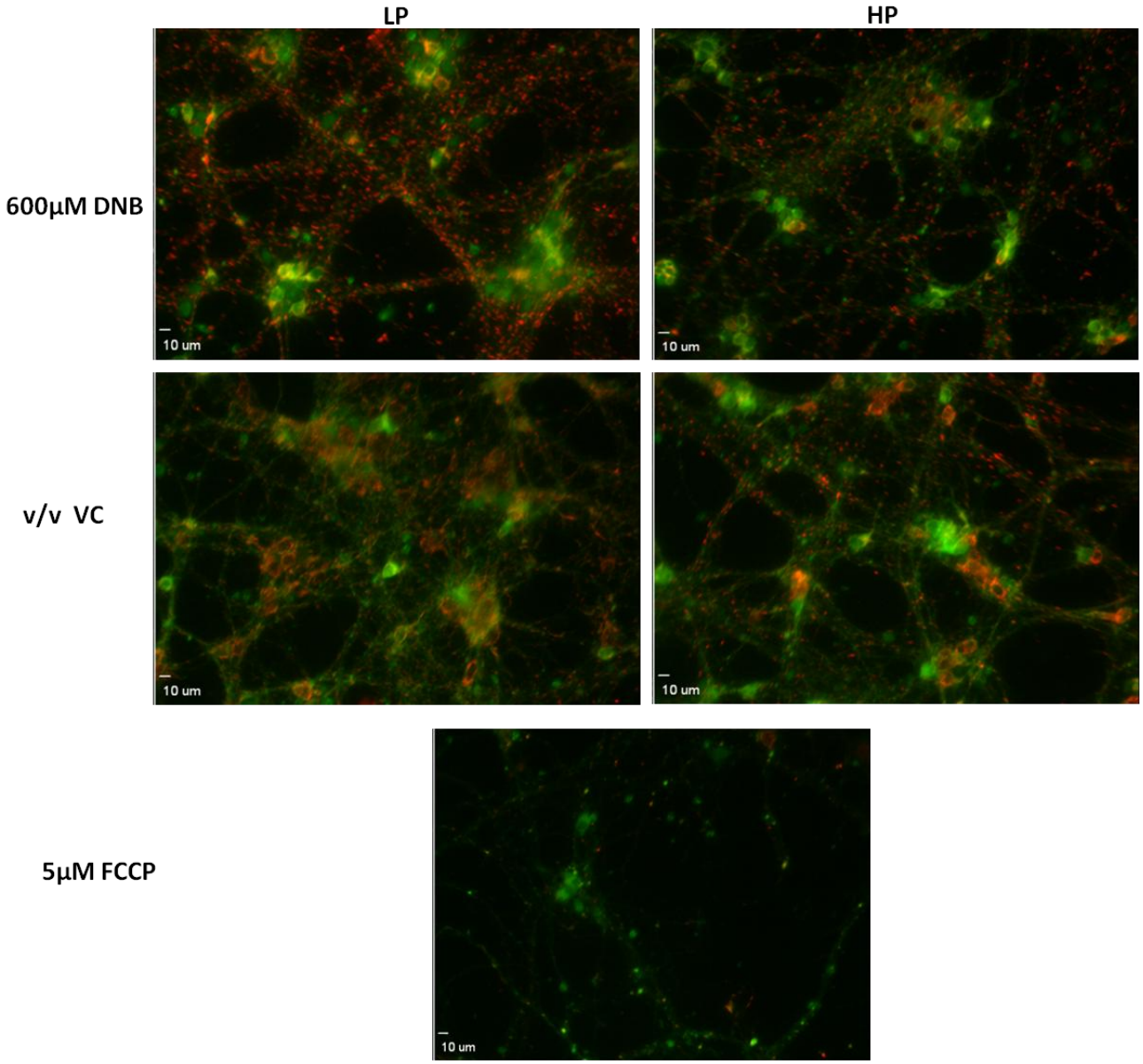

Figure 2.9. Mitochondrial Membrane Potential in Co-cultured Neurons Exposed to 600uM DNB
Low passage (LP = P4-6; left panels) and high passage (HP = P24-28; right panels) immortalized astrocytes were co-cultured with primary cortical neurons and exposed to 600uM DNB (top panel), the v/v equivalent of DMSO as a vehicle control (VC – middle panel), or 5uM FCCP (bottom panel). Neurons were incubated with JC-1, a cationic carbanocyanine dye that accumulates in mitochondria. JC-1 forms aggregates in mitochondria with intact membrane potential (red) and in depolarized mitochondria remains in the monomeric form (green).
LP = Low Passage; HP = High Passage; VC = v/v DMSO vehicle control

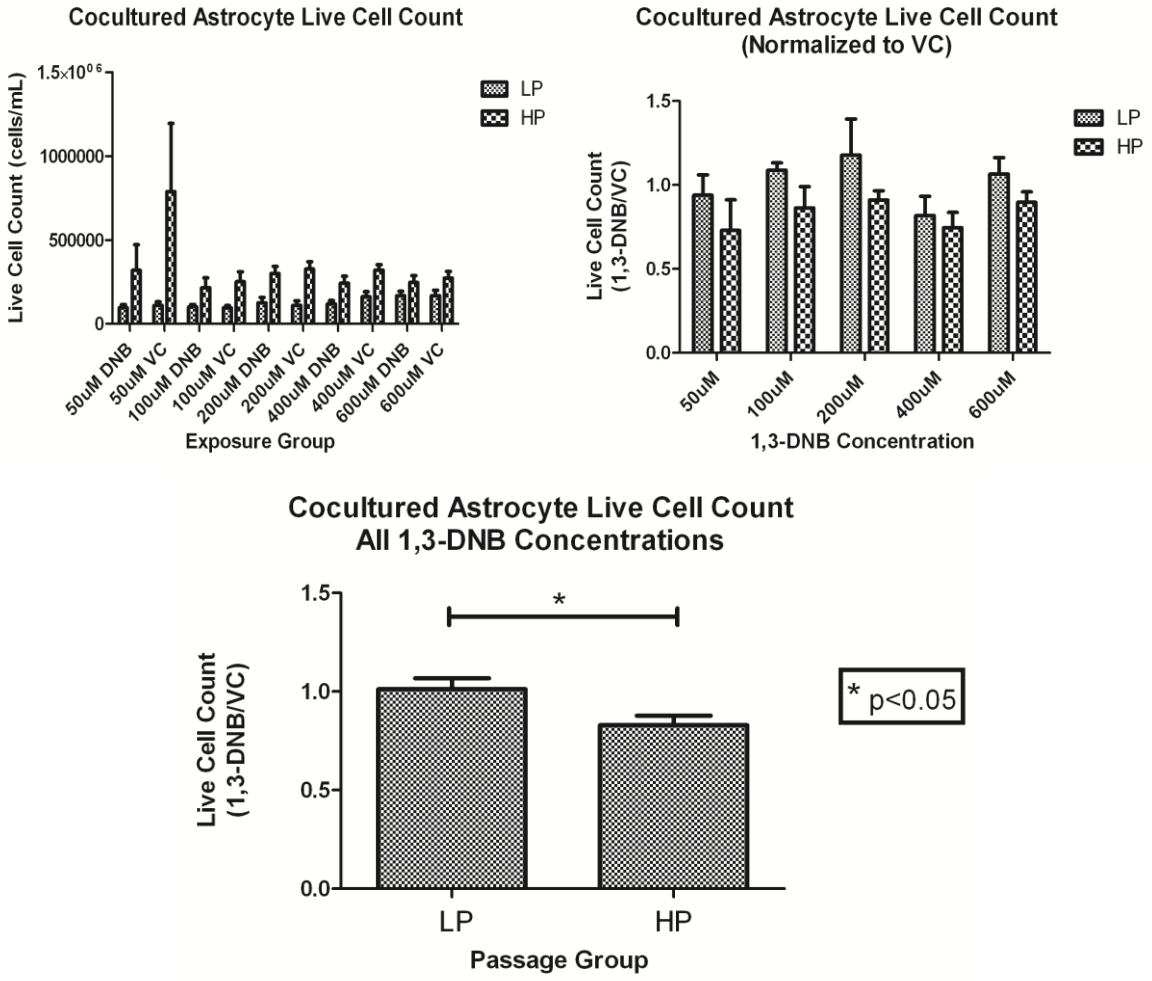

Figure 2.10. Viability of Co-cultured Immortalized Astrocytes by DNB Concentration and Passage Number

Low passage (P4-6) and high passage (P24-28) immortalized astrocytes were co-cultured with primary cortical neurons and exposed to DNB (50-600uM) or the equivalent v/v amount of DMSO. Immortalized astrocytes were trypsinized and then subsequently counted using the Countess® cell counter by trypan blue exclusion assay. Raw live cell counts are shown (Top Left). Live cell counts for DNB exposed immortalized astrocytes were then normalized to the vehicle control live cell count. Individual values of normalized live cell counts for stratified by DNB concentration (Top Right) and pooled live cell counts stratified by passage number (Bottom Center; data were uploaded to Prism software (Version 5.0, GraphPad) for statistical analysis (student's t-test).

LP = Low Passage; HP = High Passage; VC = v/v DMSO vehicle control

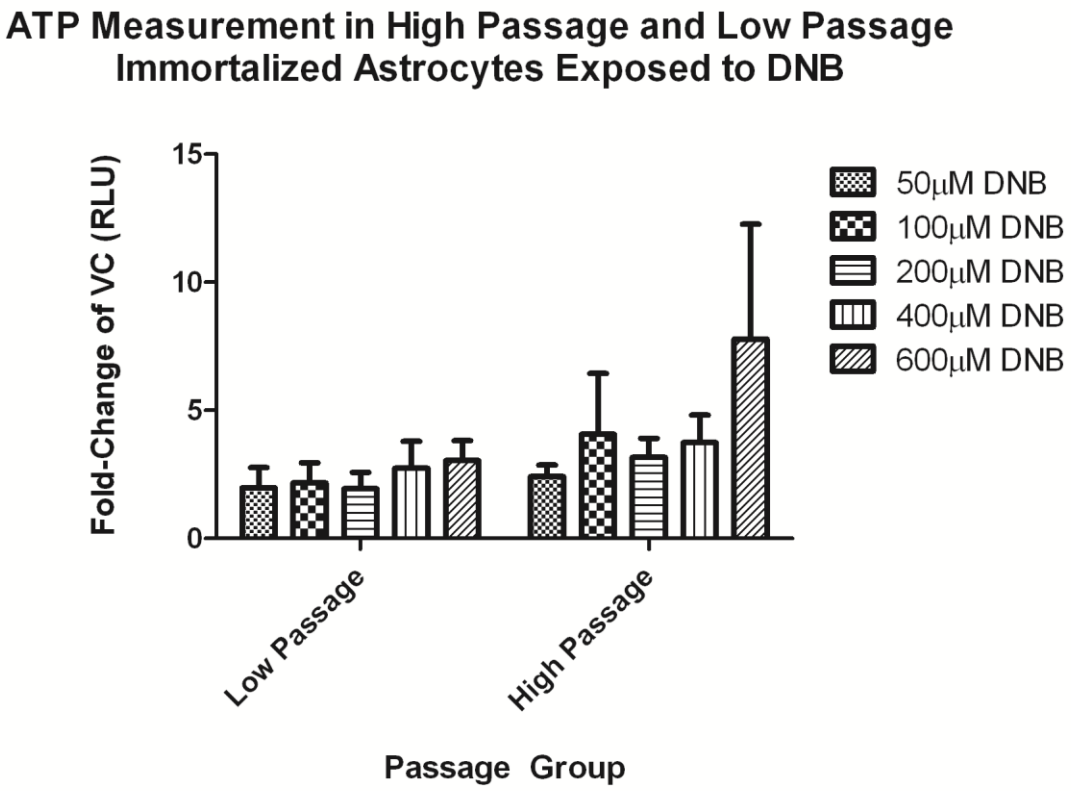

Figure 2.11. ATP Measurements in Co-cultured Immortalized Astrocytes Exposed to DNB
Low passage (P4-5) and high passage (P24-25) immortalized astrocytes were co-cultured with primary cortical neurons and exposed to DNB (50-600uM) or the equivalent v/v amount of DMSO. Astrocytes were then removed from the co-culture system, and ATP levels were measured using the PerkinElmer® ATPLite™ kit; manufacturer's protocol was followed. Data were uploaded to Prism software (Version 5.0, GraphPad) for statistical analysis (one-way ANOVA with Tukey's Test for Multiple Comparisons).
VC = v/v DMSO vehicle control

REFERENCES

1. Boumezbeur F, Mason GF, de Graaf RA, Behar KL, Cline GW, Shulman GI, et al. Altered brain mitochondrial metabolism in healthy aging as assessed by in vivo magnetic resonance spectroscopy. J Cereb Blood Flow Metab. 2010;30(1):211-21. PMCID: 2949111.

2. Rosenberg PA, Aizenman E. Hundred-fold increase in neuronal vulnerability to glutamate toxicity in astrocyte-poor cultures of rat cerebral cortex. Neurosci Lett. 1989;103(2):162-8.

3. Queiroz G, Gebicke-Haerter PJ, Schobert A, Starke K, von Kugelgen I. Release of ATP from cultured rat astrocytes elicited by glutamate receptor activation. Neuroscience. 1997;78(4):1203-8.

4. Voloboueva LA, Suh SW, Swanson RA, Giffard RG. Inhibition of mitochondrial function in astrocytes: implications for neuroprotection. J Neurochem. 2007;102(4):1383-94. PMCID: 3175820.

5. Philbert MA, Nolan CC, Cremer JE, Tucker D, Brown AW. 1,3-Dinitrobenzene-induced encephalopathy in rats. Neuropathol Appl Neurobiol. 1987;13(5):371-89.

6. Steiner SR, Philbert MA. Proteomic identification of carbonylated proteins in 1,3-dinitrobenzene neurotoxicity. Neurotoxicology. 2011;32(4):362-73. PMCID: 3158615.

7. Tjalkens RB, Ewing MM, Philbert MA. Differential cellular regulation of the mitochondrial permeability transition in an in vitro model of 1,3-dinitrobenzene-induced encephalopathy. Brain Res. 2000;874(2):165-77.

8. Miller JA, Runkle SA, Tjalkens RB, Philbert MA. 1,3-Dinitrobenzene-induced metabolic impairment through selective inactivation of the pyruvate dehydrogenase complex. Toxicol Sci. 2011;122(2):502-11. PMCID: 3155080.

9. Phelka AD, Beck MJ, Philbert MA. 1,3-Dinitrobenzene inhibits mitochondrial complex II in rat and mouse brainstem and cortical astrocytes. Neurotoxicology. 2003;24(3):403-15.

10. Phelka AD, Sadoff MM, Martin BP, Philbert MA. BCL-XL expression levels influence differential regional astrocytic susceptibility to 1,3-dinitrobenzene. Neurotoxicology. 2006;27(2):192-200.

11. Lian XY, Stringer JL. Astrocytes contribute to regulation of extracellular calcium and potassium in the rat cerebral cortex during spreading depression. Brain Res. 2004;1012(1-2):177-84.

12. Wang Y, Liu X, Schneider B, Zverina EA, Russ K, Wijeyesakere SJ, et al. Mixed inhibition of adenosine deaminase activity by 1,3-dinitrobenzene: a model for understanding cell-selective neurotoxicity in chemically-induced energy deprivation syndromes in brain. Toxicol Sci. 2012;125(2):509-21. PMCID: 3262860.

13. Rogers TB, Inesi G, Wade R, Lederer WJ. Use of thapsigargin to study Ca2+ homeostasis in cardiac cells. Biosci Rep. 1995;15(5):341-9.

14. Deckert J, Gleiter CH. Adenosine--an endogenous neuroprotective metabolite and neuromodulator. J Neural Transm Suppl. 1994;43:23-31.

15. Galloway CA, Lee H, Nejjar S, Jhun BS, Yu T, Hsu W, et al. Transgenic control of mitochondrial fission induces mitochondrial uncoupling and relieves diabetic oxidative stress. Diabetes. 2012;61(8):2093-104. PMCID: 3402299.

16. Gadaleta MN, Rainaldi G, Lezza AM, Milella F, Fracasso F, Cantatore P. Mitochondrial DNA copy number and mitochondrial DNA deletion in adult and senescent rats. Mutat Res. 1992;275(3-6):181-93.

17. Leong SF, Lai JC, Lim L, Clark JB. Energy-metabolizing enzymes in brain regions of adult and aging rats. J Neurochem. 1981;37(6):1548-56.

18. Corral-Debrinski M, Horton T, Lott MT, Shoffner JM, Beal MF, Wallace DC. Mitochondrial DNA deletions in human brain: regional variability and increase with advanced age. Nat Genet. 1992;2(4):324-9.

19. Mecocci P, MacGarvey U, Kaufman AE, Koontz D, Shoffner JM, Wallace DC, et al. Oxidative damage to mitochondrial DNA shows marked age-dependent increases in human brain. Ann Neurol. 1993;34(4):609-16.

20. Xu J, Song D, Bai Q, Zhou L, Cai L, Hertz L, et al. Role of glycogenolysis in stimulation of ATP release from cultured mouse astrocytes by transmitters and high K+ concentrations. ASN Neuro. 2014;6(1). PMCID: 3891497.

21. Wink MR, Lenz G, Braganhol E, Tamajusuku AS, Schwartsmann G, Sarkis JJ, et al. Altered extracellular ATP, ADP and AMP catabolism in glioma cell lines. Cancer Lett. 2003;198(2):211-8.

22. Wu J, Holstein JD, Upadhyay G, Lin DT, Conway S, Muller E, et al. Purinergic receptor-stimulated IP3-mediated Ca2+ release enhances neuroprotection by increasing astrocyte mitochondrial metabolism during aging. J Neurosci. 2007;27(24):6510-20.

CHAPTER III

Determine Whether or not the Degree of DNB-Induced Oxidation of Mitochondria-Related Proteins in Susceptible Brainstem Regions is Dependent on Age

INTRODUCTION

The free radical theory of aging, first put forth nearly sixty years ago, postulated that the aging process was related to the accumulation of oxidative damage to macromolecules (1). During the physiological aging process, the brain accumulates oxidative damage [reviewed by Halliwell (2)]. However, the amount of accumulated oxidative modifications to macromolecules varies by region, including age-associated increases in lipid peroxidation in cerebral hemisphere, cerebellum, and to a lesser extent, in brainstem compared to younger rats (3), increased formation of DNA adducts in substantia nigra of aged rats compared to younger rats (4), and increased protein oxidation in brainstem (5). The mitochondrion is particularly susceptible to oxidative damage, as the mitochondrion itself produces reactive oxygen species (6), (7), (8), and antioxidant concentrations decrease in brain mitochondria over time (9), (10). Additionally, there is age-dependent, regional variation in antioxidant levels in rodent brain (11) and human brain (12), (13). This evidence suggests that mitochondrial macromolecules within specific regions of the brain may be especially prone to oxidation over time.

The mitochondrial proteome in the brain accrues oxidative modifications during aging (9). Accumulation of posttranslational modifications can lead to alterations in protein function in mitochondria, some of which may be dysfunctional. Exposure to 1,3-Dinitrobenzene (DNB) in rodents results in bilaterally symmetrical spongiform lesions (14). Due in part to its ability to undergo futile redox cycling during metabolism (15), DNB has been shown to cause oxidative stress typically localized to the brainstem, where lesions are evident, including increased carbonylation in brainstem mitochondria (Dr. Stephen Steiner, unpublished data) and increased carbonylation in astrocyte mitochondria (16). Because oxidation that accrues during aging in the brain is highly region-specific and DNB selectively targets the brainstem, this study's hypothesis is that age will exacerbate mitochondrial susceptibility to DNB-induced protein oxidation in the brainstem.

Exposure to environmental neurotoxicants has been shown to cause age-dependent, regional variation in elevated oxidative stress (as noted in rodent exposure to toluene (17). However, there is very little evidence of age-related increases in *mitochondria-specific,* region-specific oxidative accumulation in response to neurotoxicant exposure. This study uses a high-throughput proteomic approach to provide novel evidence of DNB-induced mitochondrial proteome oxidation localized to brainstem mitochondria; advanced age of the animal exacerbates the extent and specific peptide loci of the mitochondrial proteome oxidation.

MATERIALS AND METHODS

Animals

Male F344 rats (1 month old, 3 month old, and 18 month old) were purchased from Harlan Laboratories and housed according to University of Michigan's University Committee on Use and Care of Animals policies. Rats were fed and watered ad libitum and housed on a 12-hour light/dark cycle.

Histology

Rats from each age group were either exposed to 10mg/kg DNB or a v/v equivalent of dimethylsulfoxide (DMSO) serving as a vehicle control (at 0h, 4h, and 24h; sacrifice occurred 12h after the 24h dose). Rats were anesthetized with isoflurane, followed by opening of the abdominal and thoracic cavity via lateral incisions. The diaphragm was cut away from the heart and lungs. Normal saline was perfused by insertion of a butterfly needle to the left ventricle, followed by an incision to the right atrium. Once the blood was cleared (approximately 7-11 minutes), the rat was perfusion fixed with 4% paraformaldehyde (PFA) (approximately 8 minutes). Directly after perfusion fixation, the rat was decapitated via guillotine. The brain was then carefully removed from the skull and placed in 4% PFA overnight prior to paraffin embedding. Embedding, hematoxylin/eosin staining, and sectioning were performed at the ULAM Pathology Core for Animal Research (University of Michigan, Ann Arbor).

Mitochondrial Isolation

Rats from each age group were either exposed to 10mg/kg DNB or a v/v equivalent of dimethylsulfoxide (DMSO) serving as a vehicle control (at 0h, 4h, and 24h; sacrifice occurred 24h after the 24h dose). Mitochondria were isolated according to the protocol (Method C) by Sims & Anderson (18), with minor modifications. Briefly, the rat was anesthetized under isoflurane, decapitated with a small animal guillotine, and the brain was rapidly removed. Brainstem and cortex were dissected from the rest of the brain in cold isolation buffer (100mM Tris, 10mM potassium-EDTA, 960mM sucrose, pH 7.4). Brainstem and cortex were then weighed and minced in cold isolation buffer. Minced tissue was then homogenized using a glass Dounce homogenizer on ice; this step was performed while being flushed with argon. Subsequent centrifugation steps followed. Prior to the Percoll gradient centrifugation step, digitonin was added to disrupt synaptosomal membranes. Mitochondria were stored at -80°C.

Detection and Identification of Mitochondria-Related Proteins and Oxidative Modification Sites (University of Michigan Peptide Synthesis and Proteomics Core and MSBioWorks, LLC, Ann Arbor, MI)

The volume of each submitted mitochondrial sample was reduced 50% and 20µL of the concentrated sample was processed by sodium dodecyl sulfate polyacrylamide gel electrophoresis (SDS-PAGE) on a 4-12% Bis-Tris Mini-gel (Invitrogen) using the MOPS buffer system and non-reducing Laemmli buffer. Each gel lane was excised into ten equal bands and these were processed by in-gel digestion using a robot (ProGest, DigiLab): bands were washed with 25mM ammonium bicarbonate followed by

acetonitrile, reduced with 10mM dithiothreitol at 60°C followed by alkylation with 50mM iodoacetamide at room temperature, digested with trypsin (Promega) for 4h at 37°C, and quenched with formic acid and the supernatant was analyzed directly without further processing. Samples were then analyzed by LC/MS/MS analyzed by nano LC/MS/MS with a Waters NanoAcquity high performance liquid chromatography (HPLC) system interfaced to a ThermoFisher Q Exactive mass spectrometer. Peptides were loaded on a trapping column and eluted over a 75µm analytical column at 350nL/min; both columns were packed with Jupiter Proteo resin (Phenomenex). The mass spectrometer was operated in data-dependent mode, with MS and MS/MS performed at 70,000 and 17,500 FWHM resolution, respectively. The fifteen most abundant ions were selected for MS/MS. Proteins were identified by reference to the UniProt rat database (forward and reverse appended with common contaminant proteins) using the Mascot search engine. Results were displayed in Scaffold software.

Pathway Analysis

UniProtID numbers for proteins <0.25-fold or >4.0-fold oxidized, as determined by %Oxidation (unweighted spectral count of oxidized protein/total unweighted spectral count), were uploaded to the Database for Annotation, Visualization, and Integrated Discovery (2). Pathways were identified by selecting Gene Ontology Term (GOTerm) Molecular Function. Options for pathway determination were set to: 3 proteins to constitute a pathway (default setting = 2), and 0.05 as a significance level for P-values and Benjamini values.

Immunohistochemical Detection of Protein Carbonylation in Brain Sections

The methods to detect protein carbonyls in fixed brain tissue were followed as described by Smerjac and Bizzozero (19). 1mo, 3mo, and 18mo rats were exposed to DNB (10mg/kg) or a v/v equivalent of DMSO as a vehicle control (i.p. injection) at 0h, 4h, and 24h; 12h after the 24h exposure, rats were anesthetized with isoflurane, followed by opening of the abdominal and thoracic cavity via lateral incisions. The diaphragm was cut away from the heart and lungs. Normal saline was perfused by insertion of a butterfly needle to the left ventricle, followed by an incision to the right atrium. Brains were removed and immersion-fixed in methacarn for approximately 2 hours followed by trimming, cassetting, and overnight immersion fixation in methacarn. Sections were then rinsed in methanol two times and 70% ethanol two times before tissue processing.

The methods to detect protein carbonyls in fixed brain tissue will be followed as described by Smerjac and Bizzozero (19). Briefly, carbonylation of proteins were detected by conversion of carbonyl groups into 2,4-dinitrophenyl hydrazones by incubation with 2,4-dinitrophenyl-hydrazine, followed by a rinse step and incubation with a primary antibody for 2,4-dinitrophenol and subsequently a horseradish peroxidase-labeled secondary antibody. Controls for this method include section incubation with iron hydroxide as a positive control or sodium borohydride as a negative control.

Statistical Analysis

Both global oxidation of MRPs (Figure 3.4) and regional oxidation (Figure 3.5) were shown as an average fold-change and compared using a Student's t-test, with $p<0.05$ considered statistically significant (Prism software, version 5.0, GraphPad).

RESULTS

Conditions and Mortality Rates of Male F344 Rats Sacrificed 24h after Last Exposure

All animals were monitored for clinical signs of intoxication throughout the exposure time course. In animals exposed at 0h, 4h, 24h with a 24h period after the last dose to sacrifice, the oldest rats (18mo) exhibited clinical signs of intoxication in DNB exposure including ataxia (100%) and chromodacryorrhea (100%); this group also exhibited a 60% mortality rate. No clinical signs were observed in the 1mo group, and only 25% of the 3mo DNB exposed animals were ataxic (Table 3.1).

Conditions and Mortality Rates of Male F344 Rats Sacrificed 12h after Last Exposure

In animals exposed at 0h, 4h, 24h with a 12h period after the last dose to sacrifice, the oldest rats (18mo) exhibited clinical signs of intoxication in DNB exposure including ataxia (100%) and chromodacryorrhea (100%); however, all of the animals survived the exposure duration. No clinical signs were observed in the 1mo or the 3mo animals (Table 3.2).

Deep Cerebellar Nuclei in 1mo, 3mo, 18mo Male F344 Rats Exposed to DNB

No lesions were found in deep cerebellar nuclei in 1mo (Figure 3.1.) or 3mo (Figure 3.2.) rats exposed to DNB. However, there was vacuolation of the neuropil in 18mo DNB exposed rats (Figure 3.3).

Effects of DNB on Global Oxidation of Mitochondria-Related Proteins (MRPs)

DNB had little to no effect on global oxidation of MRPs (Figure 3.4), suggesting that the degree of oxidation within individual regions of the brain may be more significant than the amount of MRP oxidation in the whole brain.

Effects of DNB on Regional MRP Oxidation

In young rats (1mo), DNB caused a reduction in oxidation (0.25-fold change) in only one MRP in brainstem (acetyl-CoA acetyltransferase, mitochondrial) and did not cause any changes in oxidation in any cortical MRPs (Table 3.3). DNB did not cause significant changes in MRP oxidation in brainstem or cortex of 3mo rats (Table 3.3). DNB caused the oxidation of 7 MRPs (>4.0-fold) in brainstem from 18mo animals, but none in cortex (Table 3.3).

Effects of Age on Regional MRP Oxidation

There were no differences in MRP oxidation observed in 3mo brainstem or cortex when compared to 1mo MRP oxidation; however, DNB caused the oxidation of 4 MRPs in cortex and 13 MRPs in brainstem (>4.0-fold) in 18mo animals compared to 1mo (Table 3.4).

Brainstem and Cortex MRP Oxidation

The degree to which DNB oxidizes MRPs is significantly higher in brainstem than in cortex (Figure 3.5.). With respect to MRPs oxidized >4.0-fold or greater, brainstem MRPs are approximately 3x more sensitive than cortical counterparts (Figure 3.5).

Pathways Significantly Oxidized by DNB in Brainstem

Five GOTerm Molecular Function pathways were significantly oxidized by DNB in brainstem (cation transmembrane transporter activity, nucleoside-triphosphatase activity, pyrophosphatase activity, hydrolase activity acting on acid anhydrides in phosphorous-containing anhydrides, and hydrolase activity acting on acid anhydrides). Four of the five identified pathways contain the same three proteins (cytoplasmic dynein 1 heavy chain 1, tubulin beta-2a chain, and plasma membrane calcium-transporting ATPase 2) (Table 3.5).

Age-Related Carbonylation in 1mo, 3mo, 18mo F344 Rats

In all 3 age groups, asymmetrical perinuclear staining in neurons was observed in deep cerebellar nuclei and vestibular nuclei (Figures 3.6, 3.7, 3.8) both in vehicle control and DNB exposed animals, but appears to become more pronounced in 18mo deep cerebellar nuclei (Figure 3.8). No lesions were found in deep cerebellar nuclei, vestibular nuclei, or cortex in 1mo (Figure 3.6.) or 3mo (Figure 3.7.) rats exposed to DNB. However, there was vacuolation of the neuropil in the deep cerebellar nuclei and vestibular nuclei in 18mo DNB exposed rats (Figure 3.8), but not in cortex.

DISCUSSION

There are likely multiple environmental exposures occurring over time that cause oxidative stress and contribute to a net increase in risk of developing adverse neurological outcomes during aging. This study gives evidence of increasing age exacerbating mitochondrial toxicity in the brainstem during exposure to an

environmental neurotoxicant, DNB. Exposure to DNB resulted in clinical signs of intoxication, which were most severe in the 18mo animals, and were consistent with previous findings involving DNB exposure and onset of ataxia (14). While it was previously reported that DNB exposure (10mg/kg i.p. injection) causes ataxia in rats, this study provides novel evidence of severity of clinical signs of intoxication being positively correlated with age: severe ataxia and onset of chromodacryorrhea were observed in the oldest group of animals exposed to DNB (18mo), whereas there were very few cases of ataxia in the 3mo animals (25% of exposed animals at most) and no instances of ataxia, or any other clinical signs of intoxication, in 1mo DNB-exposed animals. There is supporting evidence in the literature regarding increasing age and the increased likelihood of an environmental exposure causing adverse neurological outcomes: paraquat exposure and dopamine depletion in mice (20), cypermethrin exposure and dopaminergic neurodegeneration in rats (21), lead exposure and decreased dexterity in humans (22), and lead exposure and decreased brain volume in humans (23).

A key finding in this study is that areas of the brain affected by DNB exposure (deep cerebellar nuclei) are more susceptible to lesions in older animals than younger animals exposed to DNB. The development of vacuolated lesions in deep cerebellar nuclei in 18mo animals suggests that astrocyte foot processes are more susceptible to swelling in older animals (and is consistent with histopathological findings in previous studies on DNB exposure (14). Additionally, the development of DNB-induced lesions in 18mo animals (and not in younger DNB-exposed animals) correlates with the development of clinical signs of intoxication in DNB-exposed animals. This suggests

that the observed lesions are related to the pathophysiological mechanisms induced by DNB exposure (i.e.: an increase in reactive oxygen species (ROS)) that is likely causing the observed clinical signs of intoxication. This presumption is supported by the following evidence: astrocyte swelling is observed as a result of increased ROS and imbalances in osmotic pressure (24), and astrocyte swelling is observed in cases of ataxia caused by exposure to mycotoxin in rat (25) and megalencephalic leucoencephalopathy in humans (26).

This study provides a link between aging, regional specificity of lesions, clinical signs of DNB-induced intoxication, and specific patterns of mitochondria-related protein oxidation. Novel data put forth in this chapter gives evidence of two distinct, but potentially related concepts: that *brainstem MRPs* are more susceptible to oxidation than *cortical MRPs*, and that MRPs from mitochondria in *older* animals are more susceptible to oxidation by DNB than their *younger* counterparts. While DNB didn't cause an increase in global MRP oxidation, this suggests that specific regions of the brain (namely the brainstem) may be more susceptible to MRP oxidation than the whole brain, which may have been masked by an assessment of global MRP oxidation. This turned out to be true, as cortical MRPs showed no alterations in the degree of oxidation across age groups (zero MRPs were >4.0-fold or <0.25-fold oxidized, even in the 18mo animals exposed to DNB). However, brainstem MRPs were sensitive to DNB exposure as a function of age: in 1mo animals, one MRP was significantly less oxidized in brainstem (acetyl-CoA acetyltransferase, mitochondrial), which is active in ketone body metabolism by mitochondria (27). This suggests that significantly lower oxidation of this enzyme may contribute to the role of ketone metabolism in younger animals and may

be part of a protective mitochondrial mechanism in DNB exposure, as no lesions were observed in the youngest animals. Mitochondrial ketone body metabolism provides acetyl CoA from acetoacetyl CoA and allows for the production of energy while circumventing the need for pyruvate dehydrogenase (28); this may be important in the mitochondrial response to DNB exposure, as DNB has been shown to render pyruvate dehydrogenase inactive (29). It must be mentioned that this might only be a significant part of the mitochondrial response to DNB in the youngest group of animals and not in the 3mo animals, as lesions were not observed in the 3mo group either (and they might have a differential mitochondrial response not involving mitochondrial acetyl-CoA acetyltransferase).

There were no changes in brainstem MRP oxidation in 3mo animals, however, in 18mo animals, 7 MRPs were over 4-fold oxidized by DNB in the brainstem. Again, there were zero changes in cortical MRP oxidation in any age group, which supports the previous hypothesis in that even though DNB caused no changes in global MRP oxidation, there is regional variation in MRP susceptibility to oxidation. Additionally, within the MRPs that were found to be oxidized by proteomic analysis, brainstem MRPs had 3 times the amount of MRPs oxidized >4.0-fold than cortical MRPs. Furthermore, in MRPs that were oxidized >4.0-fold, the average level of oxidation was statistically significantly higher in brainstem than in cortex ($p<0.05$). This evidence suggests that the brainstem mitochondria were indeed more sensitive to oxidation by DNB.

There is an aging effect on cortical and brainstem MRP oxidation, with an observed >4.0-fold oxidation of 4 MRPs in cortex and 13 MRPs in brainstem compared to 1mo cortex and brainstem. Again, no changes were seen in 3mo cortex or brainstem

MRP oxidation. This gives strong evidence of an age-specific increase in MRP oxidation caused by DNB exposure.

In addition to being region-specific and increased with advanced age of the animal, DNB-induced oxidative alterations of MRPs target specific loci within these MRPs that constitute specific molecular pathways. Namely, cation transmembrane transporter, nucleoside-triphosphatase, pyrophosphatase, and hydrolase activity pathways were all identified as being constituted by significantly oxidized MRPs in the brainstem of DNB-exposed animals. Three MRPs significantly oxidized in brainstem constituted four of the five pathways identified in this analysis: cytoplasmic dynein, tubulin, and a plasma membrane calcium-transporting ATPase. This suggests that a mechanistic link between MRP oxidation and the lesions and clinical signs of intoxication seen in the oldest animals exposed to DNB may lie in mitochondrial transport. This is supported by evidence in the literature showing that cytoplasmic dynein is one of the linker proteins that bind to the microtubule and mitochondrion, and along with kinesin-1, facilitates fast transport of the mitochondrion down the microtubule in axons (30); the microtubule is composed of a tubulin heterodimer that polymerizes and depolymerizes, rendering the microtubule a dynamic component of the cytoskeleton. The plasma membrane calcium-transporting ATPases are responsible for the maintenance of intracellular (31) and extracellular (32) calcium concentrations by pumping out calcium; aberrant high intracellular calcium concentrations have been shown to affect mitochondrial transport in the brain by causing an increase in mitochondrial calcium uptake (as is seen in glutamate toxicity (33)), which can cause induction of the mitochondrial permeability transition pore (34) and in turn can disrupt

the efficiency of mitochondrial trafficking throughout the cell (35). The potentially synergistic effects of the observed DNB-induced oxidation of these three particular proteins could significantly disrupt mitochondrial transport in the brainstem of older animals, contributing to the observed DNB-induced clinical signs of intoxication in older animals.

While there was observed staining consistent with increased carbonylation in neurons in deep cerebellar nuclei in all 3 age groups compared to cortex, there were no differences in staining between vehicle control and DNB-exposed animals. However, the asymmetrical perinuclear staining did appear to be more pronounced in the deep cerebellar nuclei of 18mo animals. This suggests that the inclusion of carbonylation as part of the mechanism of vulnerability of brainstem nuclei to development of DNB-induced lesions may be more strongly associated with age than with DNB exposure. One must bear in mind that the method of carbonylation detection used in this experiment makes no distinction between carbonylated proteins and nucleic acids. Furthermore, it detects all carbonylated macromolecules throughout the entire cell, not just mitochondrial proteins; mitochondria are a repository for the accumulation of irreversible oxidative damage in DNB exposure in the brainstem (Dr. Stephen Steiner, unpublished data). One interpretation of the results obtained is that the pattern of staining observed in the perivascular region is that the primary lesion is gliovascular in origin, i.e., at the interface of the glial bed and the regional vasculature. Alternatively, perivascular vulnerability may merely be the result of increased oxidation of mitochondrial proteins in the neuronal somatic cytoplasm as suggested by more intensely stained mitochondria in the cytoplasm. This experiment provides additional

evidence of vacuolation of the neuropil in the deep cerebellar nuclei and vestibular nuclei in 18mo DNB exposed rats. This suggests that the age-related susceptibility to lesion development in these nuclei is likely due to astrocytes within those nuclei being more susceptible to oxidative stress induced by DNB.

One piece of evidence that would have added considerable value to the "aging and mitochondrial susceptibility to protein oxidation" paradigm regarding DNB exposure is *cell-specific* MRP oxidation. There were, however, issues of feasibility regarding sufficiency of mitochondrial protein concentration from neurons and astrocytes within brainstem loci in which lesions appear in DNB exposure. Had this been possible, this study would have been able to elucidate not only which MRPs are increasingly more oxidized during aging in the brainstem, but would have been able to also distinguish which MRPs might have been more highly oxidized in astrocytes compared to neurons and the resulting pathways that might have differed between the two cell types, thus giving a more clear mechanism of injury during DNB intoxication that may be influenced by aging. The hypothesis would have included astrocyte MRPs as more highly oxidized compared to neurons in DNB exposure due to evidence pointing to astrocytes as the primary cellular target in DNB exposure (14), (36). As this study stands, however, there is clear evidence of a correlation between advanced age, an increase in severity of lesions in the brainstem, clinical signs of intoxication, and an increase in MRP oxidation in brainstem, which provides important novel data on DNB-induced regional specificity of MRP susceptibility to oxidation during aging.

ACKNOWLEDGEMENTS

This research was supported by the NIH (2R01 ES08846) and the NIEHS (2T32 ES007062). We would like to thank Jackelyn Latham, Rory Landis, and Dr. Henriette Remmer for their assistance on this project.

Table 3.1. Conditions and Mortality Rates of Male F344 Rats Sacrificed 24h After Last Exposure. Number of animals affected out of total number of animals observed in parentheses. VC = Vehicle Control (DMSO), DNB = 10mg/kg 1,3-Dinitrobenzene given at 0h, 4h, and 24h; sacrificed 24h later. These animals were used for mitochondrial isolation and subsequent proteomics experiments.

Animal Age	Exposure	Hunched	Ataxia	Chromodacryorrhea	Mortality
1mo	VC	0% (0/3)	0% (0/3)	0% (0/3)	0% (0/3)
1mo	DNB	0% (0/3)	0% (0/3)	0% (0/3)	0% (0/3)
3mo	VC	0% (0/4)	0% (0/4)	0% (0/4)	0% (0/4)
3mo	DNB	75% (3/4)	25% (1/4)	0% (0/4)	0% (0/4)
18mo	VC	0% (0/3)	0% (0/3)	0% (0/3)	0% (0/3)
18mo	DNB	100% (5/5)	100% (5/5)	100% (5/5)	60% (3/5)

Table 3.2. Conditions and Mortality Rates of Male F344 Rats Sacrificed 12h After Last Exposure. Number of animals affected out of total number of animals observed in parentheses. VC = Vehicle Control (DMSO), DNB = 10mg/kg 1,3-Dinitrobenzene given at 0h, 4h, and 24h; sacrificed 12h later. These animals were used for histopathology experiments.

Animal Age	Exposure	Hunched	Ataxia	Chromodacryorrhea	Mortality
1mo	VC	0% (0/6)	0% (0/6)	0% (0/6)	0% (0/6)
1mo	DNB	0% (0/6)	0% (0/6)	0% (0/6)	0% (0/6)
3mo	VC	0% (0/6)	0% (0/6)	0% (0/6)	0% (0/6)
3mo	DNB	0% (0/6)	0% (0/6)	0% (0/6)	0% (0/6)
18mo	VC	0% (0/6)	0% (0/6)	0% (0/6)	0% (0/6)
18mo	DNB	100% (6/6)	100% (6/6)	100% (6/6)	0% (0/6)

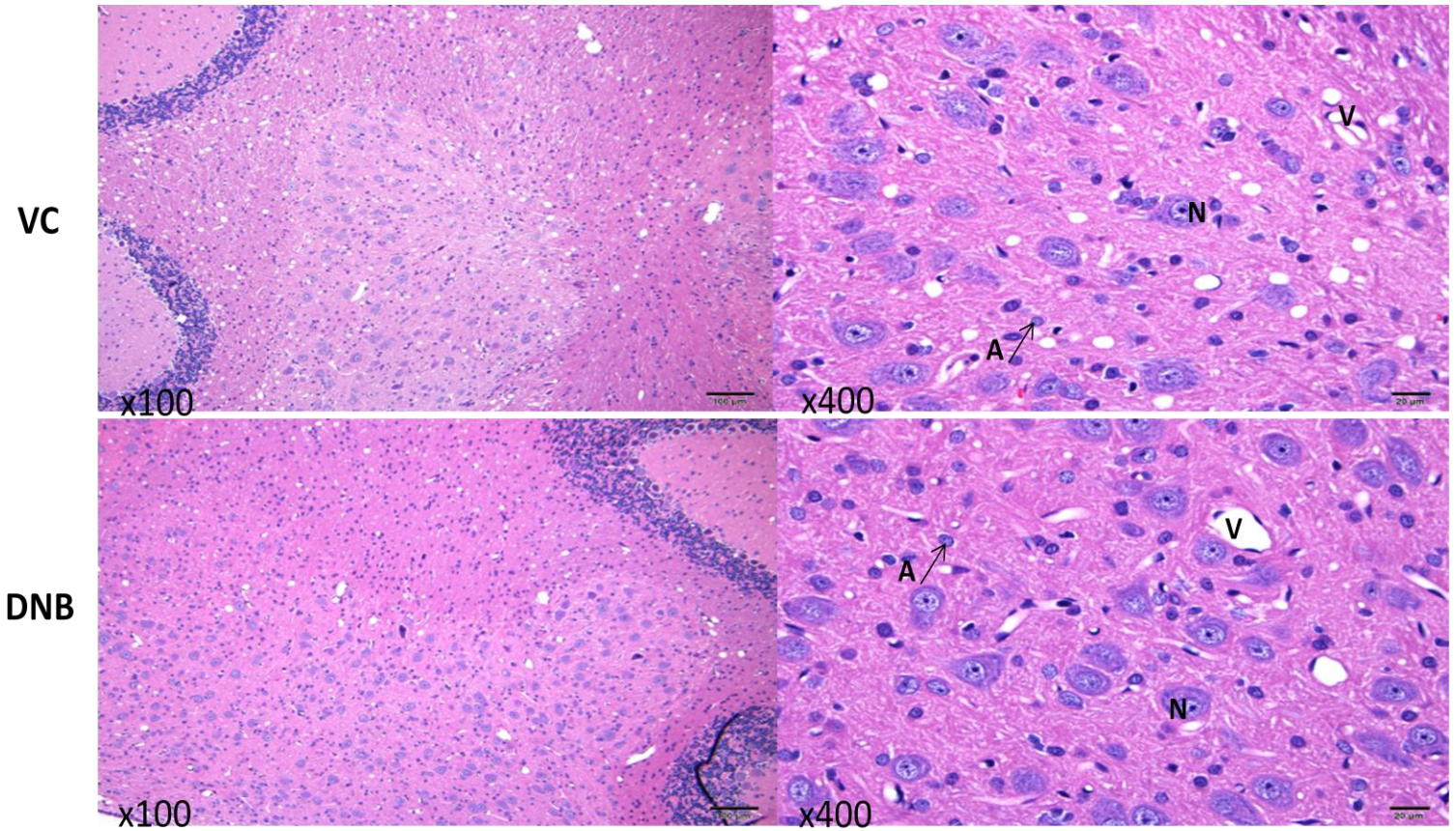

Figure 3.1. Deep Cerebellar Nuclei in 1mo Male F344 Rats Exposed to DNB
Hematoxylin and eosin staining of 1mo male F344 rats exposed to DNB (0h, 4h, 24h intraperitoneal 10mg/kg exposure with sacrifice 12h after the last exposure) or v/v equivalent of DMSO (VC) on the same time course. *(N=Neuron, V=Vasculature, A with arrow = Astrocyte). Scale bar: 100um*

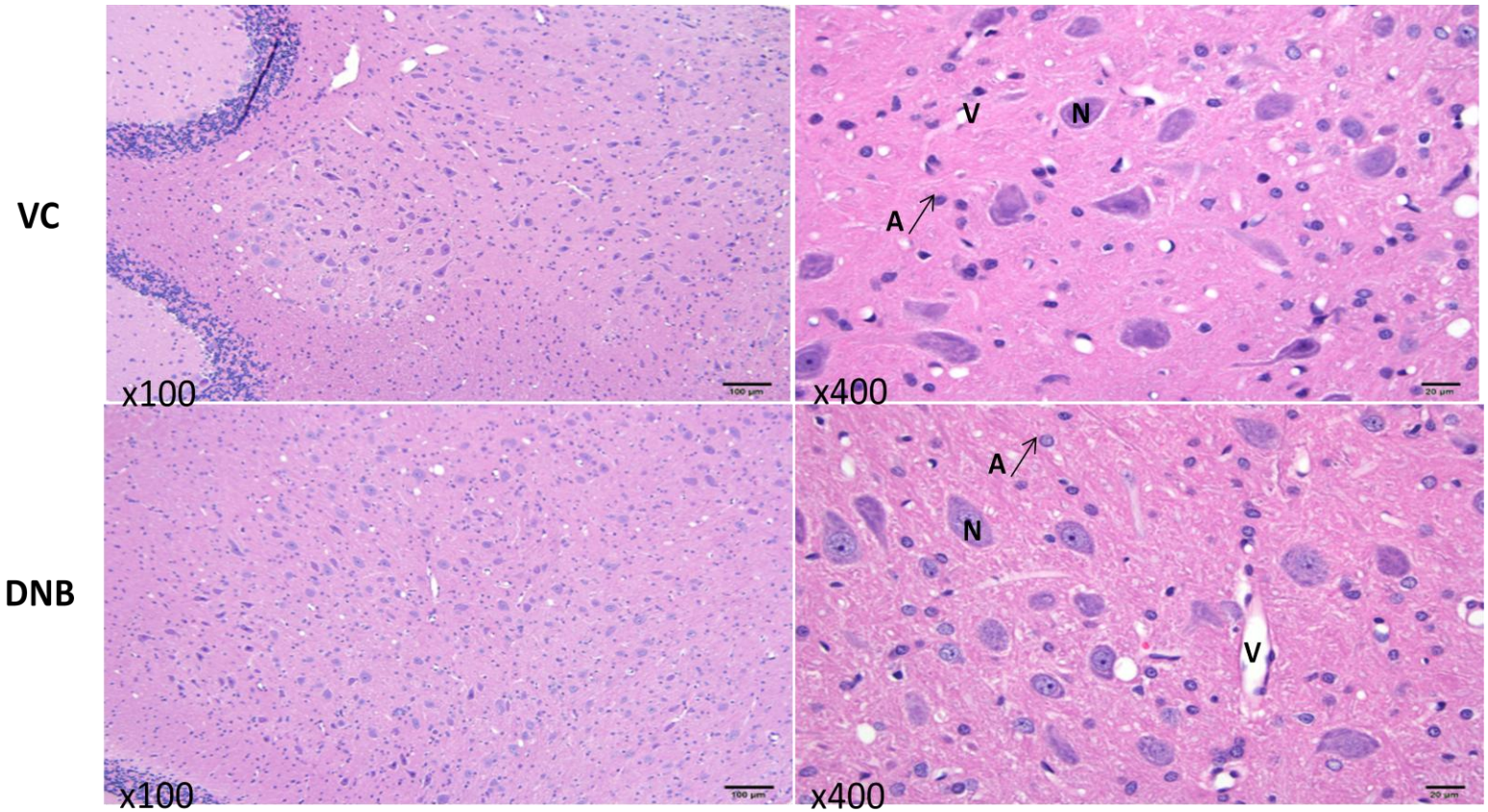

Figure 3.2. Deep Cerebellar Nuclei in 3mo Male F344 Rats Exposed to DNB
Hematoxylin and eosin staining of 3mo male F344 rats exposed to DNB (0h, 4h, and 24h intraperitoneal 10mg/kg exposure with sacrifice 12h after the last exposure) or v/v equivalent of DMSO (VC) on the same time course. *(N=Neuron, V=Vasculature, A with arrow = Astrocyte). Scale bar: 100um*

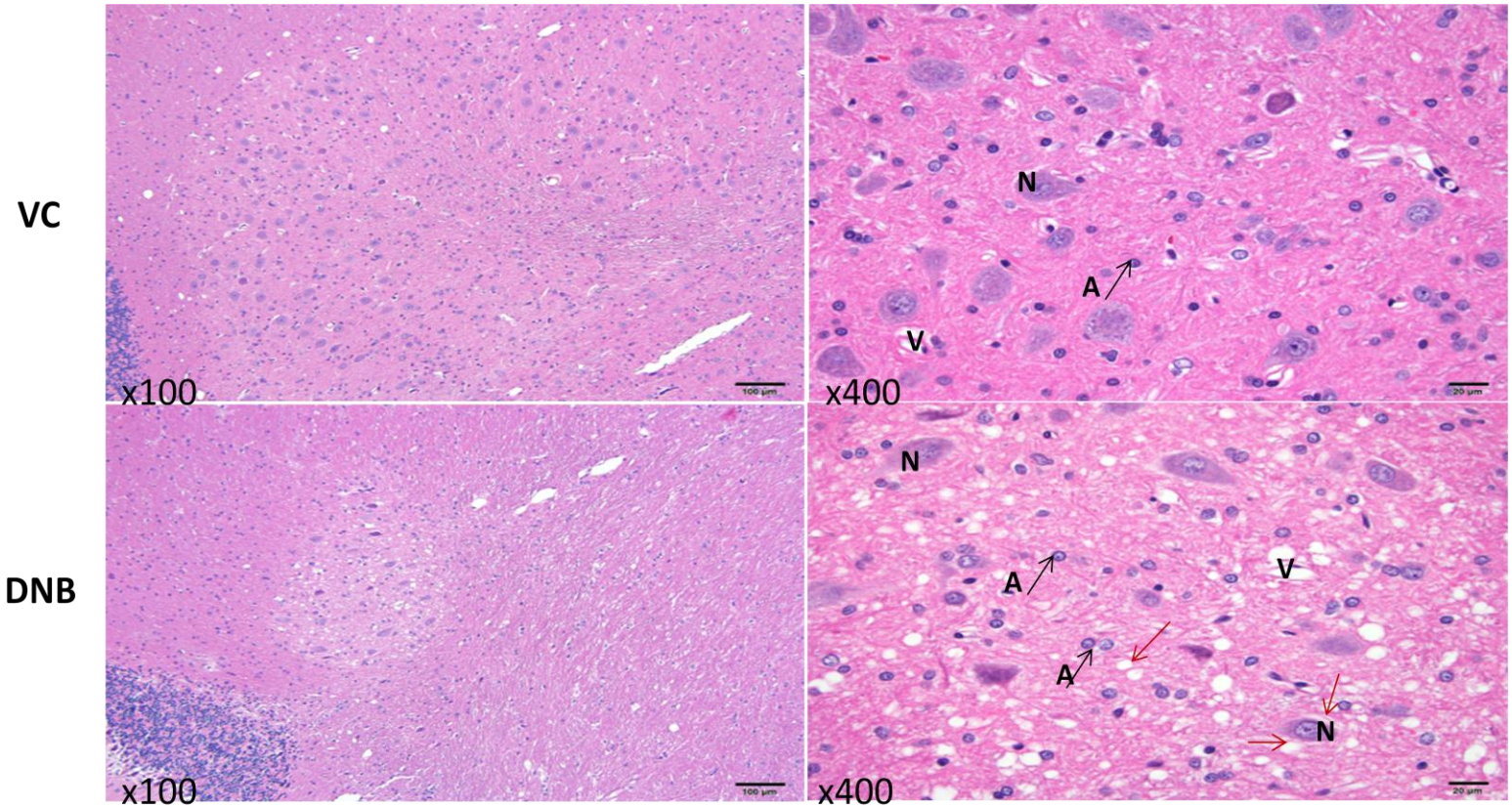

Figure 3.3. Deep Cerebellar Nuclei in 18mo Male F344 Rats Exposed to DNB
Hematoxylin and eosin staining of 18mo male F344 rats exposed to DNB (0h, 4h, and 24h intraperitoneal 10mg/kg exposure with sacrifice 12h after the last exposure) or v/v equivalent of DMSO (VC) on the same time course. *(N=Neuron, V=Vasculature, A with arrow = Astrocyte, Red Arrow = Vacuolation). Scale bar: 100um*

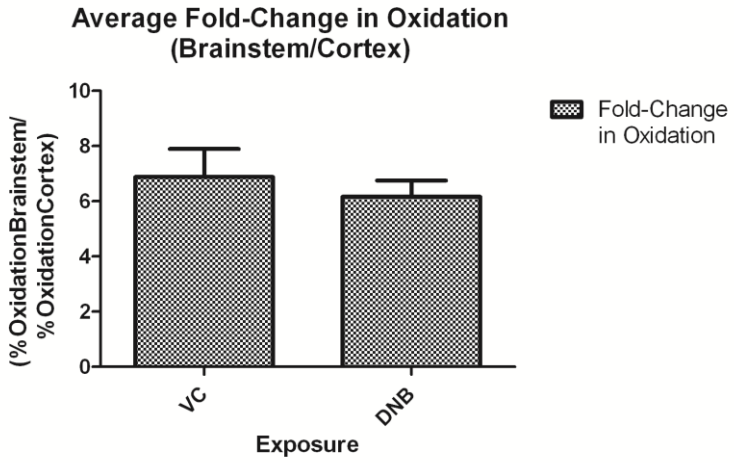

Figure 3.4. Effects of DNB on Global Oxidation of Mitochondria-Related Proteins (MRPs)
Average fold-change in oxidation of MRPs were calculated as: %Oxidation values of control brainstem divided by %Oxidation values of control cortex (VC) compared to %Oxidation values of DNB-exposed brainstem divided by %Oxidation values of DNB-exposed cortex. Data were uploaded to Prism software (Version 5.0, GraphPad) for statistical analysis (student's t-test).

Table 3.3. Effects of DNB on Regional MRP Oxidation

Identification of MRPs found to be significantly oxidized by DNB (<0.25-fold or >4.0-fold) by calculating %Oxidation (=%OxidationDNB/%OxidationVC) for brainstem and cortex within each age group of rats. Green text denotes >4.0-fold %Oxidation; red text denotes <0.25-fold %Oxidation.

Rat Age	Brainstem	Cortex	Protein Identification
1mo	1	0	Acetyl-CoA acetyltransferase, mitochondrial
3mo	0	0	-
18mo	7	0	Syntaxin-binding protein 1 Glyceraldehyde-3-phosphate dehydrogenase Tubulin beta-2A chain NADH dehydrogenase [ubiquinone] 1 alpha subcomplex subunit 6 Cytochrome c oxidase subunit 6C-2 Synaptosomal-associated protein 25 RCG58449, isoform CRA_a

Table 3.4 Effects of Age on Regional MRP Oxidation

Identification of MRPs found to be significantly oxidized by DNB (<0.25-fold or >4.0-fold) by calculating %Oxidation (=%OxidationDNB/%OxidationVC) for brainstem and cortex as a fold-change of 1mo rats. Green text denotes >4.0-fold %Oxidation.

Rat Age	Cortex	Brainstem	Protein Identification	
3mo	0	0	-	
18mo	4	13	Succinate dehydrogenase [ubiquinone] flavoprotein subunit, mitochondrial Succinyl-CoA:3-ketoacid-coenzyme A transferase 1, mitochondrial Trifunctional enzyme subunit beta, mitochondrial Glutathione S-transferase kappa 1	Cortex
			4-aminobutyrate aminotransferase, mitochondrial Cytoplasmic dynein 1 heavy chain 1 Acetyl-CoA acetyltransferase, mitochondrial Plasma membrane calcium-transporting ATPase 2 Uncharacterized protein (3) Syntaxin-binding protein 1 10 kDa heat shock protein, mitochondrial Glyceraldehyde-3-phosphate dehydrogenase Tubulin beta-2A chain NADH dehydrogenase [ubiquinone] 1 alpha subcomplex subunit 6 Cytochrome c oxidase subunit 6C-2 Synaptosomal-associated protein 25 RCG58449, isoform CRA_a	Brainstem

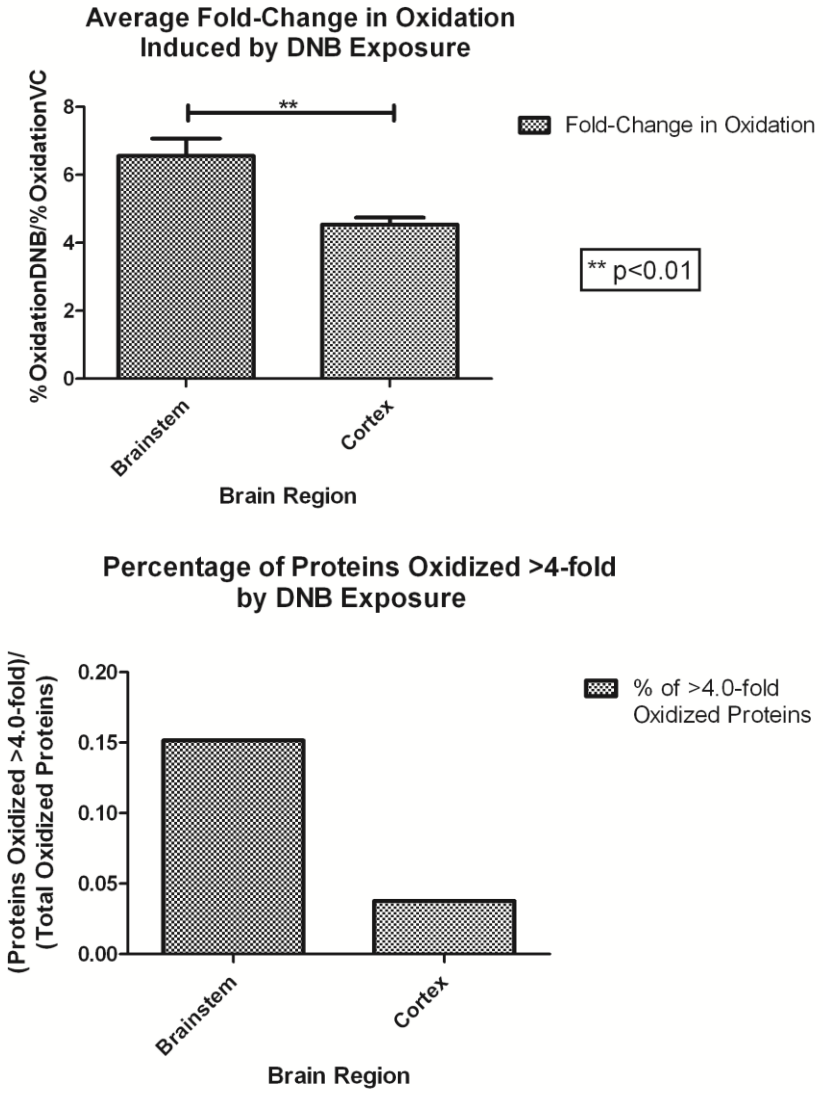

Figure 3.5. Brainstem and Cortex MRP Oxidation

Average fold-change in oxidation of MRPs were calculated as: %Oxidation values of DNB-exposed brainstem divided by %Oxidation values of control brainstem (Brainstem) compared to %Oxidation values of DNB-exposed cortex divided by %Oxidation values of control cortex (Cortex) (Top). Percentage of oxidized proteins that were oxidized >4-fold were tabulated (Bottom). Data were uploaded to Prism software (Version 5.0, GraphPad) for statistical analysis (student's t-test).

Table 3.5. Pathways Significantly Oxidized by DNB in Brainstem

UniProtID numbers for proteins <0.25-fold or >4.0-fold oxidized, as determined by %Oxidation, were uploaded to the Database for Annotation, Visualization, and Integrated Discovery (DAVID, *Nat. Protoc.* 2009). Pathways were identified by selecting GOTerm Molecular Function. Pathways distinct from control brainstem are shown.

Cation Transmembrane Transporter Activity	Nucleoside-Triphosphatase Activity	Pyrophosphatase Activity	Hydrolase Activity, acting on acid anhydrides, in phosphorous-containing anhydrides	Hydrolase Activity, acting on acid anhydrides
Synaptosomal-associated protein 25	Cytoplasmic dynein 1 heavy chain 1	Cytoplasmic dynein 1 heavy chain 1	Cytoplasmic dynein 1 heavy chain 1	Cytoplasmic dynein 1 heavy chain 1
Cytochrome c Oxidase, subunit 6-c2	Tubulin beta-2A chain	Tubulin beta-2A chain	Tubulin beta-2A chain	Tubulin beta-2A chain
Plasma membrane calcium-transporting ATPase 2	Plasma membrane calcium-transporting ATPase 2	Plasma membrane calcium-transporting ATPase 2	Plasma membrane calcium-transporting ATPase 2	Plasma membrane calcium-transporting ATPase 2

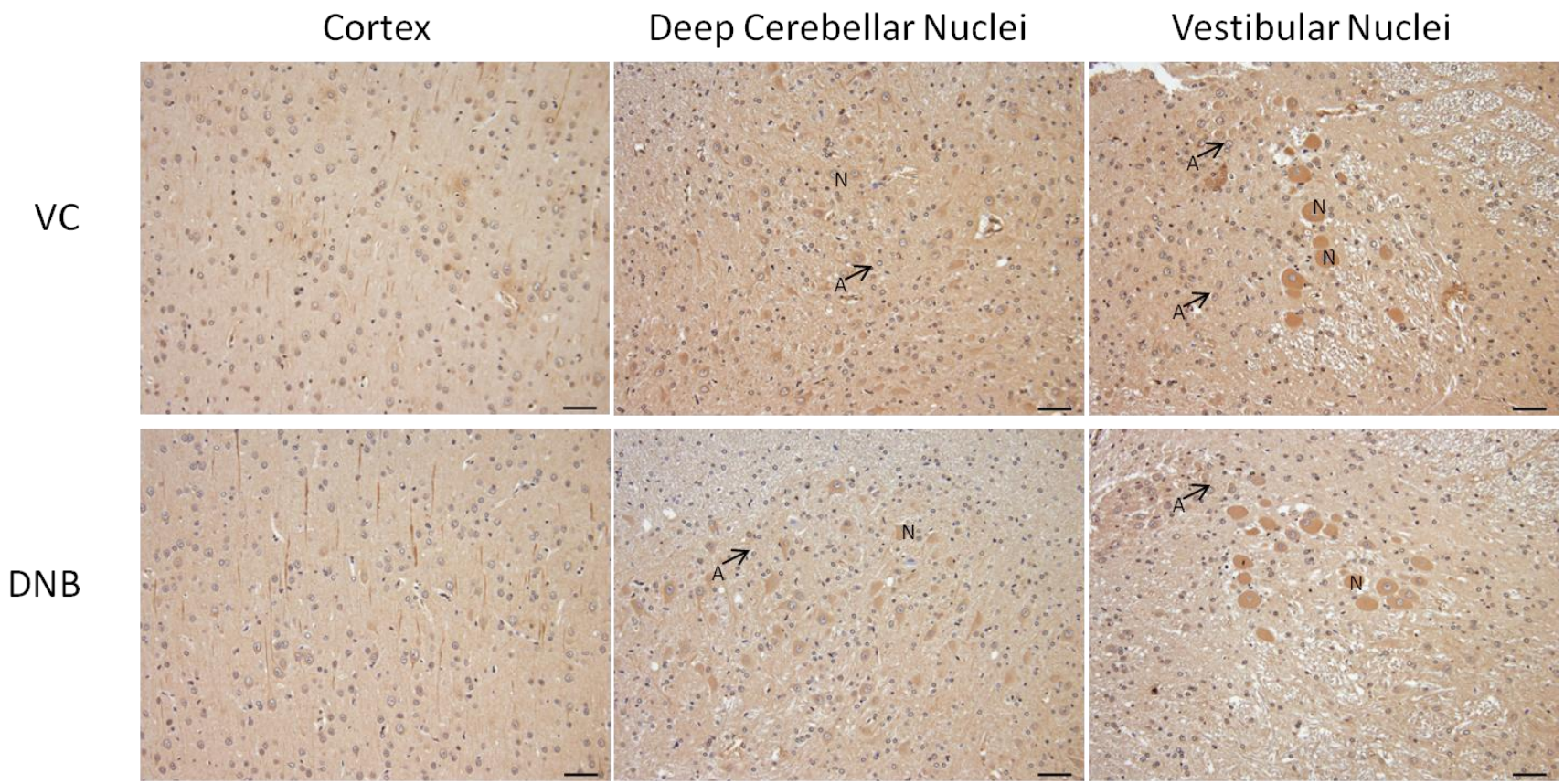

Figure 3.6. Carbonylation Detection in 1mo F344 Rats

2,4-Dinitrophenol staining of 1mo male F344 rats exposed to DNB (0h, 4h, 24h intraperitoneal 10mg/kg exposure with sacrifice 12h after the last exposure) or v/v equivalent of DMSO (VC) on the same time course. *(N=Neuron, A with arrow = Astrocyte) Scale bar: 50um*

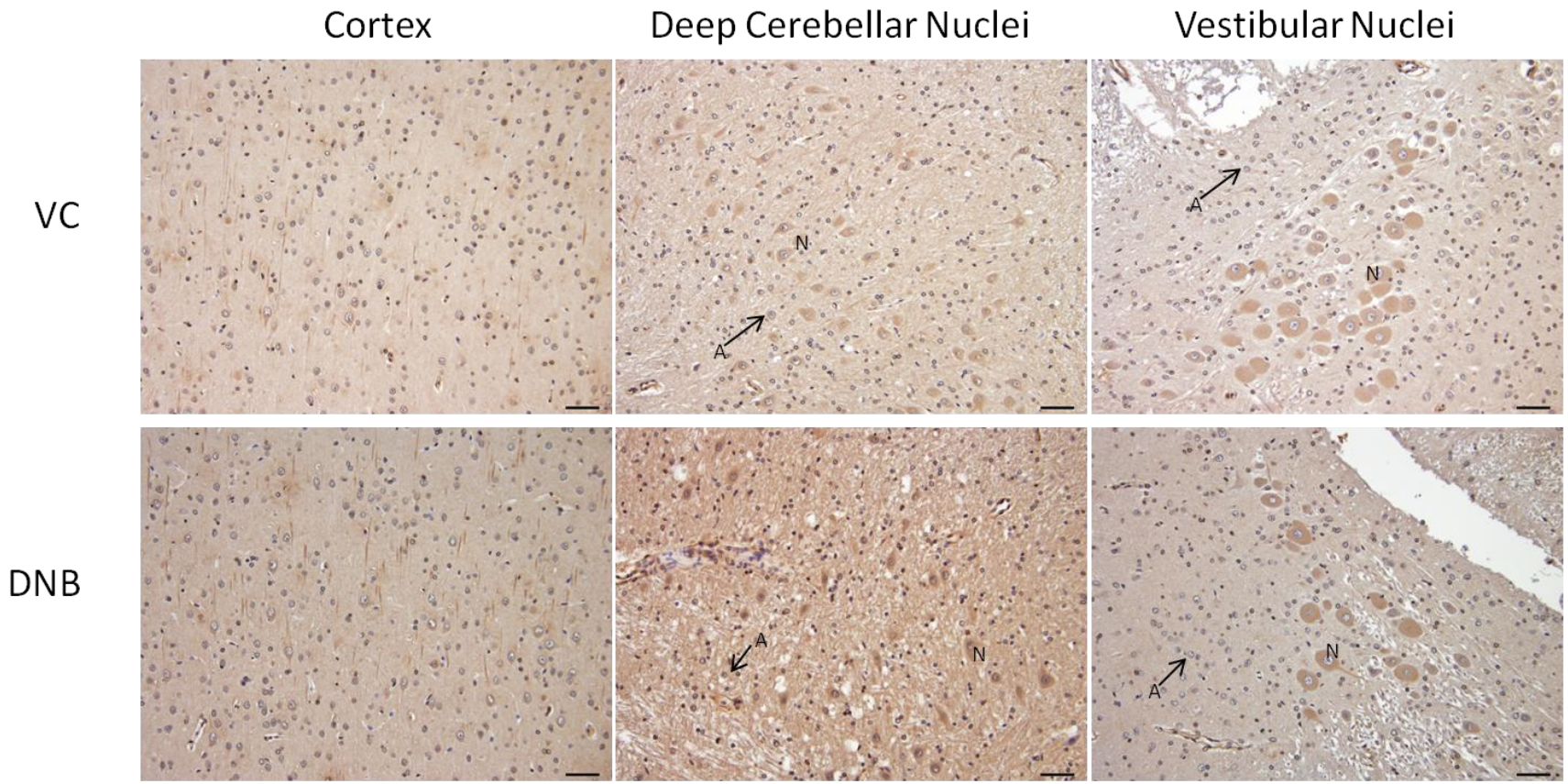

Figure 3.7. Carbonylation Detection in 3mo F344 Rats

2,4-Dinitrophenol staining of 3mo male F344 rats exposed to DNB (0h, 4h, 24h intraperitoneal 10mg/kg exposure with sacrifice 12h after the last exposure) or v/v equivalent of DMSO (VC) on the same time course. *(N=Neuron, A with arrow = Astrocyte) Scale bar: 50um*

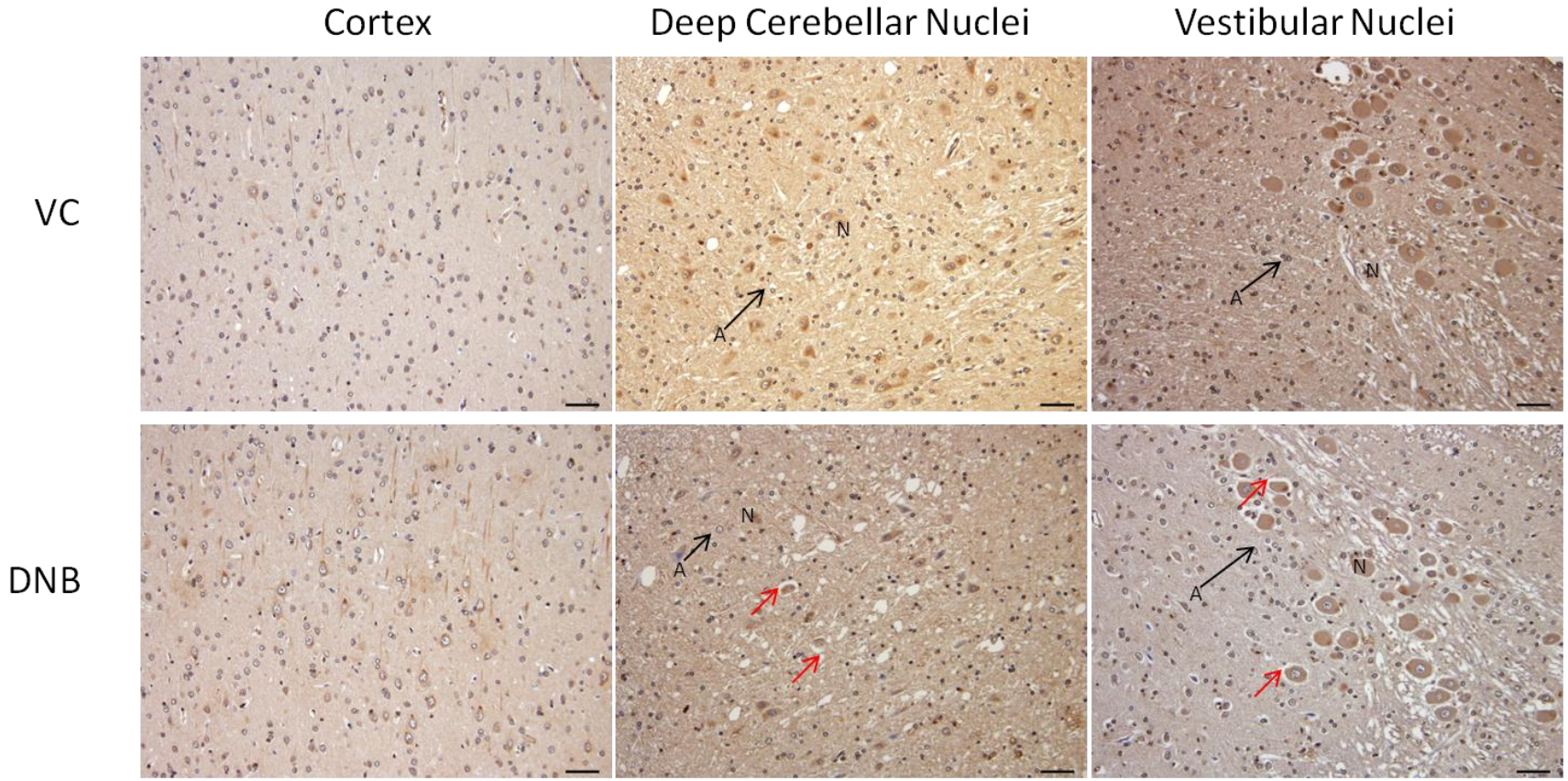

Figure 3.8. Carbonylation Detection in 18mo F344 Rats

2,4-Dinitrophenol staining of 18mo male F344 rats exposed to DNB (0h, 4h, 24h intraperitoneal 10mg/kg exposure with sacrifice 12h after the last exposure) or v/v equivalent of DMSO (VC) on the same time course. *(N=Neuron, A with arrow = Astrocyte, Red Arrow = Vacuolation). Scale bar: 50um*

REFERENCES

1. Harman D. Aging: a theory based on free radical and radiation chemistry. J Gerontol. 1956;11(3):298-300.

2. Halliwell B. Reactive oxygen species and the central nervous system. J Neurochem. 1992;59(5):1609-23.

3. Kumar P, Taha A, Sharma D, Kale RK, Baquer NZ. Effect of dehydroepiandrosterone (DHEA) on monoamine oxidase activity, lipid peroxidation and lipofuscin accumulation in aging rat brain regions. Biogerontology. 2008;9(4):235-46.

4. Giovannelli L, Decorosi F, Dolara P, Pulvirenti L. Vulnerability to DNA damage in the aging rat substantia nigra: a study with the comet assay. Brain Res. 2003;969(1-2):244-7.

5. Cardozo-Pelaez F, Song S, Parthasarathy A, Epstein CJ, Sanchez-Ramos J. Attenuation of age-dependent oxidative damage to DNA and protein in brainstem of Tg Cu/Zn SOD mice. Neurobiol Aging. 1998;19(4):311-6.

6. Turrens JF. Mitochondrial formation of reactive oxygen species. J Physiol. 2003;552(Pt 2):335-44. PMCID: 2343396.

7. Adam-Vizi V, Chinopoulos C. Bioenergetics and the formation of mitochondrial reactive oxygen species. Trends Pharmacol Sci. 2006;27(12):639-45.

8. Muller F. The nature and mechanism of superoxide production by the electron transport chain: Its relevance to aging. J Am Aging Assoc. 2000;23(4):227-53. PMCID: 3455268.

9. Perluigi M, Di Domenico F, Giorgi A, Schinina ME, Coccia R, Cini C, et al. Redox proteomics in aging rat brain: involvement of mitochondrial reduced glutathione status and mitochondrial protein oxidation in the aging process. J Neurosci Res. 2010;88(16):3498-507.

10. Imam SZ, Karahalil B, Hogue BA, Souza-Pinto NC, Bohr VA. Mitochondrial and nuclear DNA-repair capacity of various brain regions in mouse is altered in an age-dependent manner. Neurobiol Aging. 2006;27(8):1129-36.

11. Edrey YH, Oddo S, Cornelius C, Caccamo A, Calabrese V, Buffenstein R. Oxidative damage and amyloid-beta metabolism in brain regions of the longest-lived rodents. J Neurosci Res. 2014;92(2):195-205.

12. Venkateshappa C, Harish G, Mahadevan A, Srinivas Bharath MM, Shankar SK. Elevated oxidative stress and decreased antioxidant function in the human hippocampus and frontal cortex with increasing age: implications for neurodegeneration in Alzheimer's disease. Neurochem Res. 2012;37(8):1601-14.

13. Venkateshappa C, Harish G, Mythri RB, Mahadevan A, Bharath MM, Shankar SK. Increased oxidative damage and decreased antioxidant function in aging human substantia nigra compared to striatum: implications for Parkinson's disease. Neurochem Res. 2012;37(2):358-69.

14. Philbert MA, Nolan CC, Cremer JE, Tucker D, Brown AW. 1,3-Dinitrobenzene-induced encephalopathy in rats. Neuropathol Appl Neurobiol. 1987;13(5):371-89.

15. Jacobson CF, Miller MG. Species difference in 1,3-dinitrobenzene testicular toxicity: in vitro correlation with glutathione status. Reprod Toxicol. 1998;12(1):49-56.

16. Steiner SR, Philbert MA. Proteomic identification of carbonylated proteins in 1,3-dinitrobenzene neurotoxicity. Neurotoxicology. 2011;32(4):362-73. PMCID: 3158615.

17. Kodavanti PR, Royland JE, Richards JE, Besas J, Macphail RC. Toluene effects on oxidative stress in brain regions of young-adult, middle-age, and senescent Brown Norway rats. Toxicol Appl Pharmacol. 2011;256(3):386-98.

18. Sims NR, Anderson MF. Isolation of mitochondria from rat brain using Percoll density gradient centrifugation. Nat Protoc. 2008;3(7):1228-39.

19. Smerjac SM, Bizzozero OA. Cytoskeletal protein carbonylation and degradation in experimental autoimmune encephalomyelitis. J Neurochem. 2008;105(3):763-72. PMCID: 3599778.

20. Liang LP, Kavanagh TJ, Patel M. Glutathione deficiency in Gclm null mice results in complex I inhibition and dopamine depletion following paraquat administration. Toxicol Sci. 2013;134(2):366-73. PMCID: 3707437.

21. Singh AK, Tiwari MN, Upadhyay G, Patel DK, Singh D, Prakash O, et al. Long term exposure to cypermethrin induces nigrostriatal dopaminergic neurodegeneration in adult rats: postnatal exposure enhances the susceptibility during adulthood. Neurobiol Aging. 2012;33(2):404-15.

22. Grashow R, Spiro A, Taylor KM, Newton K, Shrairman R, Landau A, et al. Cumulative lead exposure in community-dwelling adults and fine motor function: comparing standard and novel tasks in the VA normative aging study. Neurotoxicology. 2013;35:154-61. PMCID: 3602137.

23. Stewart WF, Schwartz BS, Davatzikos C, Shen D, Liu D, Wu X, et al. Past adult lead exposure is linked to neurodegeneration measured by brain MRI. Neurology. 2006;66(10):1476-84.

24. Schliess F, Foster N, Gorg B, Reinehr R, Haussinger D. Hypoosmotic swelling increases protein tyrosine nitration in cultured rat astrocytes. Glia. 2004;47(1):21-9.

25. Cavanagh JB, Holton JL, Nolan CC, Ray DE, Naik JT, Mantle PG. The effects of the tremorgenic mycotoxin penitrem A on the rat cerebellum. Vet Pathol. 1998;35(1):53-63.

26. Ridder MC, Boor I, Lodder JC, Postma NL, Capdevila-Nortes X, Duarri A, et al. Megalencephalic leucoencephalopathy with cysts: defect in chloride currents and cell volume regulation. Brain. 2011;134(Pt 11):3342-54.

27. Middleton B. The oxoacyl-coenzyme A thiolases of animal tissues. Biochem J. 1973;132(4):717-30. PMCID: 1177647.

28. Veech RL. The therapeutic implications of ketone bodies: the effects of ketone bodies in pathological conditions: ketosis, ketogenic diet, redox states, insulin resistance, and mitochondrial metabolism. Prostaglandins Leukot Essent Fatty Acids. 2004;70(3):309-19.

29. Miller JA, Runkle SA, Tjalkens RB, Philbert MA. 1,3-Dinitrobenzene-induced metabolic impairment through selective inactivation of the pyruvate dehydrogenase complex. Toxicol Sci. 2011;122(2):502-11. PMCID: 3155080.

30. Pilling AD, Horiuchi D, Lively CM, Saxton WM. Kinesin-1 and Dynein are the primary motors for fast transport of mitochondria in Drosophila motor axons. Mol Biol Cell. 2006;17(4):2057-68. PMCID: 1415296.

31. Jensen TP, Buckby LE, Empson RM. Expression of plasma membrane Ca2+ ATPase family members and associated synaptic proteins in acute and cultured organotypic hippocampal slices from rat. Brain Res Dev Brain Res. 2004;152(2):129-36.

32. Talarico EF, Jr., Kennedy BG, Marfurt CF, Loeffler KU, Mangini NJ. Expression and immunolocalization of plasma membrane calcium ATPase isoforms in human corneal epithelium. Mol Vis. 2005;11:169-78.

33. Kiedrowski L, Costa E. Glutamate-induced destabilization of intracellular calcium concentration homeostasis in cultured cerebellar granule cells: role of mitochondria in calcium buffering. Mol Pharmacol. 1995;47(1):140-7.

34. Kristal BS, Dubinsky JM. Mitochondrial permeability transition in the central nervous system: induction by calcium cycling-dependent and -independent pathways. J Neurochem. 1997;69(2):524-38.

35. Guo L, Du H, Yan S, Wu X, McKhann GM, Chen JX, et al. Cyclophilin D deficiency rescues axonal mitochondrial transport in Alzheimer's neurons. PLoS One. 2013;8(1):e54914. PMCID: 3561411.

36. Tjalkens RB, Phelka AD, Philbert MA. Regional variation in the activation threshold for 1,3-DNB-induced mitochondrial permeability transition in brainstem and cortical astrocytes. Neurotoxicology. 2003;24(3):391-401.

CHAPTER IV

Are There Differences in Compensatory Molecular Pathways between Younger and Older Brainstem Mitochondria following 1,3-DNB Exposure?

INTRODUCTION

As mammals age, the ability to efficiently respond to cellular demand for adenosine triphosphate (ATP) is generally diminished. The brain, in particular, has extremely high energy demands: it accounts for only 2% of the body's mass but consumes 20% of the body's glucose (1). Thus, age-related deficits or mismatches in energy production and utilization can be especially detrimental to mental function. In a study by Dutschke, et al. (1994), aged rats showed significantly lower levels of ATP and creatine phosphate in cerebral cortex when subjected to mental activities (passive avoidance and hole board tests), compared to younger "mentally active" rats or aged rats that weren't subjected to mental tests (2), suggesting that older rats are less able to produce ATP by oxidative phosphorylation in response to metabolic demands in the brain. This is supported by evidence of an age-related decline in cytochrome oxidase activity and concurrent increase in mitochondrial size in cerebellar cortex in the aging rodent (3), age-related decreases in NADH-cytochrome c reductase activity in whole mouse brain (4),and an age-related decrease in mitochondrial electron transfer in whole mouse brain (5).

Despite supporting evidence that there is an overall decline in mitochondrial function in the brain during aging, it's important to refrain from making generalizations regarding age-related changes in mitochondrial function across brain regions: the energetic demands, specific physiological processes, cellular distribution, and spatial dynamics differ between and among different brain regions. Additionally, neurodegenerative diseases (of which age is the primary risk factor), including Alzheimer's Disease and Parkinson's Disease, manifest region-specific mitochondrial pathologies (6),(7), indicating that mitochondria within different regions of the brain are disparately susceptible to age-related modifications.

1,3-Dinitrobenzene (DNB) exposure causes the development of bilaterally symmetrical, gliovascular lesions in brainstem nuclei that form the ascending pathway of the 8th cranial nerve (8). DNB exposure results in lesions that target brainstem mitochondria, and has been shown to inhibit the pyruvate dehydrogenase complex while impairing oxidative energy metabolism (9). Additionally, mitochondrially-targeted effects of DNB include selective carbonylation of mitochondrial proteins in astrocytes (10), and induces the opening of the mitochondrial permeability transition pore in neurons from brainstem, but not neurons from cortex (11).

While it is known that DNB exposure causes mitochondrial toxicity in brainstem, there was no evidence of how age may alter the susceptibility of brainstem mitochondria to DNB. This study uses a high-throughput proteomics approach to provide novel evidence of age-related, DNB-induced, region-specific changes in mitochondria-related protein (MRP) expression. Additionally, this study maps these increases or decreases in MRP expression to molecular function pathways, giving insight into which

mitochondrial mechanisms in the brainstem are most vulnerable to dysregulation by DNB exposure and may have become more susceptible to this type of perturbation due to the aging process.

MATERIALS AND METHODS

Animals

Male F344 rats (1 month old, 3 month old, and 18 month old) were purchased from Harlan Laboratories and housed according to University of Michigan's University Committee on Use and Care of Animals policies. Rats were fed and watered ad libitum and housed on a 12-hour light/dark cycle.

Mitochondrial Isolation

Rats from each age group were either exposed to 10mg/kg DNB or a v/v equivalent of dimethylsulfoxide (DMSO) serving as a vehicle control (at 0h, 4h, and 24h; sacrifice occurred 24h after the 24h dose). Mitochondria were isolated according to the protocol (Method C) by Sims & Anderson (12), with minor modifications. Briefly, the rat was anesthetized under isoflurane, decapitated with a small animal guillotine, and the brain was rapidly removed. Brainstem and cortex were dissected from the rest of the brain in cold isolation buffer (100mM Tris, 10mM potassium-EDTA, 960mM sucrose, pH 7.4). Brainstem and cortex were then weighed and minced in cold isolation buffer. Minced tissue was then homogenized using a glass Dounce homogenizer on ice; this step was performed while being flushed with argon. Subsequent centrifugation steps

followed. Prior to the Percoll gradient centrifugation step, digitonin was added to disrupt synaptosomal membranes. Mitochondria were stored at -80°C.

Detection and Identification of Mitochondria-Related Proteins (University of Michigan Peptide Synthesis and Proteomics Core and MSBioWorks, LLC, Ann Arbor, MI)

The volume of each submitted mitochondrial sample was reduced 50% and 20µL of the concentrated sample was processed by SDS-PAGE on a 4-12% Bis-Tris Mini-gel (Invitrogen) using the MOPS buffer system and non-reducing Laemmli buffer. Each gel lane was excised into ten equal bands and these were processed by in-gel digestion using a robot (ProGest, DigiLab): bands were washed with 25mM ammonium bicarbonate followed by acetonitrile, reduced with 10mM dithiothreitol at 60°C followed by alkylation with 50mM iodoacetamide at room temperature, digested with trypsin (Promega) for 4h at 37°C, and quenched with formic acid and the supernatant was analyzed directly without further processing. Samples were then analyzed by LC/MS/MS analyzed by nano LC/MS/MS with a Waters NanoAcquity HPLC system interfaced to a ThermoFisher Q Exactive mass spectrometer. Peptides were loaded on a trapping column and eluted over a 75µm analytical column at 350nL/min; both columns were packed with Jupiter Proteo resin (Phenomenex). The mass spectrometer was operated in data-dependent mode, with MS and MS/MS performed at 70,000 and 17,500 FWHM resolution, respectively. The fifteen most abundant ions were selected for MS/MS. Proteins were identified by reference to the UniProt rat database (forward and reverse appended with common contaminant proteins) using the Mascot search engine. Results were displayed in Scaffold software.

Pathway Analysis

UniProtID numbers for proteins <0.25-fold or >4.0-fold changed were uploaded to the DAVID database (2). Fold-changes of protein were quantified as the Normalized Spectral Abundance Factor (NSAF). NSAF is calculated by first finding the Spectral Abundance Factor: (SAF = Unweighted Spectrum Count/Molecular Weight) and then normalizing to the total spectral count for that protein: ($NSAF = SAF/\sum_{Spectral\ Count}$). Pathways were identified by selecting GOTerm Molecular Function. Options for pathway determination were set to: 3 proteins to constitute a pathway (default setting = 2), and 0.05 as a significance level for P-values and Benjamini values.

RESULTS

MRP Normalized Spectral Abundance Factor (NSAF) Fold-Changes in Brainstem

Brainstem MRPs in young (1mo) control animals are comparatively more upregulated (34 proteins) than downregulated (6 proteins) (~6x difference); this does not hold true for brainstem MRPs in 1mo rats exposed to DNB (4 upregulated, 7 downregulated) (Figure 4.1, Tables 4.5 & 4.6). In 3mo control animals, there were three times as many downregulated MRPs (9 proteins) compared to upregulated MRPs (3 proteins), whereas in 3mo DNB-exposed animals, there were no upregulated MRPs, but 13 downregulated MRPs (Figure 4.1, Tables 4.7 & 4.8). In the oldest control animals (18mo), there were approximately twice as many downregulated MRPs (12 proteins) as there were upregulated MRPs (5 proteins); however, in DNB exposed 18mo animals, there were over 5x as many downregulated MRPs (11 proteins) as there were

upregulated MRPs (2 proteins) (Figure 4.1, Tables 4.9 & 4.10). This data suggests that there is an age effect on the expression of brainstem MRPs, and that DNB exposure exacerbates the increased susceptibility to downregulation of MRP expression in brainstem.

Pathways Significantly Upregulated or Downregulated in Brainstem of Control Rats

In control animals, 11 molecular function pathways were increased in 1mo brainstem (catalytic activity, nucleoside triphosphatase activity, pyrophosphatase activity, hydrolase activity, protein binding, ion transmembrane transporter activity, protein C-terminus binding, purine ribonucleotide binding, ribonucleotide binding, purine nucleotide binding, and nucleotide binding), whereas no pathways were increased in brainstem of 3mo and 18mo rats (Table 4.1.) Conversely, there were no molecular function pathways decreased in brainstem of 1mo control rats, whereas catalytic activity was decreased in brainstem of 3mo rats and protein binding was decreased in 18mo rats (Table 4.1)

Identification of MRPs in Pathways Significantly Upregulated or Downregulated in Brainstem of Control Rats

Of the 11 pathways upregulated in young control brainstem (Table 4.2), four pathways (catalytic activity, nucleoside triphosphatase activity, pyrophosphatase activity, and hydrolase activity) contain the same 3 MRPs (ATPase, Ca++ transporting, plasma membrane 2; ATPase, Na+/K+ transporting, beta 1 polypeptide; myosin ID); two pathways (protein binding, ion transmembrane transporter activity) contain the same 3 MRPs (ATPase, Ca++ transporting, plasma membrane 2; ATPase, H+ transporting, lysosomal V0 ATPase; Na+/K+ transporting polypeptide); and three pathways (purine

ribonucleotide, purine nucleotide, and nucleotide binding) contain the same 3 MRPs (ATPase, Ca++ transporting, plasma membrane 2; guanine nucleotide binding protein (G protein); myosin ID).

The three MRPs identified as involved in catalytic activity (and downregulated in 3mo control brainstem) were branched chain ketoacid dehydrogenase E1, aarF domain containing kinase 4, and aminoadipate-semialdehyde synthase (Table 4.2). Additionally, there were 3 MRPs identified as involved in protein binding and were downregulated in 18mo control brainstem: mitochondrial ribosomal protein S9, ferredoxin reductase, and NCK-associated protein 1 (Table 4.2).

Pathways Significantly Upregulated or Downregulated in Brainstem of DNB-Exposed Rats

In DNB-exposed animals, no pathways were upregulated in brainstem in *any* of the age groups. However, the same pathway (catalytic activity) was downregulated in all 3 age groups (Table 4.3).

Identification of MRPs in Pathways Significantly Upregulated or Downregulated in Brainstem of DNB-Exposed Rats

Although the same pathway (catalytic activity) was identified as upregulated by DNB exposure in brainstem MRPs across the age groups, different proteins were identified within this pathway across the age groups (Table 4.4). In 1mo DNB-exposed brainstem, the three MRPs identified in the catalytic activity pathway are as follows: DEAH (Asp-Glu-Ala-His) box polypeptide 30, lysyl-tRNA synthetase, and mitochondrial translational initiation factor 2 (Table 4.4). In 3mo DNB-exposed brainstem, the three MRPs identified in the catalytic activity pathway are as follows: sulfite oxidase, malonyl-CoA decarboxylase, and Cytochrome c oxidase subunit 3 (Table 4.4). In 18mo DNB-

exposed brainstem, the three MRPs identified in the catalytic activity pathway are as follows: biphenyl hydrolase-like (serine hydrolase), presenilin 2; chaperone, ABC1 activity of bc1 complex; and suppressor of var1, 3-like 1 (S. cerevisiae) (Table 4.4).

DISCUSSION

This study provides novel evidence of DNB-induced, region-specific, age-related changes in MRP expression. In general, there is an inverse relationship between age and number of upregulated MRPs, with 1mo control animals exhibiting the highest number of upregulated MRPs (34 total). Across control animals, there was also an increase in the number of downregulated MRPs as age increased (6 MRPs in 1mo, 9 MRPs in 3mo, and 12 MRPs in 18mo). In DNB-exposed animals, however, there was a marked decrease in the number of upregulated MRPs, even in the youngest age group (7 MRPs in 1mo, 0 MRPs in 3mo, and 2 MRPs in 18mo) while at the same time, there was an overall increase in the number of downregulated MRPs as age increased (4 MRPs in 1mo, 13 MRPs in 3mo, and 11 MRPs in 18mo). Overall, MRPs are quantified at a higher level in 1mo brainstem than older counterparts; this suggests that younger animals may be more equipped to appropriately alter metabolic profiles to mitigate the toxic effects of DNB.

This supposition is based on existing evidence supporting an overall decrease in brain mitochondrial enzyme expression and activity with advancing age: in rat brain, there's a decrease in energy metabolizing enzyme activity, including aldolase, citrate synthase, and lactate dehydrogenase (of which there's regional heterogeneity) (13). In

humans, there is an overall decrease in neural mitochondrial metabolism during the healthy aging process (14); this can be exacerbated in cases of neurodegenerative disease, such as Alzheimer's Disease (15), or in instances of exposures to environmental neurotoxicants, such as fentrazamide (16) and paraquat (17).

It is of note that, of the 106 MRPs identified as significantly upregulated or downregulated across the age groups, 26 of those (24.5% of the total) were identified as an "uncharacterized protein" or "uncharacterized protein fragment". This means that while they could still be quantified, their function is still unknown. This presents the possibility that the identified MRPs (and pathways identified based on those MRPs) may be necessary, but not sufficient, to cause the damage seen in 18mo DNB-exposed brainstem.

Both upregulated and downregulated MRPs were assembled into specific pathways based on molecular function. Since the same three MRPs make up the upregulated protein binding and ion transmembrane transporter activity pathways in 1mo control brainstem, these 3 MRPs could be mechanistically grouped together based on their participation in ion homeostasis (ATPase Ca++ transporting, plasma membrane 2 (18), ATPase H+ transporting, lysosomal V0 ATPase (19), and Na+/K+ transporting polypeptide (20)).

Even though DNB exposure causes downregulation of the same pathway in brainstem across the age groups, different MRPs were identified within each; this suggests that downregulation of *key* MRPs during aging may be necessary and/or sufficient to cause damage. This may be especially true of the 18mo animals; the three proteins constituting the "catalytic activity" pathway don't make up a discernable,

common mechanistic function (whereas the MRPs in the catalytic activity pathway in 1mo brainstem can be grouped by transcription of mtDNA and subsequent translation (DEAH (Asp-Glu-Ala-His) box polypeptide 30 (21), lysyl-tRNA synthetase (22), and mitochondrial translational initiation factor 2 (23)) and 3mo brainstem can be grouped by their function in the process of oxidative phosphorylation (sulfite oxidase (24), malonyl-CoA decarboxylase (25), and cytochrome c oxidase subunit 3 (26)). Thus, a DNB-induced decrease in the catalytic activity of biphenyl hydrolase-like serine hydrolase presenilin 2 (plays a role in mitochondrial calcium uptake and formation of the mitochondrial permeability transition pore (27)), chaperone ABC1 activity of bc1 complex (necessary for the correct conformation and function of the bc1 complex (28)), and suppressor of var1 3-like 1 (S. cerevisiae) (degrades RNA in the presence of ATP (29)) in old brainstem, while they don't functionally intersect, may be necessary to cause damage.

In summary, DNB causes a decrease in brainstem MRP expression, even in the youngest animals. However, because the youngest control animals exhibited the highest endogenous levels of MRPs, this suggests that in comparison to their older counterparts they are better equipped to respond to metabolic mitochondrial stressors, such as DNB exposure.

ACKNOWLEDGEMENTS

This research was supported by the NIH (2R01 ES08846) and the NIEHS (2T32 ES007062). We would like to thank Jackelyn Latham, Rory Landis, and Dr. Henriette Remmer for their assistance on this project.

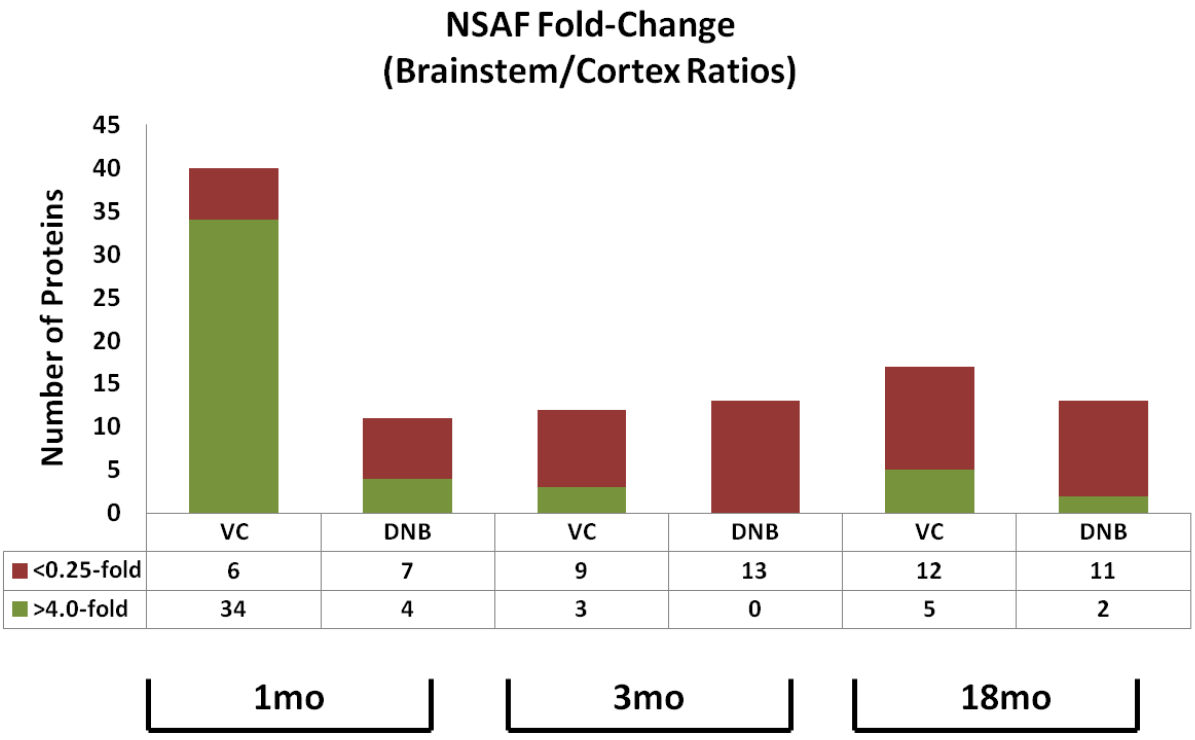

Figure 4.1. MRP Normalized Spectral Abundance Factor (NSAF) Fold-Changes in Brainstem
Identification of MRPs found to be significantly changed in brainstem (<0.25-fold or >4.0-fold) by calculating NSAF for DNB exposure and controls within each age group of rats.

Table 4.1. Pathways Significantly Upregulated or Downregulated in Brainstem of Control Rats
UniProtID numbers for MRPs <0.25-fold or >4.0-fold changed in control animals, as determined by NSAF, were uploaded to the Database for Annotation, Visualization, and Integrated Discovery (2). Pathways were identified by selecting GOTerm Molecular Function.

	1mo	3mo	18mo
↑BS	Catalytic Activity Nucleoside Triphosphatase Activity Pyrophosphatase Activity Hydrolase Activity Protein Binding Ion Transmembrane Transporter Activity Protein C-Terminus Binding Purine Ribonucleotide Binding Ribonucleotide Binding Purine Nucleotide Binding Nucleotide Binding	--	--
↓BS	--	Catalytic Activity	Protein Binding

Table 4.2. Identification of MRPs in Pathways Significantly Upregulated or Downregulated in Brainstem of Control Rats

UniProtID numbers for MRPs <0.25-fold or >4.0-fold changed in control animals, as determined by NSAF, were uploaded to the Database for Annotation, Visualization, and Integrated Discovery (2). Pathways were identified by selecting GOTerm Molecular Function. Pathways were then analyzed for identification of MRPs by UniProtID numbers.

	1mo	3mo	18mo
↑BS	**Catalytic Activity, Nucleoside Triphosphatase Activity, Pyrophosphatase Activity, Hydrolase Activity** ATPase, Ca++ transporting, plasma membrane 2 ATPase, Na+/K+ transporting, beta 1 polypeptide myosin ID **Protein Binding, Ion Transmembrane Transporter Activity** ATPase, Ca++ transporting, plasma membrane 2 ATPase, H+ transporting, lysosomal V0 ATPase Na+/K+ transporting polypeptide **Protein C-Terminus Binding** **Purine Ribonucleotide, Ribonucleotide, Purine Nucleotide, and Nucleotide Binding** ATPase, Ca++ transporting, plasma membrane 2 guanine nucleotide binding protein (G protein) myosin ID	--	--
↓BS	--	**Catalytic Activity** Branched chain ketoacid dehydrogenase E1 aarF domain containing kinase 4 aminoadipate-semialdehyde synthase	**Protein Binding** mitochondrial ribosomal protein S9 ferredoxin reductase NCK-associated protein 1

Table 4.3. Pathways Significantly Upregulated or Downregulated in Brainstem of DNB-Exposed Rats UniProtID numbers for MRPs <0.25-fold or >4.0-fold changed in DNB-exposed animals, as determined by NSAF, were uploaded to the Database for Annotation, Visualization, and Integrated Discovery (2). Pathways were identified by selecting GOTerm Molecular Function.

	1mo	3mo	18mo
↑BS	--	--	--
↓BS	Catalytic Activity	Catalytic Activity	Catalytic Activity

Table 4.4. Identification of MRPs in Pathways Significantly Upregulated or Downregulated in Brainstem of DNB-Exposed Rats

UniProtID numbers for MRPs <0.25-fold or >4.0-fold changed in DNB-exposed animals, as determined by NSAF, were uploaded to the Database for Annotation, Visualization, and Integrated Discovery (2). Pathways were identified by selecting GOTerm Molecular Function. Pathways were then analyzed for identification of MRPs by UniProtID numbers.

	1mo	3mo	18mo
↑BS	--	--	--
↓BS	**Catalytic Activity** DEAH (Asp-Glu-Ala-His) box polypeptide 30 lysyl-tRNA synthetase mitochondrial translational initiation factor 2	**Catalytic Activity** sulfite oxidase malonyl-CoA decarboxylase Cytochrome c oxidase subunit 3	**Catalytic Activity** biphenyl hydrolase-like (serine hydrolase) presenilin 2; chaperone, ABC1 activity of bc1 cmplx suppressor of var1, 3-like 1 (S. cerevisiae)

Table 4.5. Fold-Change Values of MRPs Significantly Changed in Brainstem of Control 1mo Rats
MRPs <0.25-fold or >4.0-fold changed in 1mo control animals, as determined by NSAF. Green indicates >4.0-fold change in NSAF; Red indicates <0.25-fold change in NSAF.

VC 1mo	
Fold-Change	Protein Identification
0.1582	Valyl-tRNA synthetase, mitochondrial
0.2034	Calcium/calmodulin-dependent protein kinase type II subunit alpha
0.2179	Similar to RIKEN cDNA 0710008K08 (Predicted), isoform CRA_c
0.2333	Similar to putative lipid kinase (Predicted), isoform CRA_c
0.2347	Solute carrier family 25 member 46
0.244	Alpha-aminoadipic semialdehyde synthase, mitochondrial
4.1183	Uncharacterized protein
4.2708	Uncharacterized protein
4.2708	Amphiphysin
4.4233	CD9 antigen
4.6156	Neurofilament 3, medium
4.6291	Myelin basic protein S
4.6775	Thy-1 membrane glycoprotein
4.8254	Neurofilament light polypeptide
4.8809	Transketolase
5.0165	Neurofascin, isoform CRA_d
5.0473	Sodium/potassium-transporting ATPase subunit beta-1
5.0843	Septin-8
5.202	Myelin-oligodendrocyte glycoprotein
5.491	Plasma membrane calcium-transporting ATPase 2
5.7961	RCG55135, isoform CRA_b
5.7961	Receptor expression-enhancing protein 5
5.8978	Uncharacterized protein (Fragment)
6.1011	RCG52629
6.4062	Guanine nucleotide-binding protein G(i) subunit alpha-2
6.5079	Uncharacterized protein
6.7113	Uncharacterized protein (Fragment)
6.7113	Peroxiredoxin-1
6.7113	Uncharacterized protein
6.8856	Myosin-Id
7.4739	Synaptosomal-associated protein 25
8.5416	V-type proton ATPase 116 kDa subunit a isoform 1
9.1517	Uncharacterized protein
9.1517	Uncharacterized protein
10.575	Similar to protein 4.1G (Predicted), isoform CRA_c
11.135	Uncharacterized protein
13.423	Claudin 11
18.914	Erythrocyte protein band 4.1-like 3, isoform CRA_b
19.829	Uncharacterized protein (Fragment)
24.405	Uncharacterized protein

Table 4.6. Fold-Change Values of MRPs Significantly Changed in Brainstem of DNB-Exposed 1mo Rats

MRPs <0.25-fold or >4.0-fold changed in 1mo DNB-exposed animals, as determined by NSAF. Green indicates >4.0-fold change in NSAF; Red indicates <0.25-fold change in NSAF.

DNB1mo	
Fold-Change	Protein Identification
0.0645	Putative ATP-dependent RNA helicase DHX30
0.1685	Uncharacterized protein
0.1853	Translation initiation factor IF-2
0.1977	Cytochrome c oxidase subunit 1
0.2085	Uncharacterized protein
0.218	L-2-hydroxyglutarate dehydrogenase (Predicted)
0.2224	Lysyl-tRNA synthetase
4.201	Uncharacterized protein (Fragment)
4.9424	RCG55135, isoform CRA_b
7.0714	Uncharacterized protein
7.4135	Amphiphysin

Table 4.7. Fold-Change Values of MRPs Significantly Changed in Brainstem of Control 3mo Rats
MRPs <0.25-fold or >4.0-fold changed in 3mo control animals, as determined by NSAF. Green indicates >4.0-fold change in NSAF; Red indicates <0.25-fold change in NSAF.

VC 3mo	
Fold-Change	Protein Identification
0.1255	Calcium/calmodulin-dependent protein kinase type II subunit alpha
0.1294	Alpha-aminoadipic semialdehyde synthase, mitochondrial
0.1381	L-2-hydroxyglutarate dehydrogenase (Predicted)
0.1453	Valyl-tRNA synthetase, mitochondrial
0.1624	Similar to RIKEN cDNA 0710008K08 (Predicted), isoform CRA_c
0.1998	1-phosphatidylinositol-4,5-bisphosphate phosphodiesterase beta-1
0.2071	2-oxoisovalerate dehydrogenase subunit alpha, mitochondrial (Fragment)
0.2157	Uncharacterized aarF domain-containing protein kinase 4
0.2301	Sulfite oxidase, mitochondrial
5.5227	Uncharacterized protein (Fragment)
5.5483	Cytoplasmic dynein 1 heavy chain 1
7.5938	Uncharacterized protein

Table 4.8. Fold-Change Values of MRPs Significantly Changed in Brainstem of DNB-Exposed 3mo Rats

MRPs <0.25-fold or >4.0-fold changed in 3mo DNB-exposed animals, as determined by NSAF. Green indicates >4.0-fold change in NSAF; Red indicates <0.25-fold change in NSAF.

DNB3mo	
Fold-Change	Protein Identification
0.1046	Cytochrome c oxidase subunit 3
0.1332	Protein FAM136A
0.169	RCG57079, isoform CRA_a
0.1723	Calcium/calmodulin-dependent protein kinase type II subunit alpha
0.1723	Uncharacterized protein (Fragment)
0.1928	Valyl-tRNA synthetase, mitochondrial
0.1972	Uncharacterized protein
0.1984	1-phosphatidylinositol-4,5-bisphosphate phosphodiesterase beta-1
0.2093	Malonyl-CoA decarboxylase, mitochondrial
0.2229	RCG21137
0.2442	ATP synthase protein 8
0.2442	Seryl-tRNA synthetase 2 (Predicted
0.2442	Coiled-coil domain containing 58 (Predicted), isoform CRA_c

Table 4.9. Fold-Change Values of MRPs Significantly Changed in Brainstem of Control 18mo Rats
MRPs <0.25-fold or >4.0-fold changed in 18mo control animals, as determined by NSAF. Green indicates >4.0-fold change in NSAF; Red indicates <0.25-fold change in NSAF.

VC 18mo	
Fold-Change	Protein Identification
0.0597	1-phosphatidylinositol-4,5-bisphosphate phosphodiesterase beta-1
0.0949	Similar to RIKEN cDNA 0710008K08 (Predicted), isoform CRA_c
0.1344	Calcium/calmodulin-dependent protein kinase type II subunit alpha
0.1753	NADPH:adrenodoxin oxidoreductase, mitochondrial
0.1833	Uncharacterized protein
0.2016	RCG42150
0.2091	RCG57079, isoform CRA_a
0.215	Cytochrome b
0.2264	Uncharacterized protein
0.2274	Nck-associated protein 1
0.2304	RCG21137
0.2304	Mitochondrial ribosomal protein S9
4.0321	RCG52516
4.0321	RCG44066
4.3345	Cytochrome c oxidase subunit 7A2, mitochondrial
4.3546	Uncharacterized protein
6.4513	Non-specific lipid-transfer protein

Table 4.10. Fold-Change Values of MRPs Significantly Changed in Brainstem of DNB-Exposed 18mo Rats

MRPs <0.25-fold or >4.0-fold changed in 18mo DNB-exposed animals, as determined by NSAF. Green indicates >4.0-fold change in NSAF; Red indicates <0.25-fold change in NSAF.

DNB 18mo	
Fold-Change	Protein Identification
0.1234	Uncharacterized protein
0.1426	Protein FAM54B
0.1475	RCG57079, isoform CRA_a
0.1944	Uncharacterized protein
0.2028	Uncharacterized protein
0.2139	Reticulon-1
0.2139	Biphenyl hydrolase-like (Serine hydrolase)
0.2139	Chaperone activity of bc1 complex-like, mitochondrial
0.2251	ATP-dependent RNA helicase SUPV3L1, mitochondrial
0.2292	Armadillo repeat-containing protein 10
0.2376	Calcium/calmodulin-dependent protein kinase type II subunit alpha
4.2777	Glial fibrillary acidic protein
6.06	Phosphorylase

REFERENCES

1. Magistretti PJ. Fundamental Neuroscience. 3rd ed. Larry R Squire DB, F. E. Bloom, S. du Lac, A. Ghosh, N.C. Spitzer, editor. San Diego: Academic Press; 2008.

2. Dutschke K, Nitsch RM, Hoyer S. Short-term mental activation accelerates the age-related decline of high-energy phosphates in rat cerebral cortex. Arch Gerontol Geriatr. 1994;19(1):43-51.

3. Bertoni-Freddari C, Fattoretti P, Giorgetti B, Spazzafumo L, Solazzi M, Balietti M. Age-related decline in metabolic competence of small and medium-sized synaptic mitochondria. Naturwissenschaften. 2005;92(2):82-5.

4. Navarro A, Sanchez Del Pino MJ, Gomez C, Peralta JL, Boveris A. Behavioral dysfunction, brain oxidative stress, and impaired mitochondrial electron transfer in aging mice. Am J Physiol Regul Integr Comp Physiol. 2002;282(4):R985-92.

5. Navarro A, Gomez C, Lopez-Cepero JM, Boveris A. Beneficial effects of moderate exercise on mice aging: survival, behavior, oxidative stress, and mitochondrial electron transfer. Am J Physiol Regul Integr Comp Physiol. 2004;286(3):R505-11.

6. Castellani R, Hirai K, Aliev G, Drew KL, Nunomura A, Takeda A, et al. Role of mitochondrial dysfunction in Alzheimer's disease. J Neurosci Res. 2002;70(3):357-60.

7. Abeliovich A. Parkinson's disease: Mitochondrial damage control. Nature. 2010;463(7282):744-5.

8. Philbert MA, Nolan CC, Cremer JE, Tucker D, Brown AW. 1,3-Dinitrobenzene-induced encephalopathy in rats. Neuropathol Appl Neurobiol. 1987;13(5):371-89.

9. Miller JA, Runkle SA, Tjalkens RB, Philbert MA. 1,3-Dinitrobenzene-induced metabolic impairment through selective inactivation of the pyruvate dehydrogenase complex. Toxicol Sci. 2011;122(2):502-11. PMCID: 3155080.

10. Steiner SR, Philbert MA. Proteomic identification of carbonylated proteins in 1,3-dinitrobenzene neurotoxicity. Neurotoxicology. 2011;32(4):362-73. PMCID: 3158615.

11. Tjalkens RB, Phelka AD, Philbert MA. Regional variation in the activation threshold for 1,3-DNB-induced mitochondrial permeability transition in brainstem and cortical astrocytes. Neurotoxicology. 2003;24(3):391-401.

12. Sims NR, Anderson MF. Isolation of mitochondria from rat brain using Percoll density gradient centrifugation. Nat Protoc. 2008;3(7):1228-39.

13. Leong SF, Lai JC, Lim L, Clark JB. Energy-metabolizing enzymes in brain regions of adult and aging rats. J Neurochem. 1981;37(6):1548-56.

14. Boumezbeur F, Mason GF, de Graaf RA, Behar KL, Cline GW, Shulman GI, et al. Altered brain mitochondrial metabolism in healthy aging as assessed by in vivo magnetic resonance spectroscopy. J Cereb Blood Flow Metab. 2010;30(1):211-21. PMCID: 2949111.

15. Hirai K, Aliev G, Nunomura A, Fujioka H, Russell RL, Atwood CS, et al. Mitochondrial abnormalities in Alzheimer's disease. J Neurosci. 2001;21(9):3017-23.

16. Schmuck G, Freyberger A, Ahr HJ, Stahl B, Kayser M. Effects of the new herbicide fentrazamide on the glucose utilization in neurons and erythrocytes in vitro. Neurotoxicology. 2003;24(1):55-64.

17. Chen L, Yoo SE, Na R, Liu Y, Ran Q. Cognitive impairment and increased Abeta levels induced by paraquat exposure are attenuated by enhanced removal of mitochondrial H(2)O(2). Neurobiol Aging. 2012;33(2):432 e15-26.

18. Shutov LP, Kim MS, Houlihan PR, Medvedeva YV, Usachev YM. Mitochondria and plasma membrane Ca2+-ATPase control presynaptic Ca2+ clearance in capsaicin-sensitive rat sensory neurons. J Physiol. 2013;591(Pt 10):2443-62. PMCID: 3678036.

19. Hughes SM, Moroni-Rawson P, Jolly RD, Jordan TW. Submitochondrial distribution and delayed proteolysis of subunit c of the H+-transporting ATP-synthase in ovine ceroid-lipofuscinosis. Electrophoresis. 2001;22(9):1785-94.

20. Lovell MA, Xiong S, Markesbery WR, Lynn BC. Quantitative proteomic analysis of mitochondria from primary neuron cultures treated with amyloid beta peptide. Neurochem Res. 2005;30(1):113-22.

21. Wang Y, Bogenhagen DF. Human mitochondrial DNA nucleoids are linked to protein folding machinery and metabolic enzymes at the mitochondrial inner membrane. J Biol Chem. 2006;281(35):25791-802.

22. Dias J, Octobre G, Kobbi L, Comisso M, Flisiak S, Mirande M. Activation of human mitochondrial lysyl-tRNA synthetase upon maturation of its premitochondrial precursor. Biochemistry. 2012;51(4):909-16.

23. Spencer AC, Spremulli LL. The interaction of mitochondrial translational initiation factor 2 with the small ribosomal subunit. Biochim Biophys Acta. 2005;1750(1):69-81.

24. Gardlik S, Rajagopalan KV. Oxidation of molybdopterin in sulfite oxidase by ferricyanide. Effect on electron transfer activities. J Biol Chem. 1991;266(8):4889-95.

25. Jobgen WS, Fried SK, Fu WJ, Meininger CJ, Wu G. Regulatory role for the arginine-nitric oxide pathway in metabolism of energy substrates. J Nutr Biochem. 2006;17(9):571-88.

26. Musser SM, Stowell MH, Chan SI. Cytochrome c oxidase: chemistry of a molecular machine. Adv Enzymol Relat Areas Mol Biol. 1995;71:79-208.

27. Yun B, Lee H, Ghosh M, Cravatt BF, Hsu KL, Bonventre JV, et al. Serine hydrolase inhibitors block necrotic cell death by preventing calcium overload of the mitochondria and permeability transition pore formation. J Biol Chem. 2014;289(3):1491-504. PMCID: 3894331.

28. Brasseur G, Tron G, Dujardin G, Slonimski PP, Brivet-Chevillotte P. The nuclear ABC1 gene is essential for the correct conformation and functioning of the cytochrome bc1 complex and the neighbouring complexes II and IV in the mitochondrial respiratory chain. Eur J Biochem. 1997;246(1):103-11.

29. Wang DD, Shu Z, Lieser SA, Chen PL, Lee WH. Human mitochondrial SUV3 and polynucleotide phosphorylase form a 330-kDa heteropentamer to cooperatively degrade double-stranded RNA with a 3'-to-5' directionality. J Biol Chem. 2009;284(31):20812-21. PMCID: 2742846.

CHAPTER V

Conclusion & Future Directions

The vestibulocochlear nerve (the VIIIth cranial nerve) provides the ascending sensory input for the auditory and vestibular systems of the brain, and functions to maintain both balance and hearing. The vestibular and auditory branches of this nerve innervate specific brainstem nuclei, including the vestibular nuclei and inferior colliculi (1). Exposure to 1,3-Dinitrobenzene (DNB) causes gliovascular lesions in precisely those regions of the brain supplied by the VIIIth cranial nerve (2). Despite the lack of any morphological changes in the nerve root (Philbert – unpublished observations), it is not clear whether or not the gliovascular lesions produced by DNB in the brainstem are the product of primary damage to the nerve *per se* or direct insult to astrocytes in the brainstem: morphological evidence points to the latter. Nevertheless, auditory function and neuronal activity provide insights into the interplay between function and susceptibility. Unilateral rupture of the tympanic membrane reduces glucose consumption in vulnerable regions ipsilateral to the deafened ear while exposure of the intact ear to white noise exacerbates the lesion in the contralateral brainstem in animals that were also exposed to DNB (3). These findings provide compelling evidence that that metabolic demand (and, therefore, mitochondrial workload) in response to the level of auditory function and lesion severity are closely interrelated.

Astrocytes provide structural collateral stabilization to neurons, trophic biochemical support, participate in regulatory volume decrease through the management of ions in the extracellular space and actively maintain the integrity of the blood-brain-barrier: all functions that require energy and, by extension, functional mitochondria (4). Astrocytes are a primary cellular target of DNB as indicated by the rapid onset of focal oncotic necrosis observed in vulnerable brainstem nuclei adjacent to the IV^{th} ventricle prior to neuronal involvement (2). One important way in which astrocytes protect neurons is by releasing adenosine triphosphate (ATP) into the extracellular space, which is dephosphorylated to adenosine which itself binds to the A_1 receptor on the neuronal surface and attenuates synaptic transmission (5). An increase in extracellular adenosine has been shown to occur rapidly in a concentration-dependent fashion following exposure of DI-TNC_1 immortalized astrocytes to DNB *in vitro* (6). This finding *in vitro* is consistent with the idea adenosine is either passively (through loss of membrane integrity) or actively (through as yet unidentified membrane transport mechanisms) released by astrocytes into the extracellular space where it may act as a silencing neurotransmitter on neuronal adenosine receptors following DNB exposure. The functional consequence of this sequence of events us that DNB exposure causes ataxia in rats due to development of lesions in the vestibular system (2).

While DNB exposure causes diminution of proprioception that manifests as ataxia, the physiological aging process provides for time-dependent degradation of audiovestibular function: in humans, increased age is associated with increased numbers of amyloid plaque in the vestibulocochlear nerve (mainly confined to the glia)

(7). Epidemiological studies support the link between age-related loss of function of the sensory pathways of the vestibulocochlear nerve: sixty-three percent of people in the United States over the age of 70 have hearing loss (8), and 40% of people over the age of 65 living in the United States living at home will fall at least once per year, with 75% of deaths due to falls occurring in this age group (9). Additionally, a recent study investigated the link between incidence of falls and hearing loss in older adults in the United States, and found that the transition from normal hearing to mild hearing loss is associated with a 3-fold increased odds of reporting a fall within the last year (10). These clinical and epidemiological findings in humans are supported by experimental studies in rodents.

Older mice exhibit higher levels of oxidized mitochondrial glutathione and mtDNA in the brain compared to younger mice, which was found to be inversely related with motor coordination in the older mice (11). These data suggest that age-related loss of function of the vestibular and auditory systems may be linked, and may be a result of mitochondrial and glial dysfunction manifesting over time. This attenuation of function during the aging process was hypothesized to increase mitochondrial susceptibility in the brainstem to DNB-induced neurotoxicity; this overarching hypothesis was tested using *in vitro* methods investigating neuroprotective functions of astrocytes exposed to DNB as a function of passage number, and *in vivo* methods investigating the role of aging in regionally differential mitochondrial susceptibility to protein oxidation and differential MRP expression in DNB exposure.

PASSAGE EFFECT IN ASTROCYTES – SURROGATE FOR AGING

Astrocytes provide neuronal support by composing the blood brain barrier and releasing neuroprotective factors such as adenosine; DNB exposure causes breakdown of the former (observed as astrocytic foot process swelling) (2) and induction of the latter (6). Despite their responsibility to maintain the neuronal extracellular environment, astrocytes in the aging brain lose their ability to perform neuroprotective functions, including maintenance of neuronal mitochondrial membrane potential (12).

While immortalized cells are used in laboratories because of their relative ease and reproducibility of results regardless of how many times they are passaged, this study provides novel data on DNB-induced functional changes in high passage immortalized astrocytes (DI-TNC_1) compared to low passage immortalized astrocytes. Metrics of mitochondrial function were assessed in monoculture DI-TNC_1 astrocytes and in DI-TNC_1 astrocytes co-cultured with primary neurons, as were neuroprotective functions.

Monoculture high passage DI-TNC_1 astrocytes contain mitochondria that are more sensitive to DNB exposure than low passage DI-TNC_1 astrocytes; there was an observed passage#-dependent susceptibility to first mitochondrial flickering events and a concurrent decrease in mitochondrial aspect ratio in which high passage DI-TNC_1 astrocytes exhibit an *earlier* first flickering event and decrease in mitochondrial aspect ratio compared to low passage DI-TNC_1 astrocytes. Based on mitochondrial dynamics in monoculture DI-TNC_1 astrocytes, the described passage effect may be an acceptable surrogate for the aging of astroctyes *in vitro*, as these same mitochondrial dynamics are altered significantly in the aged brain (mitochondrial volume increase in aged rat brain (13), decreased mitochondrial membrane potential in senescence-accelerated mice

prone (SAMP8) mouse astrocytes (14). These measurements of mitochondrial dynamics correlate with an attenuation of high passage DI-TNC_1 astrocyte proliferation compared to low passage DI-TNC_1 astrocyte proliferation, suggesting that the observed disturbances in mitochondrial dynamics in high passage DI-TNC_1 astrocytes are reflective of decreased mitochondrial function, as cellular proliferation is an "energy-expensive" process.

In a co-culture system, high passage DI-TNC_1 astrocytes exhibited less effective neuroprotective functions than low passage DI-TNC_1 astrocytes. This was evident in data presented in Chapter II in which low passage DI-TNC_1 astrocytes prevented neuronal depolarization to a greater extent than high passage DI-TNC_1 astrocytes in DNB exposure and prevented mitochondrial depolarization in neurons to a greater extent than high passage DI-TNC_1 astrocytes in DNB exposure. Furthermore, low passage DI-TNC_1 astrocytes were better able to survive DNB exposure in a co-culture system, which suggests that not only do mitochondria from low passage DI-TNC_1 astrocytes have the ability to function such that they preserve astrocytic functions in response to the neuronal environment, but also maintain astrocyte viability in DNB exposure. This level of resistance to DNB exposure was not observed in high passage DI-TNC_1 astrocytes.

This study provides compelling evidence supporting a mitochondrial role in the passage effect observed in astrocytes in DNB exposure indicating that the observed changes are necessary for DNB-induced neurotoxicity. However, the data in this aim do not assume sufficiency to cause lesions as observed in DNB exposure. Neurotoxicity caused by DNB involves multiple factors, some of which have already

been elucidated in astrocytes: adenosine release by DI-TNC_1 astrocytes (6) and carbonylation of specific mitochondrial proteins in DI-TNC_1 astrocytes (15). Due to the regionally-specific nature of lesions induced by DNB exposure, the current aim ignores any inherent, physiological differences there might be between brainstem astrocytes and other astrocytes; since DI-TNC_1 astrocytes are derived from diencephalon, which doesn't incur lesions in DNB exposure, this aim may be overlooking some of these as of yet unknown, potentially functional differences in astrocytes from different regions of the brain. However, this study adds to the current body of data utilizing DI-TNC_1 astrocytes to investigate cell-specific changes in DNB exposure in that it investigates the role of aging by way of passage number as a proxy for the aging process.

To further elucidate mitochondrial mechanisms that may be affected by passage number in DNB exposure, the co-culture experiments investigating intracellular calcium dynamics in neurons may be expanded. The current data shows that DNB exposure causes a decrease in free cytosolic calcium in neurons co-cultured with both low and high DI-TNC_1 astrocytes, with the low passage DI-TNC_1 astrocytes exhibiting more pronounced prevention of depolarization (as measured by free intracellular calcium concentrations). Because mitochondria are a storage compartment for intracellular calcium in neurons (16) and the ability of mitochondria to buffer the intracellular space by sequestering calcium diminishes in the aging brain (17), it's possible that neurons co-cultured with low passage DI-TNC_1 astrocytes mimics a "younger" phenotype in which the observed lower intracellular calcium concentration in neurons caused by DNB exposure compared to neurons co-cultured with high passage DI-TNC_1 astrocytes is due to an increase in mitochondrial calcium sequestration. This could be determined by

utilizing a mitochondrially-permeant, calcium-indicating dye (such as Rhod2 AM) concurrently with a dye that fluoresces upon binding with free cytosolic calcium (such as Fluo4 AM) and time-lapse fluorescence imaging as performed in Chapter II.

Future work aiming to determine whether or not high passage DI-TNC_1 astrocytes are an acceptable proxy for aged astrocytes *in vivo* could include a proteomic analysis of methionine oxidation and MRP expression in isolated mitochondria from both low passage DI-TNC_1 astrocytes and high passage DI-TNC_1 astrocytes. This would provide a direct contrast with data presented in Chapters III & IV of this dissertation, and place the observed *in vivo* data from those two chapters further in context with the metrics of neuroprotection observed in Chapter II.

AGE-ASSOCIATED, DNB-INDUCED SPECIFIC OXIDATIVE PROTEOMIC MODIFICATIONS IN BRAINSTEM MITOCHONDRIA

While it is generally true that the brain becomes more oxidized with age, the type of macromolecule that's targeted for oxidation and the degree to which oxidation occurs on these macromolecules can vary by region (18), (19), (20). In this study, not only were brainstem MRPs more prone to DNB-induced oxidation than cortical MRPs, the degree to which the oxidation occurred in brainstem MRPs was significantly higher than their cortical counterparts. This suggests that there is regional variation in susceptibility to DNB-induced MRP oxidation, and that increased oxidation to MRPs in aggregate may be part of the mechanism of injury in the development of lesions in the brainstem due to DNB exposure. However, Chapter III provides convincing evidence that the sheer amount of oxidation incurred by the mitochondrial proteome during aging which becomes exacerbated by DNB exposure might not fully explain lesion development;

there is clear specificity with which DNB-induced oxidation occurs. This is true with regards to both *region* (in 1mo animals, there is a decrease in oxidation in one MRP in brainstem, no changes observed in 3mo animals, and an increase in oxidation in 7 MRPs in 18mo brainstem; no decreases below 0.25-fold or increases above 4.0-fold in %Oxidation were observed in cortex) and *age* (there was an observed >4.0-fold oxidation of 4 MRPs in cortex and 13 MRPs in brainstem compared to 1mo cortex and brainstem, and no changes were seen in 3mo cortex or brainstem MRP oxidation).

Age was associated with the development of DNB-induced lesions; only in the brainstem of the oldest animals was there an observed vacuolation pattern typical of DNB exposure (2) and consistent with the swelling of astrocyte processes (21). There must be careful interpretation of this data when using the observed MRP oxidation data to explain the mechanism behind lesion development: the mitochondria used in the proteomics experiment were isolated from animals exposed to DNB at 0h, 4h, and 24h with a 24h lapse between the last exposure and animal sacrifice; this exposure timeline was only used for the mitochondrial isolation experiments due to the high mortality rate in the oldest group of DNB-exposed animals (60%). For this purpose, we used the following exposure timeline for the remaining experiments (hematoxylin and eosin-stained sections for lesion analysis; immunohistochemistry for presence of carbonylation): 0h, 4h, and 24h with a 12h lapse between the last exposure and animal sacrifice. That said, it is likely that the specificity and amount of MRP oxidation observed would be attributed to a more severe pattern of lesion in brainstem of the oldest DNB-exposed animals, as the development of lesions in the brainstem of the oldest DNB-exposed animals was still observed in a shorter exposure timeline.

Additionally, in each group of exposure timelines, the oldest animals exposed to DNB presented with ataxia at a rate of 100%.

In addition to causing widespread oxidation in brainstem MRPs, DNB also causes specific oxidation in brainstem MRPs that constitute distinct molecular pathways: cation transmembrane transporter, nucleoside-triphosphatase, pyrophosphatase, and hydrolase activity. The same three MRPs constituted 80% of the pathways identified as significantly oxidized in brainstem by DNB: cytoplasmic dynein, tubulin, and a plasma membrane calcium-transporting ATPase. All three of these proteins are involved in mitochondrial transport: dynein is one of the linker proteins that binds to both the mitochondrion and the microtubule, facilitating mitochondrial transport in neurons (22), tubulin heterodimers form the microtubule on which the mitochondrion is transported throughout the cell, and calcium-transporting ATPases regulate intracellular and extracellular calcium levels; if intracellular calcium concentrations are elevated in the brain, the induction of the mitochondrial permeability transition pore may occur (23), which can alter the pattern of mitochondrial transport throughout the cell (24). Because cytoplasmic dynein, tubulin, and calcium-transporting ATPases participate in mitochondrial transport, it's plausible that part of the mechanism of DNB neurotoxicity in the brainstem related to advanced age results from the inability of the neural cells in this region to respond to localized demand for ATP. This is supported by evidence showing that in rodents presenting with neurodegenerative pathologies, mitochondrial trafficking in the brain is diminished (25). A resulting hypothesis might be, then, that the observed DNB-induced oxidation to dynein, tubulin, and calcium-transporting ATPases in the brainstem may result in functional changes to those

proteins, providing a mechanistic basis for the observed lesions and clinical signs of intoxication in the oldest animals exposed to DNB. Relevant future experiments would include conducting activity assays on these proteins purified from the brainstem of old animals exposed to DNB.

Because DNB targets brainstem astrocytes prior to the appearance of neuronal effects (2), future work might include the proteomic analysis of cell-specific oxidative modifications to MRPs in brainstem. For the purposes of this study, the lack of sufficiency of protein concentrations from each respective cell type in affected regions of the brainstem prevented a proteomic analysis of this type. Because there are significant age-associated increases in both neuron (26), (27) and astrocyte oxidation (28), (29) in the brain, it is likely that there will be significant increases oxidation in each cell type in old animals; however, due to astrocytes being a cellular target of DNB, it could be hypothesized that astrocytes would likely accrue more oxidative damage than neurons in the brainstem in DNB exposure, even in the oldest animals.

MITOCHONDRIA-RELATED PROTEIN EXPRESSION AS A FUNCTION OF AGE, BRAIN REGION, AND DNB EXPOSURE

In this study, increased expression of MRPs in young control brainstem correlates with resistance against lesion development in the brainstem and presentation of clinical signs of intoxication during DNB exposure. This suggests that younger animals have compensatory molecular pathways in the brainstem that aid in the response to DNB-induced neurotoxicity, which was indeed shown to be true in Chapter IV. In young control animals, there were 11 distinct molecular function pathways upregulated in the brainstem, whereas there were no upregulated pathways in either

3mo or 18mo brainstem. In fact, catalytic activity was downregulated in 3mo brainstem and protein binding was decreased in the 18mo brainstem in control animals, suggesting that the physiological aging process itself causes a decrease in cohesive pathways involving MRPs. Interestingly, DNB exposure caused the downregulation of the same pathway in the brainstem of every age group (catalytic activity). However, the proteins that constituted the catalytic activity pathway were different for each age group. This suggests that while DNB exposure causes a decrease in very specific MRPs in the brainstem that participate in catalysis, the reactions which require catalysis by these MRPs are targeted differentially by DNB in an age-dependent manner. That is, the observed downregulation in brainstem MRPs induced by DNB may be made more susceptible due to the physiological aging process.

While the observed changes in MRP expression appear to be necessary to confer age-related mitochondrial susceptibility to DNB-induced neurotoxicity, it has not been determined sufficient to describe aging effects on this relationship in totality. It is indeed true that young control animals display increased expression of MRPs compared to older control animals *and* that DNB exposure drastically decreases MRP expression compared to each respective age-matched control. However, there are factors affecting protein expression itself that are of particular importance to mitochondrial proteins in the aging brain. Because mtDNA only contains 37 genes, 13 of which contain the genes for enzymes in the electron transport chain, the majority of MRPs are expressed by nuclear genes (nuclear genes encode 99% of mitochondrial proteins; 1% are encoded by mtDNA) (30). In order for a protein to be imported into the mitochondrion for use, it must contain a targeting signal to be recognized by the mitochondrion and must be in

the proper conformation (30), as most mitochondrially-imported proteins are kept in an unfolded conformation prior to import (31). Aging is known to decrease the efficiency of this process: protein misfolding increases in the brain during aging (32), and increased oxidative stress (as is often associated with increases in age) inhibits the protein import into mitochondria (33).

Additionally, DNB exposure causes the selective carbonylation of mitochondrial heat shock protein 70 (mtHsp70) in astrocytes (15). Because mtHsp70 is a molecular chaperone that uses ATP to translocate mitochondrially-targeted polypeptides from the cytosol to the mitochondrial matrix (34), the decrease in MRP expression caused by DNB even in the youngest age group could be related to dysregulation of brainstem MRP import and processing in astrocytes; the loss of regulation of protein folding itself during aging in the brain likely exacerbated the effects of DNB in the oldest animals.

Because many MRPs first exist as “precursor peptides” (31) that can easily become misfolded, recent work has shown that mitochondria may be able to more efficiently respond to localized demands for ATP by maintaining higher amounts of mRNA for mitochondrially-tagged proteins in a close vicinity to the mitochondrion [Reviewed by Devaux, et al. (35)]. This suggests that levels of mRNA specific to MRPs, not just MRP expression itself, may be very important to the ability of the mitochondrion to respond to localized ATP demands, which is likely diminished in aged animals exposed to DNB.

Future work investigating the role of aging and DNB exposure on proper MRP import and processing would involve procuring the cytosolic fraction of proteins in addition to the mitochondrial fraction to compare the concentrations of mitochondrially-

tagged peptides destined for the mitochondrion versus those that actually gain entry to the organelle. This experiment could be done using the same LC/MS-MS techniques used in this study. Additionally, to assess for proper protein folding, one could use the results generated from the LC/MS/MS to compile a list of MRPs of interest, purify the protein, and assess for secondary protein structure by using circular dichroism or protein nuclear magnetic resonance.

ADDITIONAL CONSIDERATIONS

Sex-Specific Differences in Neural Function across the Lifespan – Relevance to Current Study

This study utilized only male rats for the investigation of aging effects on mitochondrial susceptibility to DNB-induced neurotoxicity. Therefore, these results may not be as easily extended to include the total population. That said, the experimental design excluded female rats for reasons of simplicity: estrogen acts as a neuroprotective hormone in cases of stroke [reviewed by Liu and Yang (36)], Parkinson's Disease [(reviewed by Bourque (37)], and Alzheimer's Disease [reviewed by Correia (38)]. While male rodents do express estrogen receptors in the brain (39), females typically have higher and more variable circulating concentrations of estrogen compared to males (40). Therefore, estrogenic effects on endpoints measured in this study could have potentially masked or exaggerated the results, as the concentration of estrogen fluctuates with the animal's age (40).

Because of the potentially confounding role of estrogen in its ability to be neuroprotective, it would likely introduce a differential response to DNB between male and female rats. This supposition is reinforced by a body of recent evidence suggesting that astrocytes are involved with estrogenic neuroprotective pathways in response to

manganese exposure (41), in Alzheimer's Disease (42), and in 1-methyl-4-phenyl-1,2,3,6-tetrahydropyridine (MPTP) exposure in male mice (43). Because astrocytes are a primary cellular target in DNB exposure (2), the pathophysiological mechanisms with which male and female rodents respond to DNB may differ. Additionally, estrogen can interact directly with mitochondria by binding directly to Complex V of the electron transport chain, causing inhibition of this complex (44). Therefore, not only does estrogen interact with the cellular target of DNB, but also with an important organellar target of DNB, the mitochondrion, further establishing sex-specific differences related to estrogen as a potential confounder.

Moreover, there is evidence supporting age-related, sex-specific differences in mitochondrial function in the aging rodent brain (in which females retain mitochondria that are more functional than mitochondria in males) (45), which may or may not have anything to do with estrogen itself. In the human brain, men exhibit age-related decreases in whole brain and frontal and temporal lobe volume, whereas in women, significant age-related losses in volume occur in the parietal lobes and hippocampus (46). The same study also found sex-specific differential glucose metabolism that varied across regions of the brain (46).

Because there are as of yet undetermined mechanisms underlying neurotoxic effects of environmental exposures, this study may be excluding important factors in the female brain that confer mitochondrial susceptibility to neurotoxicity. The most obvious oversight may be in the aforementioned role of estrogen in neuroprotection. However, there are more overlapping neural mechanisms between the male and female brain

than not; thus, this study still highlights important insight into the role of aging on mitochondrial susceptibility to DNB toxicity.

CONCLUDING REMARKS

This body of work gives supporting evidence of age-related mitochondrial susceptibility to DNB-induced neurotoxicity. Because both *in vivo* and *in vitro* methods were utilized in this study, it provides not only an in-depth look at the neuroprotective capacity of astrocytes due to their age *in vitro*, but also gain insight into specific mitochondrial posttranslational modifications as a result of aging and induced by DNB exposure *in vivo*, which gives a more inclusive picture of physiological aging compared to what is offered by *in vitro* techniques.

This study highlights the intersection between mitochondrial insults that may accrue during the lifespan and additional mitochondrial stress induced by exposure to DNB. Data put forth in this dissertation supports the hypotheses that astrocytes are less able to perform neuroprotective functions as they age, that DNB exposure causes age-related, region-specific, significant oxidative damage to MRPs, and that DNB exposure causes an age-related, region-specific decrease in MRP expression. These results indicate that the observed age-related alterations to astrocyte mitochondrial dynamics and resultant neuroprotective functions, and specific damage to brainstem MRPs as a result of DNB exposure are necessary to produce lesions and manifest as ataxia. There are, however, other components of the mechanism by which DNB induces damage to the brainstem with a resultant loss of function of the vestibular and

auditory system: adenosine release by astrocytes (6), carbonylation of specific MRPs in astrocytes (15), increased cerebral blood flow (47), decreases of glutathione concurrent with increases in glucose consumption in astrocytes (48), and region-specific alterations to astrocyte mitochondrial membrane potential (49). Thus, the data presented in this study is novel in that it includes an aging component in mitochondrial susceptibility to DNB neurotoxicity (and is necessary to induce injury), but alone is not sufficient to explain the mechanisms involved in DNB neurotoxicity.

While DNB is known to cause gliovascular lesions confined to specific brainstem nuclei (2) which cause ataxia due to loss of function in the vestibulocochlear system, there is an age-related decrease in the function of the vestibulocochlear system as well, as evidenced by the increased incidence of falls and loss of hearing in the elderly population in the United States (8), (9). The physiological aging process induces vulnerabilities, such as an overall increase in mitochondrial oxidative stress, the blood-brain barrier becomes leaky, and astrocyte function declines. These functional declines are not confined to those areas in which DNB exposure causes lesions, but instead have been observed globally in the brain. In either DNB exposure or aging, decreases in function in the vestibular and auditory systems are typically not sufficient to cause death; rather, the morphological alterations are precipitating events in the progression toward an increased risk of mortality/morbidity (9).

The question still remains, then, what renders brainstem astrocytes and mitochondria more *vulnerable* to DNB-induced damage (a condition that is exacerbated by the aging process); conversely, what makes cortical astrocyte mitochondria more *resistant* to this

age-related susceptibility to damage caused by DNB exposure remains to be investigated.

REFERENCES

1. Sanders RD, Gillig PM. Cranial Nerve VIII: Hearing and Vestibular Functions. Psychiatry (Edgmont). 2010;7(3):17-22. PMCID: 2861521.

2. Philbert MA, Nolan CC, Cremer JE, Tucker D, Brown AW. 1,3-Dinitrobenzene-induced encephalopathy in rats. Neuropathol Appl Neurobiol. 1987;13(5):371-89.

3. Ray DE, Abbott NJ, Chan MW, Romero IA. Increased oxidative metabolism and oxidative stress in m-dinitrobenzene neurotoxicity. Biochem Soc Trans. 1994;22(4):407S.

4. Volobouéva LA, Suh SW, Swanson RA, Giffard RG. Inhibition of mitochondrial function in astrocytes: implications for neuroprotection. J Neurochem. 2007;102(4):1383-94. PMCID: 3175820.

5. Pascual O, Casper KB, Kubera C, Zhang J, Revilla-Sanchez R, Sul JY, et al. Astrocytic purinergic signaling coordinates synaptic networks. Science. 2005;310(5745):113-6.

6. Wang Y, Liu X, Schneider B, Zverina EA, Russ K, Wijeyesakere SJ, et al. Mixed inhibition of adenosine deaminase activity by 1,3-dinitrobenzene: a model for understanding cell-selective neurotoxicity in chemically-induced energy deprivation syndromes in brain. Toxicol Sci. 2012;125(2):509-21. PMCID: 3262860.

7. Fujii M, Goto N, Okada A, Kida A, Kikuchi K. Distribution of amyloid bodies in the aged human vestibulocochlear nerve. Acta Otolaryngol. 1996;116(4):566-71.

8. Lin FR, Thorpe R, Gordon-Salant S, Ferrucci L. Hearing loss prevalence and risk factors among older adults in the United States. J Gerontol A Biol Sci Med Sci. 2011;66(5):582-90. PMCID: 3074958.

9. Rubenstein LZ. Falls in older people: epidemiology, risk factors and strategies for prevention. Age Ageing. 2006;35 Suppl 2:ii37-ii41.

10. Lin FR, Ferrucci L. Hearing loss and falls among older adults in the United States. Arch Intern Med. 2012;172(4):369-71. PMCID: 3518403.

11. Pallardo FV, Asensi M, Garcia de la Asuncion J, Anton V, Lloret A, Sastre J, et al. Late onset administration of oral antioxidants prevents age-related loss of motor co-ordination and brain mitochondrial DNA damage. Free Radic Res. 1998;29(6):617-23.

12. Lin DT, Wu J, Holstein D, Upadhyay G, Rourk W, Muller E, et al. Ca2+ signaling, mitochondria and sensitivity to oxidative stress in aging astrocytes. Neurobiol Aging. 2007;28(1):99-111.

13. Bertoni-Freddari C, Fattoretti P, Casoli T, Spagna C, Meier-Ruge W, Ulrich J. Morphological plasticity of synaptic mitochondria during aging. Brain Res. 1993;628(1-2):193-200.

14. Garcia-Matas S, Gutierrez-Cuesta J, Coto-Montes A, Rubio-Acero R, Diez-Vives C, Camins A, et al. Dysfunction of astrocytes in senescence-accelerated mice SAMP8 reduces their neuroprotective capacity. Aging Cell. 2008;7(5):630-40.

15. Steiner SR, Philbert MA. Proteomic identification of carbonylated proteins in 1,3-dinitrobenzene neurotoxicity. Neurotoxicology. 2011;32(4):362-73. PMCID: 3158615.

16. Thayer SA, Miller RJ. Regulation of the intracellular free calcium concentration in single rat dorsal root ganglion neurones in vitro. J Physiol. 1990;425:85-115. PMCID: 1189839.

17. Tonkikh AA, Carlen PL. Impaired presynaptic cytosolic and mitochondrial calcium dynamics in aged compared to young adult hippocampal CA1 synapses ameliorated by calcium chelation. Neuroscience. 2009;159(4):1300-8.

18. Yanar K, Aydin S, Cakatay U, Mengi M, Buyukpinarbasili N, Atukeren P, et al. Protein and DNA oxidation in different anatomic regions of rat brain in a mimetic ageing model. Basic Clin Pharmacol Toxicol. 2011;109(6):423-33.

19. Kumar P, Taha A, Sharma D, Kale RK, Baquer NZ. Effect of dehydroepiandrosterone (DHEA) on monoamine oxidase activity, lipid peroxidation and lipofuscin accumulation in aging rat brain regions. Biogerontology. 2008;9(4):235-46.

20. Giovannelli L, Decorosi F, Dolara P, Pulvirenti L. Vulnerability to DNA damage in the aging rat substantia nigra: a study with the comet assay. Brain Res. 2003;969(1-2):244-7.

21. Garman RH. Histology of the central nervous system. Toxicol Pathol. 2011;39(1):22-35.

22. Pilling AD, Horiuchi D, Lively CM, Saxton WM. Kinesin-1 and Dynein are the primary motors for fast transport of mitochondria in Drosophila motor axons. Mol Biol Cell. 2006;17(4):2057-68. PMCID: 1415296.

23. Kristal BS, Dubinsky JM. Mitochondrial permeability transition in the central nervous system: induction by calcium cycling-dependent and -independent pathways. J Neurochem. 1997;69(2):524-38.

24. Guo L, Du H, Yan S, Wu X, McKhann GM, Chen JX, et al. Cyclophilin D deficiency rescues axonal mitochondrial transport in Alzheimer's neurons. PLoS One. 2013;8(1):e54914. PMCID: 3561411.

25. Du H, Guo L, Yan S, Sosunov AA, McKhann GM, Yan SS. Early deficits in synaptic mitochondria in an Alzheimer's disease mouse model. Proc Natl Acad Sci U S A. 2010;107(43):18670-5. PMCID: 2972922.

26. Kumar A, Foster TC. Linking redox regulation of NMDAR synaptic function to cognitive decline during aging. J Neurosci. 2013;33(40):15710-5. PMCID: 3787496.

27. Nunomura A, Tamaoki T, Motohashi N, Nakamura M, McKeel DW, Jr., Tabaton M, et al. The earliest stage of cognitive impairment in transition from normal aging to Alzheimer disease is marked by prominent RNA oxidation in vulnerable neurons. J Neuropathol Exp Neurol. 2012;71(3):233-41. PMCID: 3288284.

28. Klamt F, Gottfried C, Tramontina F, Dal-Pizzol F, Da Frota ML, Jr., Moreira JC, et al. Time-related increase in mitochondrial superoxide production, biomolecule damage and antioxidant enzyme activities in cortical astrocyte cultures. Neuroreport. 2002;13(12):1515-8.

29. Schipper HM, Vininsky R, Brull R, Small L, Brawer JR. Astrocyte mitochondria: a substrate for iron deposition in the aging rat substantia nigra. Exp Neurol. 1998;152(2):188-96.

30. Schmidt O, Pfanner N, Meisinger C. Mitochondrial protein import: from proteomics to functional mechanisms. Nat Rev Mol Cell Biol. 2010;11(9):655-67.

31. Lionaki E, Tavernarakis N. Oxidative stress and mitochondrial protein quality control in aging. J Proteomics. 2013;92:181-94.

32. Naidoo N, Ferber M, Master M, Zhu Y, Pack AI. Aging impairs the unfolded protein response to sleep deprivation and leads to proapoptotic signaling. J Neurosci. 2008;28(26):6539-48. PMCID: 2925257.

33. Wright G, Terada K, Yano M, Sergeev I, Mori M. Oxidative stress inhibits the mitochondrial import of preproteins and leads to their degradation. Exp Cell Res. 2001;263(1):107-17.

34. Chacinska A, Koehler CM, Milenkovic D, Lithgow T, Pfanner N. Importing mitochondrial proteins: machineries and mechanisms. Cell. 2009;138(4):628-44.

35. Devaux F, Lelandais G, Garcia M, Goussard S, Jacq C. Posttranscriptional control of mitochondrial biogenesis: spatio-temporal regulation of the protein import process. FEBS Lett. 2010;584(20):4273-9.

36. Liu R, Yang SH. Window of opportunity: estrogen as a treatment for ischemic stroke. Brain Res. 2013;1514:83-90. PMCID: 3664650.

37. Bourque M, Dluzen DE, Di Paolo T. Neuroprotective actions of sex steroids in Parkinson's disease. Front Neuroendocrinol. 2009;30(2):142-57.

38. Correia SC, Santos RX, Cardoso S, Carvalho C, Santos MS, Oliveira CR, et al. Effects of estrogen in the brain: is it a neuroprotective agent in Alzheimer's disease? Curr Aging Sci. 2010;3(2):113-26.

39. Zhang JQ, Cai WQ, Zhou DS, Su BY. Distribution and differences of estrogen receptor beta immunoreactivity in the brain of adult male and female rats. Brain Res. 2002;935(1-2):73-80.

40. Simpson E, Rubin G, Clyne C, Robertson K, O'Donnell L, Jones M, et al. The role of local estrogen biosynthesis in males and females. Trends Endocrinol Metab. 2000;11(5):184-8.

41. Lee E, Sidoryk-Wegrzynowicz M, Yin Z, Webb A, Son DS, Aschner M. Transforming growth factor-alpha mediates estrogen-induced upregulation of glutamate transporter GLT-1 in rat primary astrocytes. Glia. 2012;60(7):1024-36. PMCID: 3353324.

42. Ramirez CM, Gonzalez M, Diaz M, Alonso R, Ferrer I, Santpere G, et al. VDAC and ERalpha interaction in caveolae from human cortex is altered in Alzheimer's disease. Mol Cell Neurosci. 2009;42(3):172-83.

43. Tripanichkul W, Sripanichkulchai K, Finkelstein DI. Estrogen down-regulates glial activation in male mice following 1-methyl-4-phenyl-1,2,3,6-tetrahydropyridine intoxication. Brain Res. 2006;1084(1):28-37.

44. Zheng J, Ramirez VD. Rapid inhibition of rat brain mitochondrial proton F0F1-ATPase activity by estrogens: comparison with Na+, K+ -ATPase of porcine cortex. Eur J Pharmacol. 1999;368(1):95-102.

45. Guevara R, Gianotti M, Roca P, Oliver J. Age and sex-related changes in rat brain mitochondrial function. Cell Physiol Biochem. 2011;27(3-4):201-6.

46. Murphy DG, DeCarli C, McIntosh AR, Daly E, Mentis MJ, Pietrini P, et al. Sex differences in human brain morphometry and metabolism: an in vivo quantitative

magnetic resonance imaging and positron emission tomography study on the effect of aging. Arch Gen Psychiatry. 1996;53(7):585-94.

47. Romero I, Brown AW, Cavanagh JB, Nolan CC, Ray DE, Seville MP. Vascular factors in the neurotoxic damage caused by 1,3-dinitrobenzene in the rat. Neuropathol Appl Neurobiol. 1991;17(6):495-508.

48. Romero IA, Lister T, Richards HK, Seville MP, Wylie SP, Ray DE. Early metabolic changes during m-Dinitrobenzene neurotoxicity and the possible role of oxidative stress. Free Radic Biol Med. 1995;18(2):311-9.

49. Tjalkens RB, Phelka AD, Philbert MA. Regional variation in the activation threshold for 1,3-DNB-induced mitochondrial permeability transition in brainstem and cortical astrocytes. Neurotoxicology. 2003;24(3):391-401.